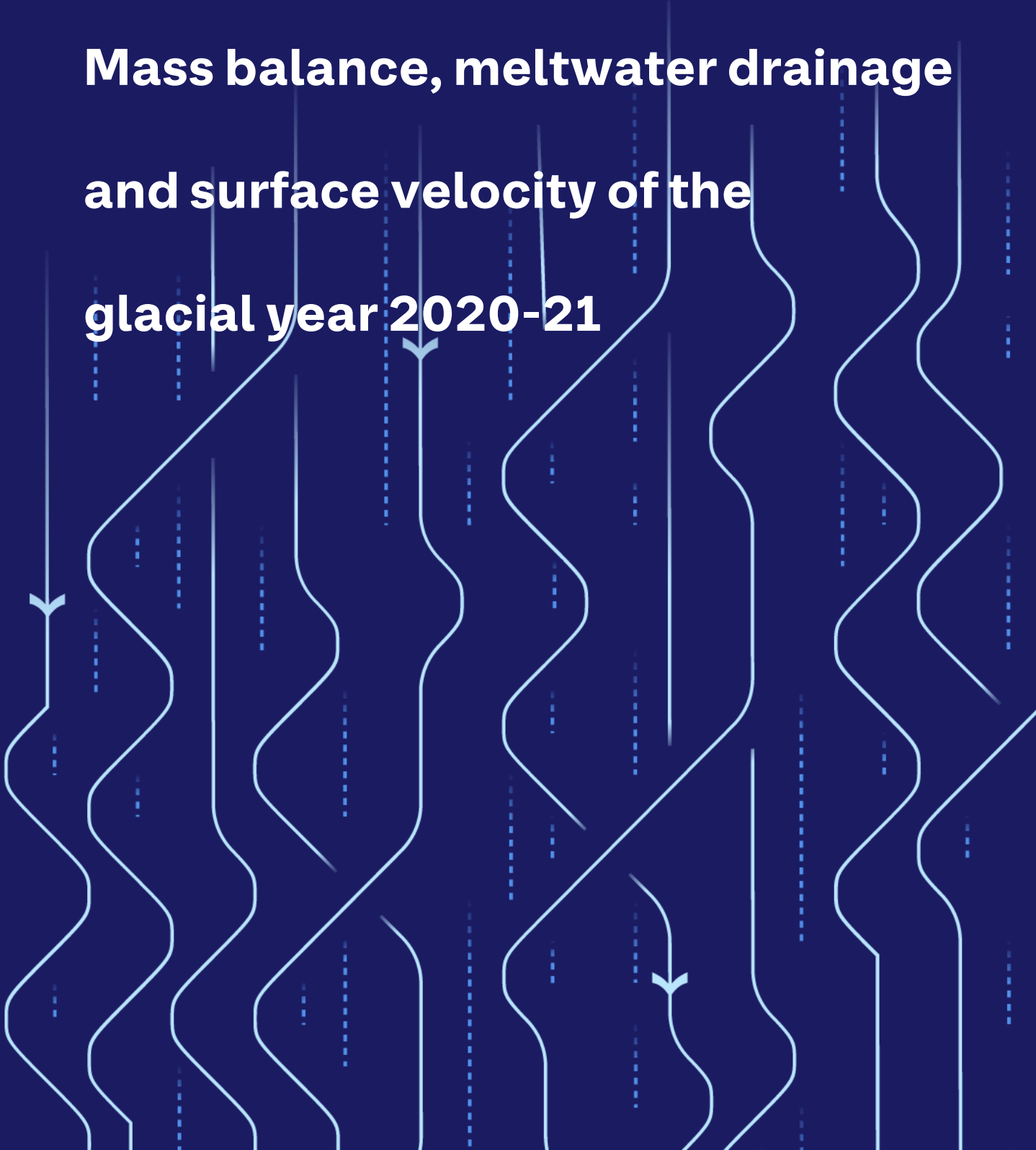


VATNAJÖKULL:

**Mass balance, meltwater drainage
and surface velocity of the
glacial year 2020-21**

The background features a series of vertical, wavy white lines on a dark blue background. These lines represent meltwater drainage paths. Three white arrows point downwards, indicating the direction of flow: one on the left side, one in the center, and one on the right side. The lines are solid in some sections and dashed in others, suggesting different flow characteristics or measurement points.



VATNAJÖKULL:

Mass balance, meltwater drainage and surface velocity of the glacial year 2020-21

Höfundar

Finnur Pálsson, Andri Gunnarsson Eyjólfur Magnússon, Hlynur Skagfjörð Pálsson, Hrafnhildur Hannesdóttir, Ragnar Þórhallsson, Sveinbjörn Steinþórsson

Dagsetning

Febrúar 2022

Lykilsíða

Skýrsla LV nr	LV-2022-009	Dagsetning	Febrúar 2022
Fjöldi Síðna	58	Upplag	1
Dreifing	<input checked="" type="checkbox"/> Birt á vef LV	<input checked="" type="checkbox"/> Opin	<input type="checkbox"/> Takmörkuð til [Dags.]
Titill	VATNAJÖKULL: Mass balance, meltwater drainage and surface velocity of the glacial year 2020-21		
Höfundar/fyrirtæki	Finnur Pálsson, Andri Gunnarsson Eyjólfur Magnússon, Hlynur Skagfjörð Pálsson, Hrafnhildur Hannesdóttir, Ragnar Þórhallsson, Sveinbjörn Steinþórsson, Institute of Earth Sciences University of Iceland, RH-1-22		
Verkefnisstjóri	Andri Gunnarsson		
Unnið fyrir	Landsvirkjun		
Samvinnuaðilar			
Útdráttur	In the glaciological year 2020-21 the winter balance for Vatnajökull was 90% of the average, over the observation period from 1991-92. The total summer mass loss was 17% more than average since 1995 (26% more than average since 1991-92). The net balance was negative as it has been since 1994-95 (except 2014-15), and mass loss 2.6-fold the average since 1994-95 (1.9-fold the average since 1991-92).		
Lykilorð	Vatnajökull, mass balance, afkoma		

Samþykki verkefnisstjóra
Landsvirkjunar



Contents:

1. Introduction
2. Diary
3. Mass balance measurements
 - 3.1 Methods
 - 3.2 Results of mass balance measurements
 - 3.2.1. Tungnaárjökull
 - 3.2.2. Köldukvíslarjökull
 - 3.2.3. Dyngjujökull
 - 3.2.4. Brúarjökull
 - 3.2.5. Eyjabakkajökull
 - 3.2.6. Breiðamerkurjökull
 - 3.2.7. Síðujökull
 - 3.2.8. Grímsvötn
 - 3.3. The mass balance record for Vatnajökull
4. Surface velocity measurements
5. Melt water runoff
6. Conclusions

Figures:

- Figure 1. Outlets of Vatnajökull and location of mass balance sites in 2020_21.
- Figure 2. Maps showing point values of specific in m water equivalent (m_{we}), 2020_21.
- Figure 3. a. Specific point mass balance (m_{we}), along all mass balance profiles 2020_21.
b. Specific point mass balance as a function of elevation on central flow lines on Vatnajökull outlets.
- Figure 4. Specific mass balance of Vatnajökull (m_{we}) 2020_21. Top: winter, Centre: summer Bottom: net balance.
- Figure 5. Top left: The difference between winter balance in 2020_21 and the average winter balance 1995_96 to 2019_20. Top right: The difference between summer balance in 2021 and the average summer balance 1996 to 2020. Lower left: The difference between net balance in 2020_21 and the average net balance 1995_96 to 2019_20. (Blue is higher than average balance and red lower than average).
- Figure 6. Mass balance at a central flow line on Tungnaárjökull 2020_21, and average mass balance 1991_92 to 2019_20 (*the horizontal red lines indicate st. dev. of the variability at the survey site during the survey period*).
- Figure 7. Specific mass balance at a central flow line on Köldukvíslarjökull 2019_20, and average mass balance 1991_92 to 2019_20.
- Figure 8. Mass balance at a central flow line on Dyngjujökull 2020_21, and average mass balance 1992_93 to 2019_20.
- Figure 9. Mass balance at two flow lines on Brúarjökull 2020_21, and average mass balance 1992_93 to 2019_20.
- Figure 10. Mass balance at a central flow line on Eyjabakkajökull 2020_21, and average mass balance 1995_96 to 2019_20.
- Figure 11. Mass balance at a central flow line on Breiðamerkurjökull 2020_21, and average mass balance 1995_96 to 2019_20.
- Figure 12. Mass balance at a central flow line on Síðujökull 2019_20, and average mass balance 2004_05 to 2019_20.
- Figure 13. Mass balance at a central flow line towards Grímsvötn 2020_21, and average mass balance 1991_92 to 2019_20.

- Figure 14. Vatnajökull winter (left) and summer (right) mass balance plotted against net mass balance for the survey period 1991_92 to 2020_21.
- Figure 15. Specific mass balance record for Vatnajökull (top), and selected Vatnajökull outlets 1991_92-2020_21.
- Figure 16. Cumulative specific surface mass balance Vatnajökull and selected Vatnajökull outlets 1991_92 – 2019_20.
- Figure 17. The relation between net annual balance (bn) and accumulation area ratio (AAR) and bn and equilibrium line altitude (ELA), for Vatnajökull outlets during the survey period.
- Figure 18. Average summer surface velocity at survey sites in 2021.
- Figure 19. Surface elevation change relative to spring 2010 (upper panel) and average surface velocity (lower panel) at mb sites on Dyngjujökull in 1992 to 2021.
- Figure 20. Surface elevation change relative to spring 2010 (upper panel) and average surface velocity (lower panel) at mb sites on Eyjabakkajökull in 1995 to 2021.
- Figure 21. Location of surface elevation profiles surveyed in field trips to Vatnajökull in 2021. Survey in spring is shown with red and autumn survey in blue.
- Figure 22. Water divides and drainage basins of selected rivers draining water from Vatnajökull.
- Figure 23. The temporal variation of the average annual meltwater runoff to selected river catchments.

Tables:

Table I. Melt water drainage to selected rivers.

Appendixes:

- Appendix A: Surface mass balance at survey sites 2020_21.
- Appendix B: Surface mass balance distribution by elevation in 2020_21.
- Appendix C: Coordinates at velocity measurement sites.
- Appendix D: Measured surface velocity on Vatnajökull in 2020_21.
- Appendix E: Melt water runoff to selected rivers in summer 2021 derived from summer ablation.
- Appendix F: Records of surface elevation change and surface velocity at mass balance survey sites on Vatnajökull.

1. INTRODUCTION

In 1992 (glacial year 1991_92) a program of surface mass balance measurements was started for Vatnajökull by the Science Institute University of Iceland (now Institute of Earth Sciences, IES) in collaboration with the National Power Company (NPC). For the first year the program was limited to the western part of the glacier, but then expanded to include the northern outlets as well. In 1996 this study was further expanded to include southern outlets, with support from The European Union (Framework IV - Environment and Climate, TEMBA project 1996-1997). This program was extended 1998–2000 with further support from EU (Framework IV - Environment and Climate, ICEMASS project, 1998-2000). In 2000-2002 NPC and IES continued the program. In 2003-2005 IES participated in a multinational research project, which was financially supported by The European Union (EVK2-CT-2002-00152 SPICE). IES was responsible for obtaining data sets for calibration of models of the mass balance and dynamics of Vatnajökull. This work was also supported by The National Power Company of Iceland and The National Road Authority and was a continuation of the TEMBA-project of 1996-97 and ICEMASS project 1998-2001.

Since then IES and NPC have continued a similar program. Mass balance measurements on the southeast outlet Breiðamerkurjökull is financially supported by the National Road Authority.

The aim of the collaborative work of NPC and IES is to improve understanding of the mass balance and melt water runoff from glaciers. This work in combination with energy balance measurements by NPC and IES on Vatnajökull will be used for calibration of models of the surface energy and mass balance of Vatnajökull.

This report describes the field measurements, mass balance, melt water runoff and GPS survey, for the glaciological year 2020_21.

2. DIARY

April 13-14: installation of melt wires, maintenance of AWSs on Breiðamerkurjökull.

May 1-7, June 3 and 8: measurements of the winter balance, setup of AWSs.

August 10: maintenance of AWSs on Breiðamerkurjökull

October 15-18: summer balance measurements, take down of AWSs;

November 26-27: summer balance measurements

In all expeditions the locations of mass balance stakes were measured with Kinematic GPS (or fast static GPS) for surface velocity calculation.

The following members of staff of the Institute of Earth Sciences, University of Iceland, carried out the fieldwork on Vatnajökull: Finnur Pálsson, Sveinbjörn Steinþórsson, Eyjólfur Magnússon with Andri Gunnarsson and Ragnar Þórhallsson (National Power Company), Hlynur Skagfjörð Pálsson (Reykjavík Rescue Team) and Hrafnhildur Hannesdóttir.

3. MASS BALANCE MEASUREMENTS

The purpose of the mass balance measurements is to describe the temporal and spatial distribution of the components of the mass balance. The mean annual values of the components and their variation from year to year are analyzed and related to meteorological conditions and climatic variability. The results are used in studies of changes in the glacier volume, estimates of meltwater contribution to glacial rivers, mass balance modeling, evaluation of altitudinal and regional variations of mass balance in response to climatic variations, and to assess the hydrometeorological and dynamic response of the ice cap to climate change.

The mass balance was determined by a stratigraphic method, measuring changes in thickness and density relative to the summer surface. The winter balance was estimated by drilling ice cores through the winter layer in the spring. Ablation was monitored from markers; snow stakes were put up on the glacier and wires were drilled down in the ablation area. The summer balance was measured in the autumn.

3.1 Methods

Measurements of the surface mass balance on a large ice cap like Vatnajökull are impractical in terms of cost with conventional techniques and sampling density that are typically used on small glaciers. The spatial variability of the mass balance may, however, be predictable on the flat large outlets of such an ice cap given data on several profiles extending over the elevation range of the glacier. The precipitation generally increases with elevation and decreases with the distance from the coast, but both the

distribution of snowfall and redistribution of snow by drift depend on the prevailing wind direction during the winter. The summer melting depends mainly on the altitude and the albedo of the glacier surface. Therefore, we have used observations along a limited number of flowlines, which span the elevation ranges of the outlets to assess aerial estimates of surface mass balance. Each profile describes the variation with elevation, but together they also describe the lateral variation of the mass balance. Recently, modern over-snow vehicles and helicopters have allowed fast traverses to ensure successful fieldwork despite frequently poor weather conditions. The error for individual point measurement is estimated $\sim 30 \text{ cm}_{\text{we}}$ for both summer and winter balance. The error for the glacier wide specific mass balance, based on area integral of mass balance, is however considered smaller, since the error for individual survey sites is independent.

The winter mass balance (b_w) is defined as the mass of snow accumulated during the winter months, the summer balance (b_s) is the mass balance during the summer, and the net balance (b_n) is defined as their sum. The specific mass balance is expressed in terms of the equivalent thickness of water. All mass balance components apply to a time interval between given measurement dates, which are not fixed from one year to another. The dates in the autumn are separated by approximately one calendar year, which roughly coincides with the glaciological year defined as October 1st to September 30th. Snow cores are drilled in April-May through the winter layer and profiles of the density are measured. The summer balance is derived in the autumn from measurements of the changes in the snow core density during the summer in the accumulation area and from

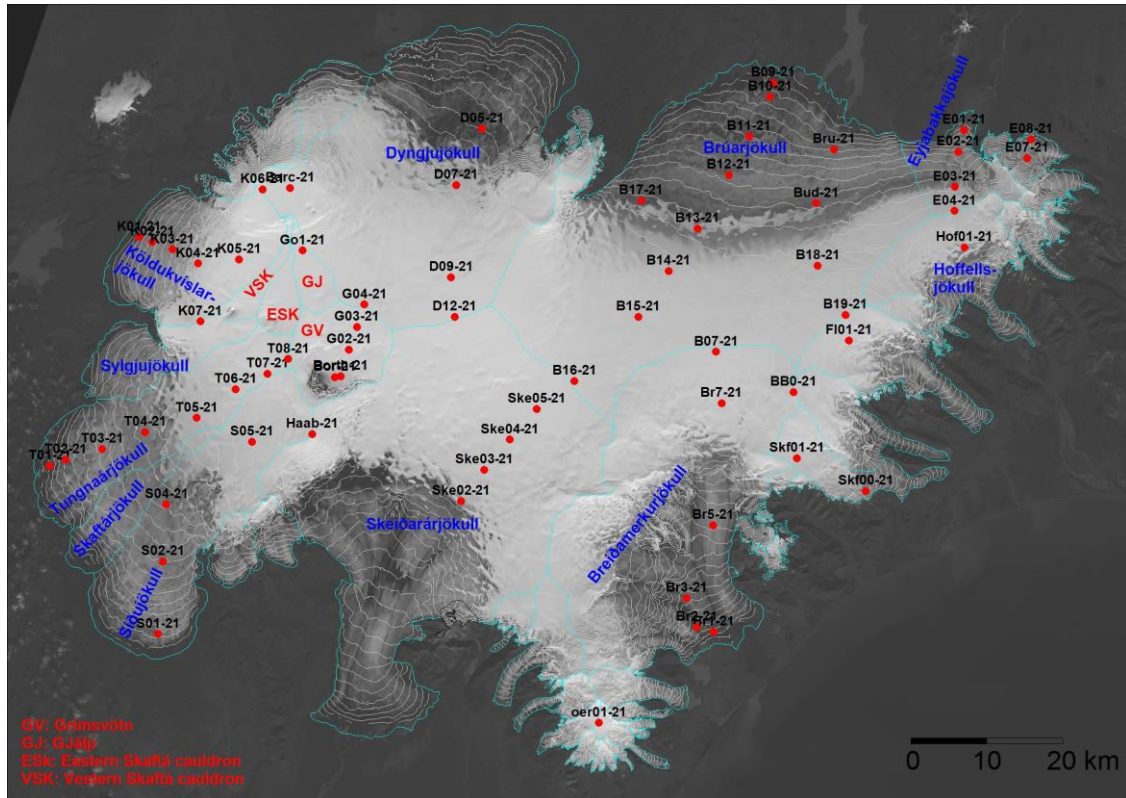


Figure 1. Outlets of Vatnajökull and location of mass balance survey sites 2020_21.

readings at stakes and wires drilled into the ice in the ablation areas. Digital maps are created for winter, summer and net balance for the whole ice cap based on the in-situ measurements. The mass balance is calculated over both the ice and water drainage basins. The summer balance over the water basin is an estimate of meltwater contribution to rivers and groundwater storage. This estimate, however, does not include precipitation that falls as rain on the glacier or snow, which falls and melts during the summer. As conventional for the north hemisphere we define the glaciological year from the start of October to the end of September next year and the period draining meltwater from the glacier during the summer from start of June through September. It would be misleading to include May in the summer period because runoff from the glacier melt in May is delayed due to refreezing during the elimination of

the frost in the surface layer.

3.2 Results of mass balance measurements.

Winter mass balance measurements were done at 67 sites in spring 2021 (Fig. 1). The specific mass balance at individual sites is shown in Fig. 2. Most survey sites are on approximate central flow lines at individual outlets. The specific mass balance along the flow lines is given in Fig 3. for the glacier outlets: Síðujökull, Tungnaárjökull, Köldukvíslarjökull, Dyngjujökull, Brúarjökull (west and east), Eyjabakkajökull, Breiðamerkurjökull, SE-Vatnajökull, Skeiðarárjökull accumulation zone and the ice catchment of Grímsvötn.

Digital maps for winter, summer and net balance are shown in Figure 4. The mass balance of individual outlet is discussed in the following subsections.

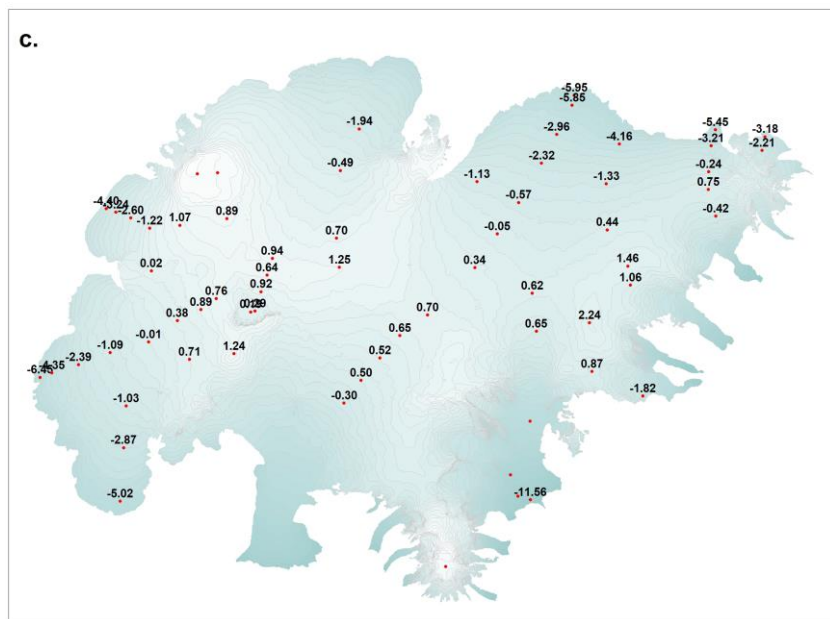
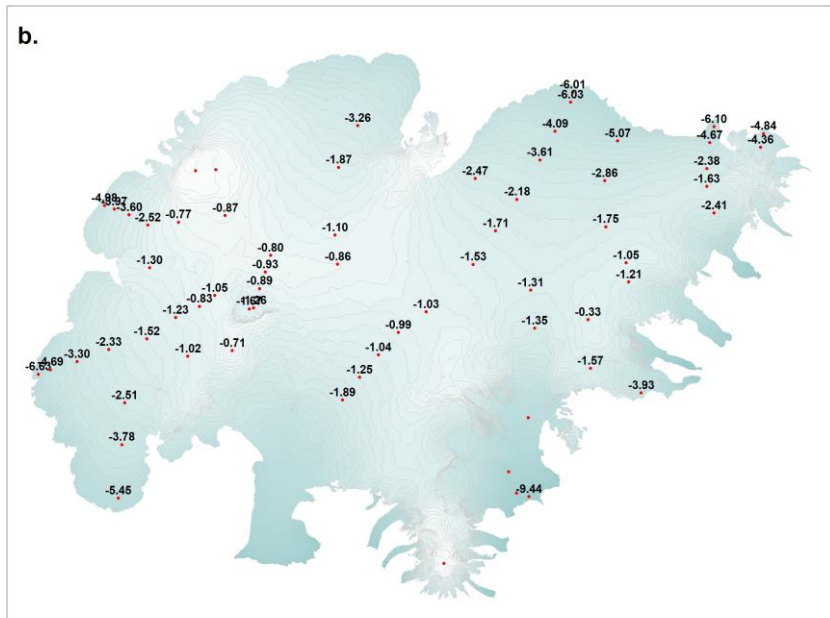
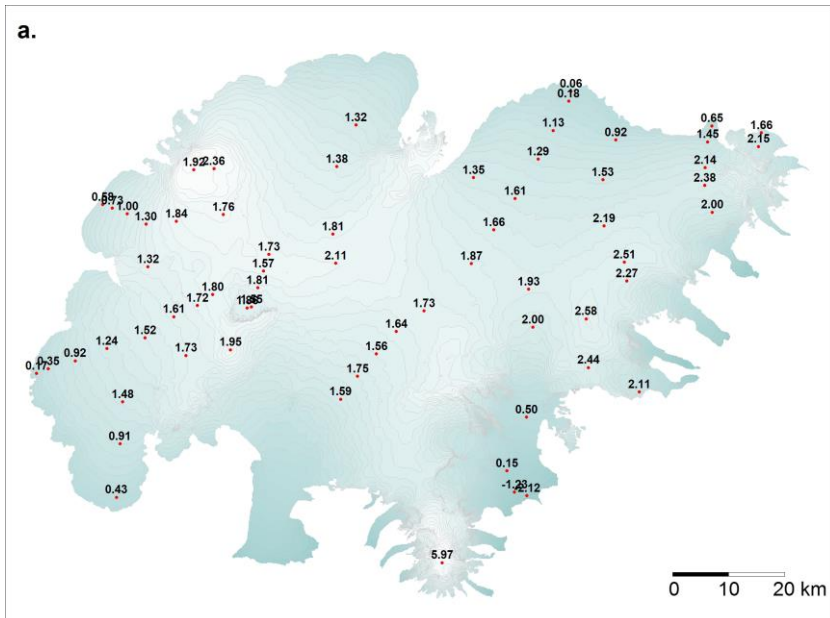


Figure 2. Maps showing point values of specific surface mass balance in m_{we} , 2020_21. a. winter, b. summer, c. net balance.

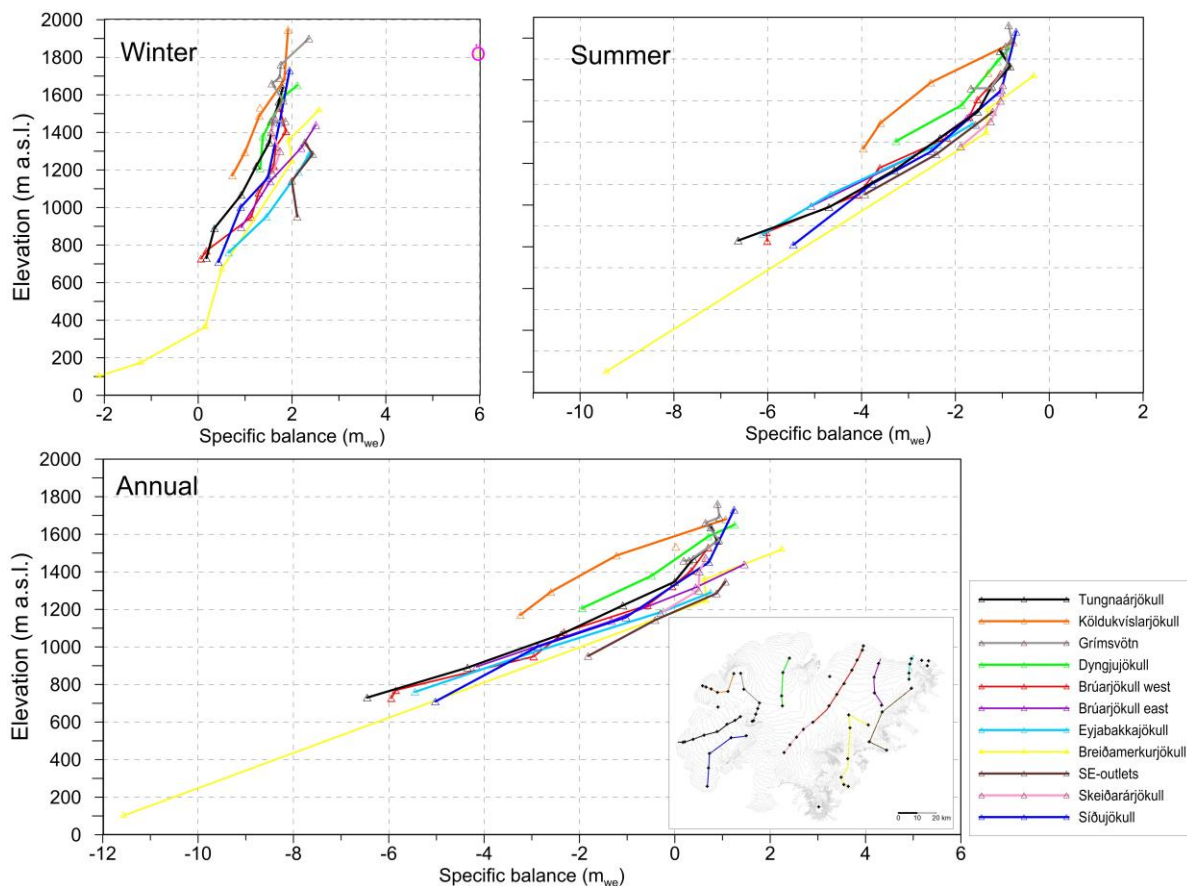


Figure 3. a. Specific mass balance (m_{we}), at survey sites along all mass balance profiles 2020_21.

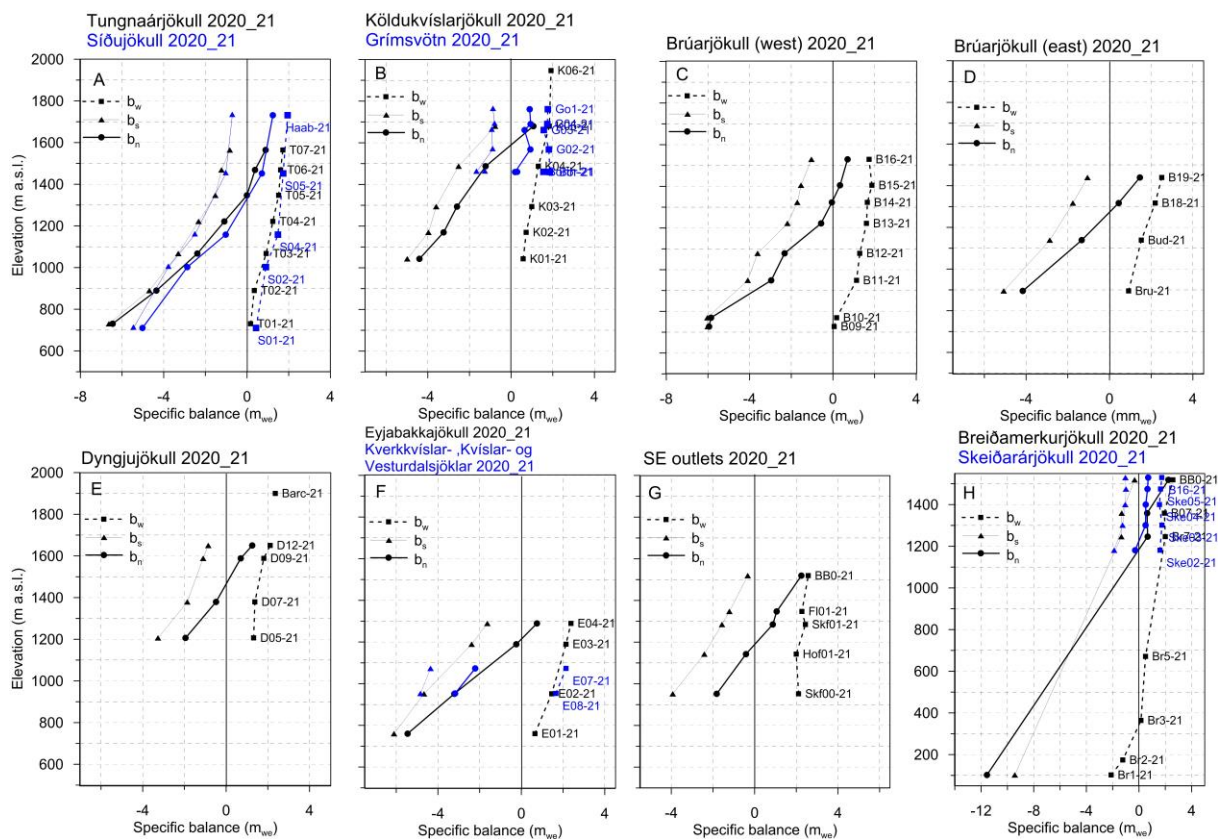


Figure 3. b. Specific point mass balance (m_{we}) 2020_21 as a function of elevation on central flow lines on Vatnajökull outlets.

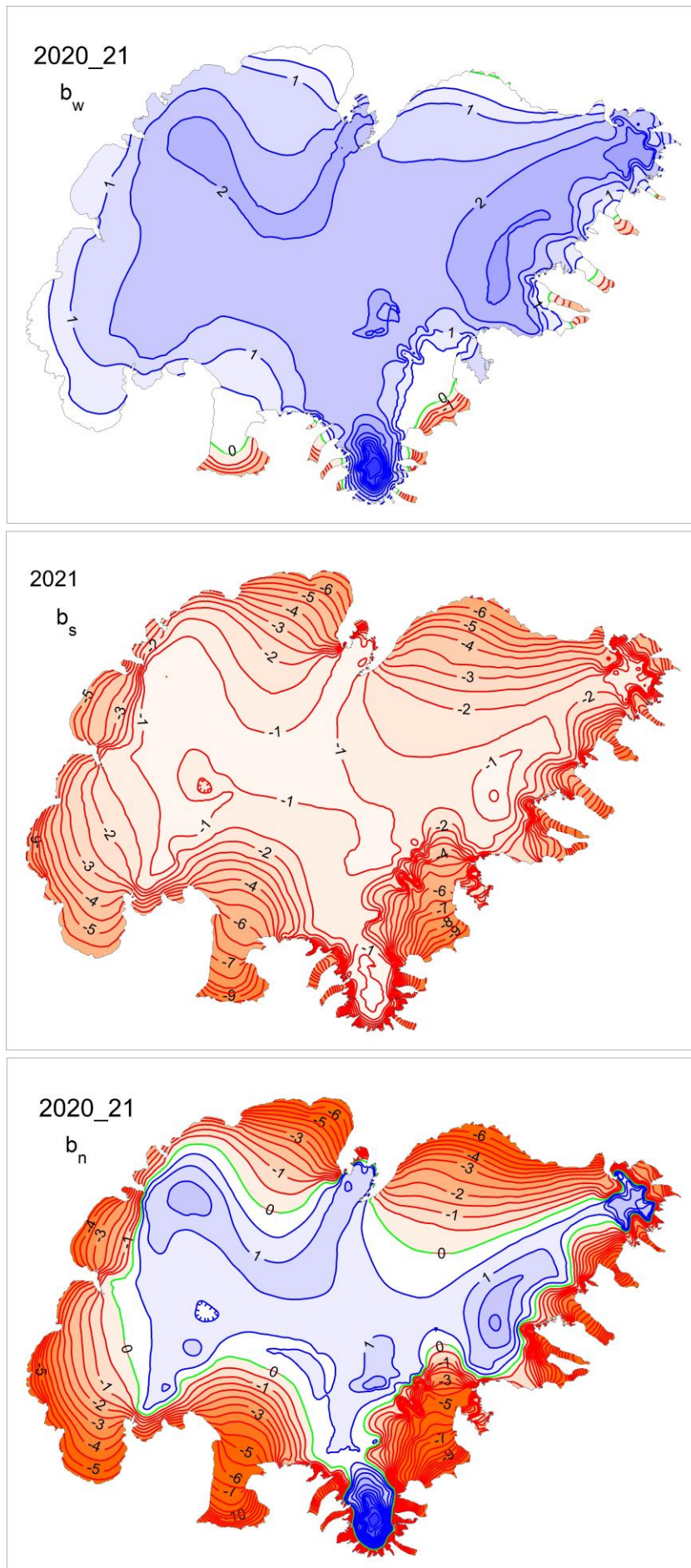


Figure 4. Specific mass balance (m_{we}) maps of Vatnajökull 2020_21. Top: winter, Centre: summer, Bottom: net balance.

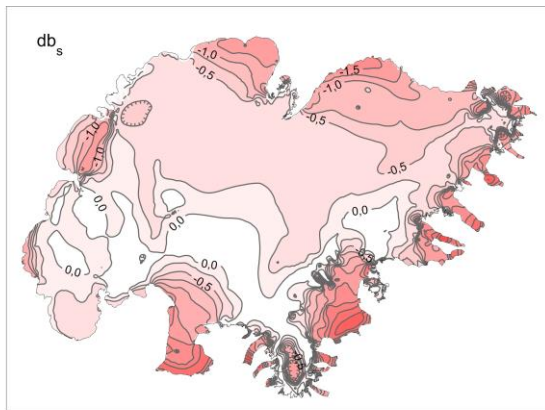
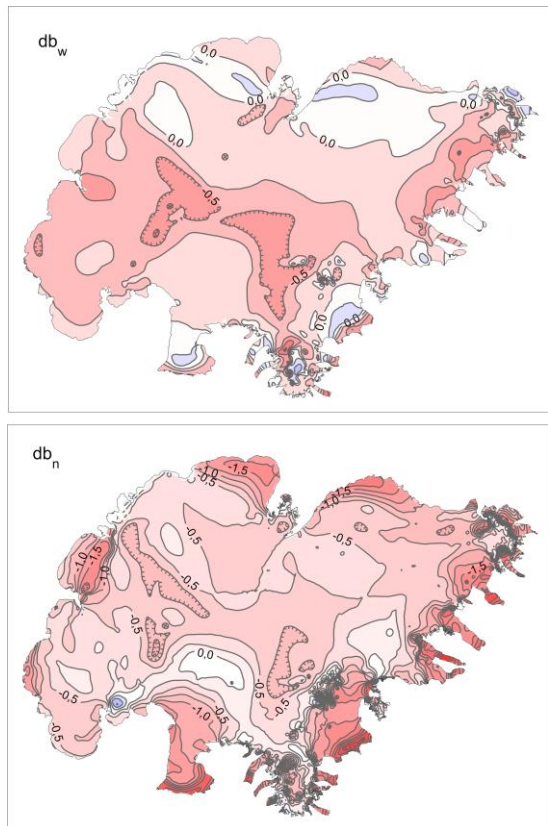


Figure 5. Top left: The difference between winter balance in 2020_21 and the average winter balance 1995_96 to 2019_20. Top right: The difference between summer balance in 2021 and the average summer balance 1996 to 2020. Lower left: The difference between net balance in 2020_21 and the average net balance 1995_96 to 2019_20.

(Blue is higher than average balance and red less than average).

A surface DEM is needed for surface area distribution and delineation of ice divides for individual outlets and catchments. The currently used surface DEM is mostly based on SPOT5 satellite images in 2010*, and partly from LiDAR survey 2010 -11 and -12 (**Jóhannesson et al. 2013), but the large set of GPS profiles measured in spring 2020 was used to locally shift the older DEMs. This DEM represents the surface of 2020 but cut to the glacier terminus of autumn 2019, was used in all area distributions; ice and water divides were not reworked.

The weather in the autumn 2020 was wet and rather warm but mid-November to mid-February extremely dry. From mid-February to late-April snow gradually collected, followed by a cold dry period till late May.

Figure 5 (top left) shows that the winter accumulation is under average at almost everywhere, except in the mid elevation range on the northern outlets, and lower elevations in the south. Winter melting at the low-lying S-outlets slightly less than average. Most of June was rather cold with

snow accumulating on larger portion of the glacier. Real summer with high melts rates started in the first week of July month, with peak melt rates in the last week of August.

Relatively little dust precipitated on the glacier during summer, so average albedo was quite high for most of the summer.

*SPOT 5 HRG images were made available by the French Space Agency (CNES) through the ISIS (Incentive for the Scientific use of Images from the SPOT system) program and SPOT 5 HRS digital elevation models by the Spot Image project Planet Action (www.planet-action.org) and the SPIRIT SPOT 5 stereoscopic survey of Polar Ice.

**Jóhannesson, T., Björnsson, H., Magnússon, E., Guðmundsson, S., Pálsson, F., Sigurðsson, O., Thorsteinsson, T., and Berthier, E.: Ice-volume changes, bias estimation of mass-balance measurements and changes in subglacial lakes derived by lidar mapping of the surface Icelandic glaciers, *Ann. Glaciol.*, 54, 63–74, doi:10.3189/2013AoG63A422,2013.

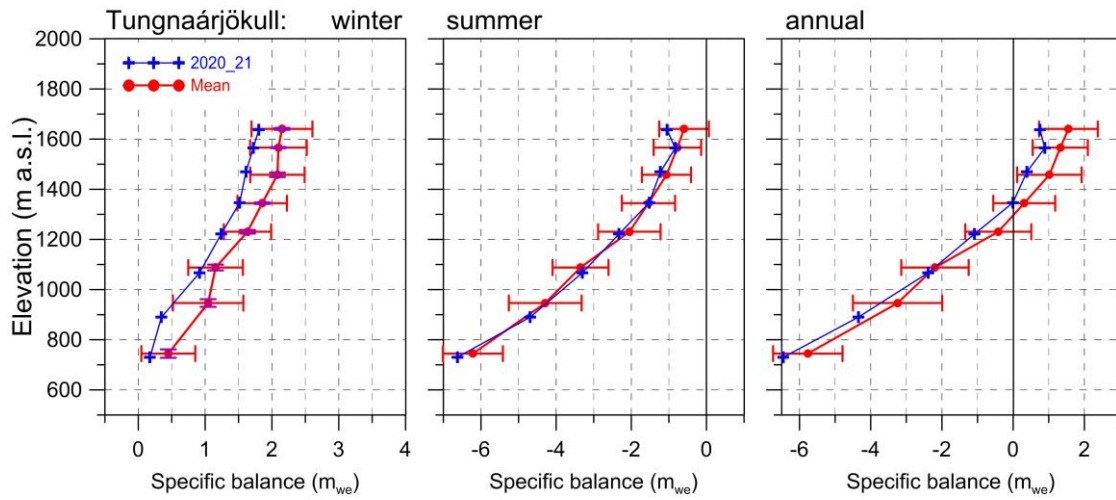


Figure 6. Mass balance at a central flow line of Tungnaárjökull 2020_21 and average mass balance 1991_92 to 2019_20 (the horizontal red lines indicate std. dev of the variability at the survey site during the survey period).

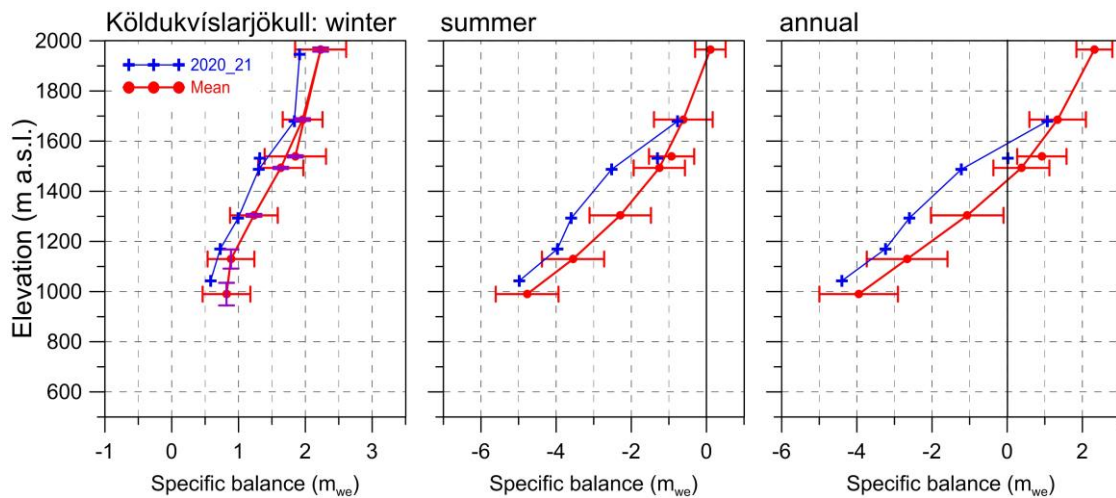


Figure 7. Mass balance at a central flow line of Köldukvíslarjökull 2020_21 and average mass balance 1991_92 to 2019_20.

3.2.1 Tungnaárjökull.

Area = 330 km²

$B_w = 0.37 \text{ km}^3_{we}$; $b_w = 1.11 \text{ m}_{we}$

$B_s = -0.90 \text{ km}^3_{we}$; $b_s = -2.72 \text{ m}_{we}$

$B_n = -0.53 \text{ km}^3_{we}$; $b_n = -1.61 \text{ m}_{we}$

ELA = 1350 m a.s.l. (at profile)

AAR = 31 %

(The terms are defined at the foot of this page)

Variation of mass balance along a central flow line on Tungnaárjökull is shown in Fig. 6. The winter accumulation was almost 1std. (~0.5 m) less than average at almost all survey sites. The total winter balance was only 73% of the average. Summer mass loss was at average at all survey sites especially at the highest where

dust from Grímsvötn probably enhanced the melt. In total summer mass loss was 4% over average of the survey period. Similar applies to the net balance. In total the net mass loss amounted to 0.5 m more than average (45% more) of the survey period. This is the 27th year out of the 30 surveyed with negative net balance on Tungnaárjökull catchment.

3.2.2 Köldukvíslarjökull

Area = 289 km²

$B_w = 0.36 \text{ km}^3_{we}$; $b_w = 1.24 \text{ m}_{we}$

$B_s = -0.74 \text{ km}^3_{we}$; $b_s = -2.56 \text{ m}_{we}$

$B_n = -0.38 \text{ km}^3_{we}$; $b_n = -1.32 \text{ m}_{we}$

ELA = 1590 m a.s.l. (at profile)

AAR = 34 %

For each ice catchment basin, B_w , B_s and B_n are water equivalent volumes of winter, summer and net balance, ELA the equilibrium line altitude, and AAR is the accumulation area ratio.

Variation of mass balance along a central flow line on Köldukvíslarjökull is shown in Fig. 7. The winter accumulation was close to average at ~1700 m but well under average at the other. The total winter accumulation was at average was 0.25 m less than average (84%). Summer mass loss was much more than (1 to 1.5 std.) average at all survey sites except the highest that were close to average. In total summer mass loss was 32% over the average during the survey period. In total the net mass loss was 0.9 m more than that of an average year of the survey period (~2.8 times the average). This is the 25th year out of the 30 surveyed with negative net balance.

3.2.3 Dyngjujökull

Area = 1039 km²

$B_w = 1.59 \text{ km}^3_{we}$; $b_w = 1.53 \text{ m}_{we}$

$B_s = -2.33 \text{ km}^3_{we}$; $b_s = -2.24 \text{ m}_{we}$

$B_n = -0.74 \text{ km}^3_{we}$; $b_n = -0.71 \text{ m}_{we}$

ELA = 1465 m a.s.l. (at profile)

AAR = 53 %

Variation of mass balance along a flow line on Dyngjujökull is shown on Fig. 8. Mass balance is not measured at the lowest elevations but assumed to be

correlated (as a function of elevation) to that of Brúarjökull and Köldukvíslarjökull. The site measurements show less than average snow accumulation in the upper part of the accumulation zone, but slightly over average at the lower two. The total winter accumulation is estimated 95% of the survey period.

Summer mass loss was almost 1 std. more than average over the survey period at all survey sites. The net balance was negative by -0.71 m_{we} while the average for Dyngjujökull is only slightly negative (-0.03 m_{we}), so the mass loss in 2020_21 is ~25 fold the average loss.

Dyngjujökull has often had mass balance close to zero, and the net balance has been estimated positive in at least 11 years of the three-decade period of almost continuous mass loss for Vatnajökull as a whole. The inland, Dyngjujökull, is the outlet of Vatnajökull closest to mass equilibrium during the survey period.

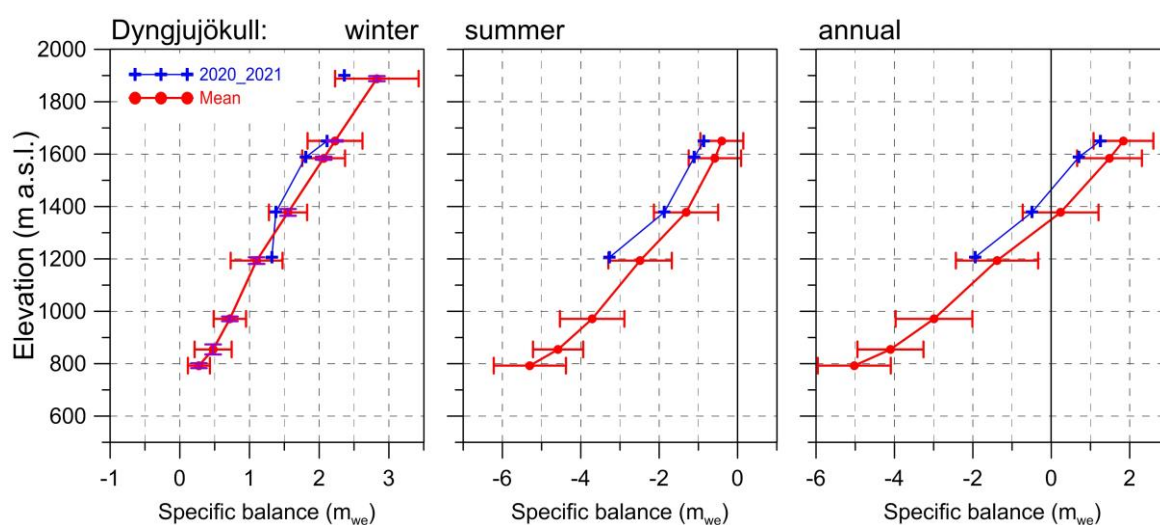


Figure 8. Mass balance at a central flow line on Dyngjujökull 2020_21 and average mass balance 1991_92 to 2019_20 (except 1998_99 – 2003_04 at all but the top elevation).

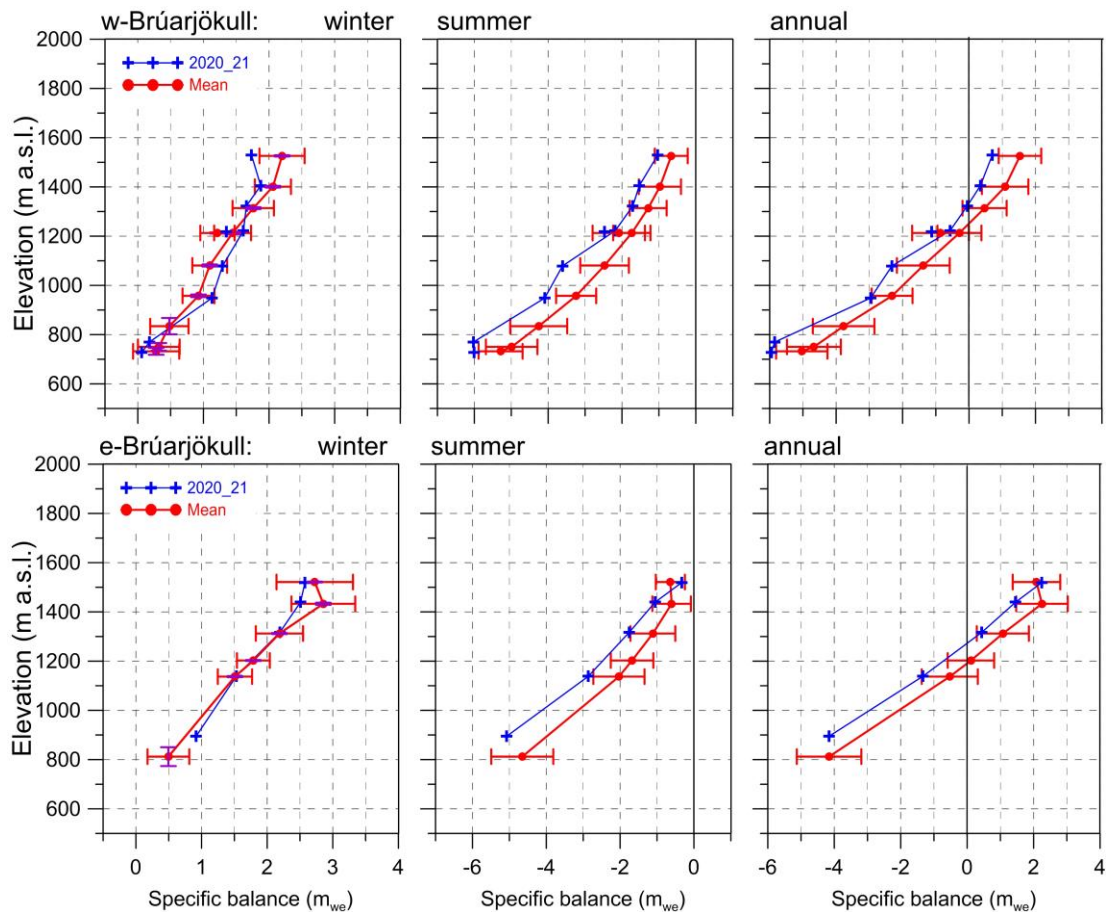


Figure 9. Mass balance at two flow lines on Brúarjökull 2020_21 and average mass balance 1992_93 to 2019_20.

3.2.4 Brúarjökull

Area = 1500 km²

$B_w = 2.41 \text{ km}^3_{we}$; $b_w = 1.61 \text{ m}_{we}$

$B_s = -3.67 \text{ km}^3_{we}$; $b_s = -2.45 \text{ m}_{we}$

$B_n = -1.26 \text{ km}^3_{we}$; $b_n = -0.84 \text{ m}_{we}$

ELA = 1335 m a.s.l. (western flow line)

ELA = 1270 m a.s.l. (eastern flow line)

AAR = 48 %

Variation of mass balance along two flow lines on Brúarjökull is shown on Fig. 9. At the western flow line accumulation was well over average (1 std.) at middle elevation range, but well under at the three highest and two lowest survey sites. At the eastern survey line accumulation was close to average in the mid elevation range, but far under average at the highest two, at Breiðabunga, which is most prone to precipitation from south and eastern wind directions. The distribution of the

snow accumulation reflects prevailing path of the Atlantic low-pressure systems south and east of Iceland, for long periods of the winter, resulting in precipitation in northern winds. The winter accumulation was in total about at average. Summer mass loss was almost 1 std. more than average at all survey sites, except the highest on Breiðabunga where it was under average, probably due to snowfall in summer. In total the mass loss in summer was exceeded the average by 29 %. The net balance was about 1 std. less than average at almost all the survey sites. In total the net balance was negative by -0.87 m_{we} , almost 3-fold the average mass loss of the survey period. During the survey period, there have been 8 years of positive balance and 21 years with negative net balance.

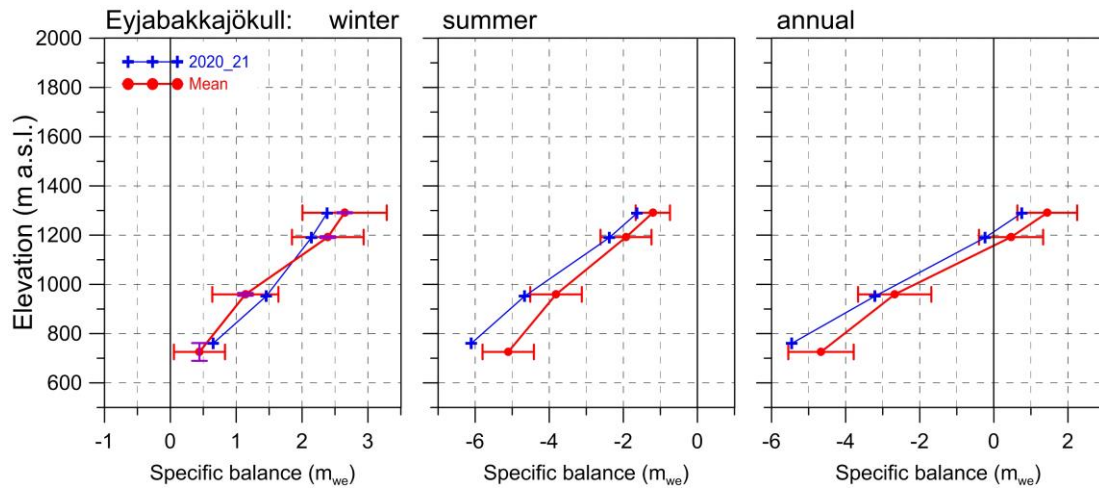


Figure 10. Mass balance at a central flow line of Eyjabakkajökull 2020_21 and average mass balance 1995_96 to 2019_20.

3.2.5 Eyjabakkajökull

Area = 106 km²
 $B_w = 0.19 \text{ km}^3_{we}$; $b_w = 1.82 \text{ m}_{we}$
 $B_s = -0.35 \text{ km}^3_{we}$; $b_s = -3.30 \text{ m}_{we}$
 $B_n = -0.16 \text{ km}^3_{we}$; $b_n = -1.48 \text{ m}_{we}$
 ELA = 1215 m a.s.l. (at profile)
 AAR = 27 %

Variation of mass balance along a central flow line on Eyjabakkajökull is shown on Fig. 10. As on at the contiguous E-Brúarjökull accumulation was less than average all sites in the mid elevation range, but less than average at the highest. The total winter accumulation was at average of the survey period. Summer mass loss was by far more than average at all survey

sites, but much less than average close to average ELA (probably due to summer snowfall). The total summer mass loss was about 23% more than average. The net balance was negative by 1.7-fold that of the average of the survey period, and has been negative for all but 3 years of the 26 years of survey.

3.2.6 Breiðamerkurjökull

Area = 925 km²
 $B_w = 1.26 \text{ km}^3_{we}$; $b_w = 1.37 \text{ m}_{we}$
 $B_s = -2.75 \text{ km}^3_{we}$; $b_s = -2.98 \text{ m}_{we}$
 $B_n = -1.49 \text{ km}^3_{we}$; $b_n = -1.61 \text{ m}_{we}$
 ELA = 1185 m a.s.l. (at profile)
 AAR = 52

Variation of mass balance along a

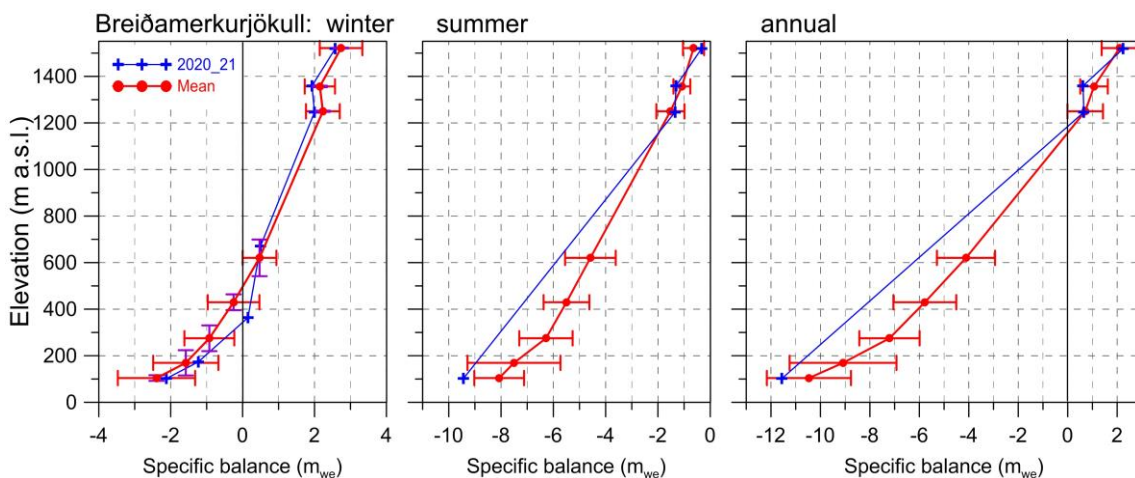


Figure 11. Mass balance at a central flow line of Breiðamerkurjökull 2020_21 and average mass balance 1995_96 to 2019_20.

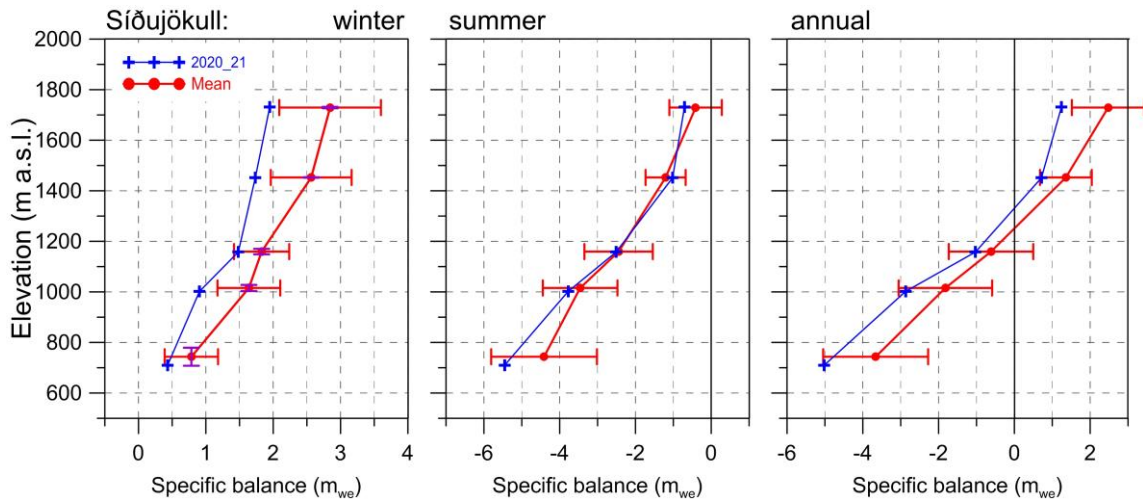


Figure 12. Mass balance at a central flow line of Síðujökull 2020_21 and average mass balance 2004_05 to 2019_20.

central flow line on Breiðamerkurjökull is shown on Fig. 11.

Winter accumulation was slightly under average at the survey sites in the accumulation zone. At the lower sites in the ablation zone mass loss in winter was less than average. The total winter balance was 92% of the average of the survey period. Summer mass loss was not far from to average in the accumulation zone, except at the highest on Breiðabunga (same as E-Brúarjökull), but more than 1 std. over average in the lowest ablation zone. As this is written the two upper sites of the ablation zone have not been visited, so the results presented are preliminary. The total summer mass loss was close to 15% more than average during the survey period. The net mass loss was almost 45% more than in an average year.

In addition to mass loss due to surface melt Breiðamerkurjökull loses in the order of 0.5 km^3 annually via calving into the marginal lake Jökulsárlón; this mass loss is not accounted for here.

3.2.7 Síðujökull

Area = 410 km^2

$B_w = 0.49 \text{ km}^3_{we}$; $b_w = 1.20 \text{ m}_{we}$

$B_s = -1.20 \text{ km}^3_{we}$; $b_s = -2.93 \text{ m}_{we}$

$B_n = -0.71 \text{ km}^3_{we}$; $b_n = -1.73 \text{ m}_{we}$

ELA = 1335 m a.s.l. (at profile)

AAR = 36 %

Variation of mass balance along a central flow line on Síðujökull is shown in Fig. 12.

The winter snow accumulation was ~1std. less than average at all survey sites. The total winter balance was only 74% of the average (since 2004_05). Summer mass loss was at average at all sites except the lowest, where it was far more than average. The total summer mass loss was at the average during the survey period. Net mass loss was ~34% more than average during the 16-year survey period. Her the only year of positive net balance was of 2014_2015.

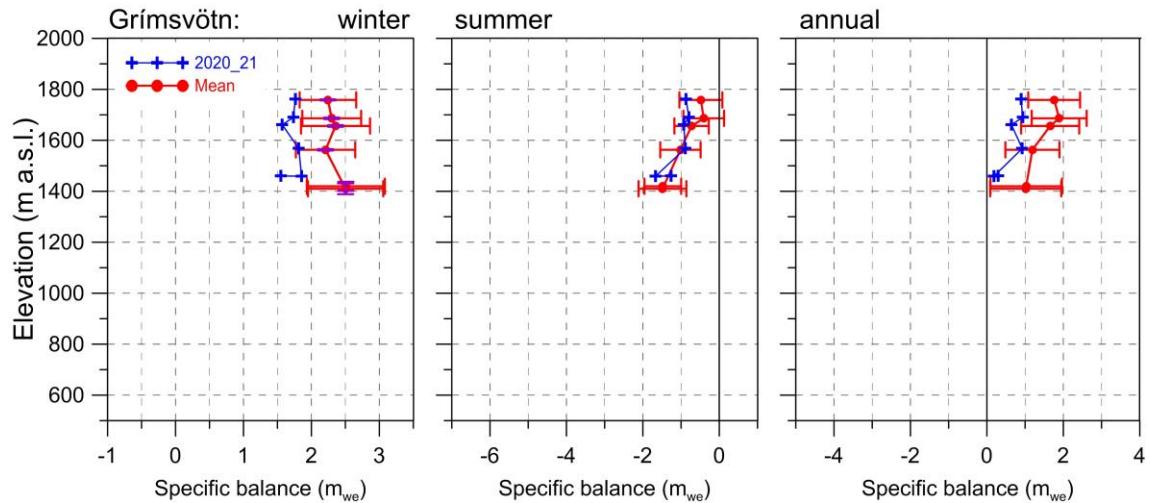


Figure 13. Mass balance at a flow line towards Grímsvötn 2020_21 and average mass balance 1991_92 to 2019_20.

3.2.6 Grímsvötn-Gjálp

Area = 174 km²
 $B_w = 0.24 \text{ km}^3_{we}$; $b_w = 1.80 \text{ m}_{we}$
 $B_s = -0.15 \text{ km}^3_{we}$; $b_s = -1.08 \text{ m}_{we}$
 $B_n = 0.09 \text{ km}^3_{we}$; $b_n = 0.714 \text{ m}_{we}$

Variation of mass balance at sites close to a flow line from Bárðarbunga towards Grímsvötn center is shown in Fig. 13. Snow accumulation was almost 1 std. less than average at all survey sites, and total winter accumulation only 77% the average.

Summer mass loss was more than average at all but two sites; total summer mass loss 33% over the average. Net balance was positive as always (except 2010), now by only 47% of the average. In addition to surface mass loss in summer, geothermal melt in the Grímsvötn catchment area is on the order of 0.2 km³ annually, this is not accounted for here.

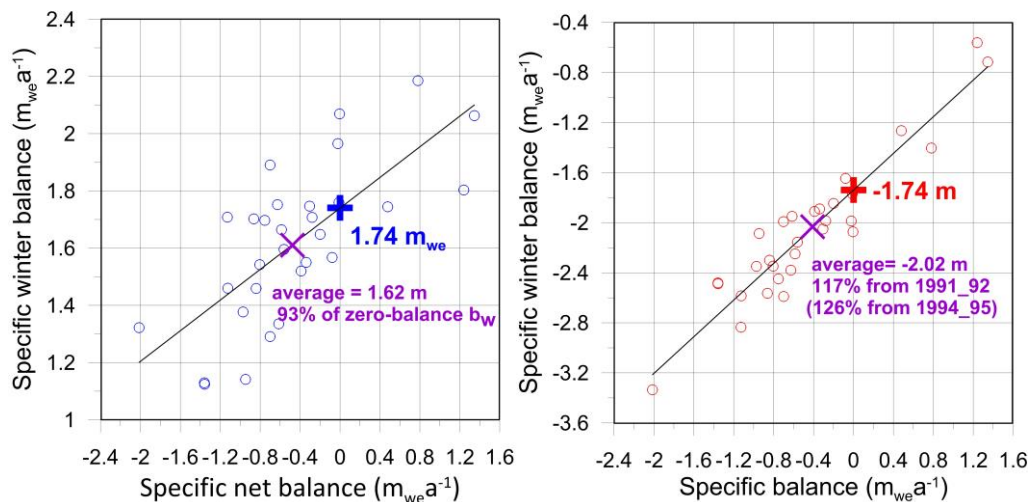


Figure 14. Vatnajökull winter (left) and summer (right) mass balance plotted against net mass balance for the survey period 1991_92 to 2020_21.

3.3 Vatnajökull: mass balance record

From the digital mb maps (Fig. 4) the glacier wide volumes of winter, summer and net balances for Vatnajökull have been calculated by integration and are as follows:

Area = 7770 km²
B_w = 11.35 km³_{we} ; b_w = 1.46 m_{we}
B_s = -20.08 km³_{we} ; b_s = -2.59 m_{we}
B_n = -8.73 km³_{we} ; b_n = -1.13 m_{we}
AAR = 49%;

(balance values as a function of elevation are tabulated in appendix D) The weather in the autumn and first winter months 2020_21, was wet and rather warm, but from late November 2020 to early February almost no snow was accumulated in Grímsvötn (data from snow elevation meter), an extremely dry period for most of Vatnajökull. In Grímsvötn snow accumulation started again at a steady rate till late April, then a dry period again to the end of May. June was cold and snow accumulated in the upper part until a sudden start of summer melt on the last days of June. Distribution of the winter snow was not typical (see fig. 5a). In general, there was less snow than average on most of the icecap, by far less in the west and south, but more than average in the mid elevation range of the northern outlets, most likely collected in spells of snowfall in northern winds. The total winter balance was ~90% of the average (over the observation period from 1991_92). Inland the summer months were warm with prevailing western winds and extremely dry calm and warm weather in East Iceland. The total summer mass loss was ~17% over the average since 1995 (almost 26% over the average since 1992).

The zero-mass balance mass turnover for Vatnajökull (current topography) is estimated from the zero net balance crossover of the linear trend of b_w plotted against b_n and equivalently b_s against b_n (see fig 14.) and found to be close to 1.74 m_{we} (13.5 km³_{we}). The winter balance 2020_21 is only 84% of the estimated zero-mass balance turnover (0-mbt), while the average b_w of the survey period is close 93% of the 0-mbt. The summer balance of 2021 is -0.85 m (or 67%) more negative than 0-mbt. On average the summer mass loss has been 17% (average of summers 1992-2021) higher than 0-mbt, 26% for the period of 1995-2021.

This clearly shows that the high mass loss of the past 3 decades is governed by too much mass loss during summer rather than too little snow accumulation during winter.

The net balance of 2020_21 is negative by 1.9-fold that of the period since 1991_92 (2.6-fold the average of the period since 1994_95), the 5th in row of years with highest mass loss of the survey period (see fig. 15).

The net balance has been negative since 1994_95 (except for 2014_15). After a short period of positive and close to zero mass balance, both 2018_19 and 2020_21 is comparable to the 15-year period (1995_96 to 2009_10) of high mass loss.

During the period of high net mass loss since 1994_95, the northern outlets have had several years of close to zero and positive mass balance. After 2010 both winter and summer balance are highly variable, much more so than the 15 prior years of high mass loss, this is seen for all the mb records presented in figure 15. The variability of the winter balance is by far more prominent for the outlets closest to sea. That part of the glacier receives precipitation from all south and east wind directions, and thus has high snow accumulation in

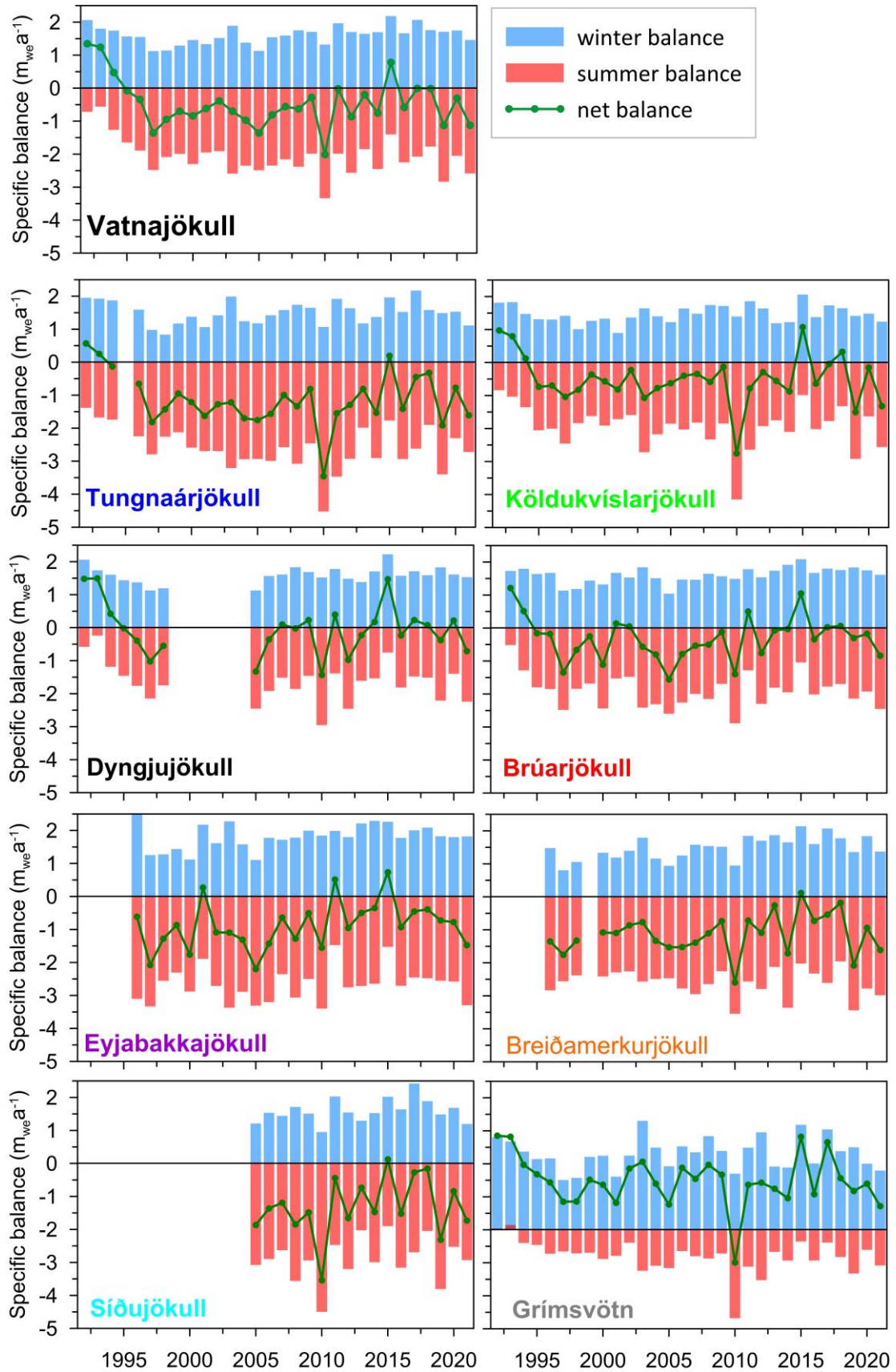


Figure 15. Specific mass balance record for Vatnajökull(top), and selected Vatnajökull outlets 1991_92-2020_21.

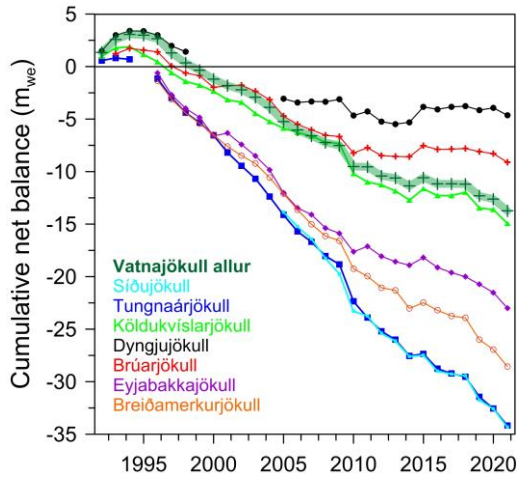


Figure 16. Cumulative specific surface mass balance Vatnajökull and selected Vatnajökull outlets 1991_92 – 2019_20.

Atlantic low-pressure systems are just south and east of Iceland. The cumulative net balance curves for the outlets of Vatnajökull in Fig. 17 show that all outlets have been losing mass since 1994_95. During the period of high mass loss, the mass loss speed is about -0.5 - -0.6 $m_{we}a^{-1}$ for the northern outlets but -1.1 - -1.5 $m_{we}a^{-1}$ for the south and western outlets. After 2010 there is a distinct difference between the north inland (Dyngjujökull and Brúarjökull) and the south and west coastal (Breiðamerkurjökull, Tungnaárjökull and Síðujökull) outlets in that there is sudden change in the mass balance trend for northern. The trend changes from $-0.5ma^{-1}$ to about zero for the northern while there is little change for the others. The east outlet Eyjabakkajökull behaves like the coastal and is in fact close to sea, while Köldukvíslarjökull is more similar to the northern, although the mb rate change after 2010 is less significant. The cumulative mb for Vatnajökull is very similar to Köldukvíslarjökull, with a slope of -0.75 ma^{-1} in the period of high mass loss, but -0.35 ma^{-1} after 2010.

During the survey period starting 1991_92 Vatnajökull lost ~ 120 km^3 of ice or thinned ~ 15 m due to surface

mass loss (summing from the start of high mass loss in 1994_95 yields 150 km^3 or 19 m thinning). Non-surface mass balance is estimated (calving, geothermal melt, internal friction, eruptions) ~ 0.2 m_{we} for Vatnajökull in a paper by Tómas Jóhannesson and others (Jóhannesson, T., Pálmason, B., Hjartarson, Á., Jarosch, A., Magnússon, E., Belart, J., et al. (2020). Non-surface mass balance of glaciers in Iceland. *J. Glaciol.* 66, 685–697. doi:10.1017/jog.2020.37) which amounts to a loss of ~ 55 km^3 or 7 m average thinning since 1994_95.

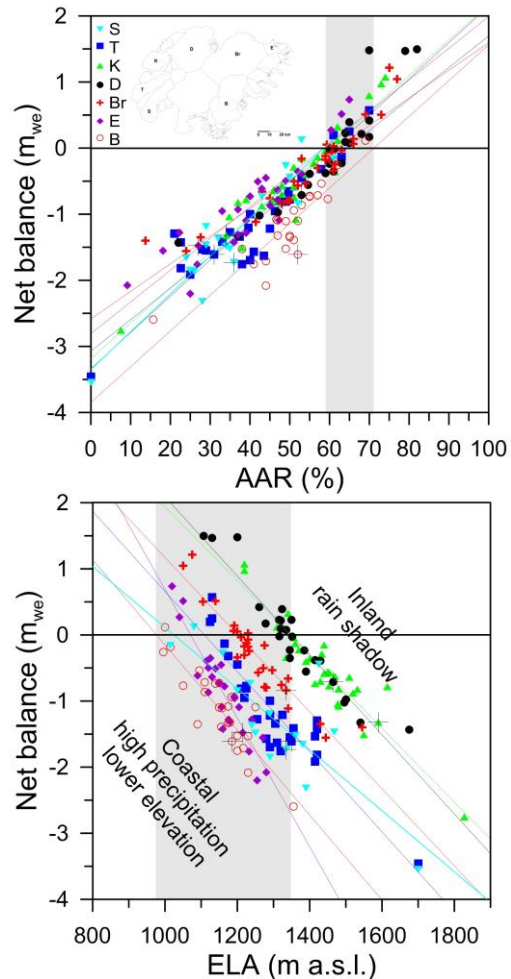


Figure 17. The relation between net annual balance (b_n) and accumulation area ratio (AAR) (upper) and b_n and equilibrium line altitude (ELA), for Vatnajökull outlets during the survey period. (This year's points are marked with a black +).

In Fig. 17 the relation of the annual net balance to the accumulation area ratio (AAR) and equilibrium line altitude (ELA) is shown for different outlets over the survey period. The b_n -AAR gradient is similar for all outlets, about 0.5 m_{we} for 10% change in AAR. The zero-balance AAR varies for different outlets in the range 60-65%, similar for all outlets except for the southern outlet Breiðamerkurjökull. Breiðamerkurjökull is far from equilibrium, the ablation area is too large. A large part of the outlet has carved 200-300 m deep valley into the former sediment bed, and the surface and bed elevation has lowered accordingly. Similarly, the zero-balance ELA varies from about 1000-1100 m a.s.l. for the southern outlets to 1400 m a.s.l. for the NW outlets. The b_n -ELA slope is similar for all outlets -0.6 m_{we} per 100 m, except Eyjabakkajökull with a slope of -1.0 m_{we} per 100 m and Síðujökull

with a slope of -0.45 m_{we} per 100 m (for Síðujökull possibly due to outliers in the data set).

4. SURFACE VELOCITY MEASUREMENTS

The average summer surface velocity of the glacier surface at the survey was calculated from fast static or kinematic GPS (accuracy about $\sim 10 \text{ cm}$) positioning of the ablation stakes/wires. In 2021 all sites were surveyed in spring and autumn and many in June. At a few sites stakes from previous years were found and resurveyed, making it possible to calculate surface velocity over a year or longer time span. The average summer surface velocity is shown in Figure 18.

At sites close to the glacier terminus very small horizontal movement is measured. This indicates that the glacier snouts are almost stagnant. In

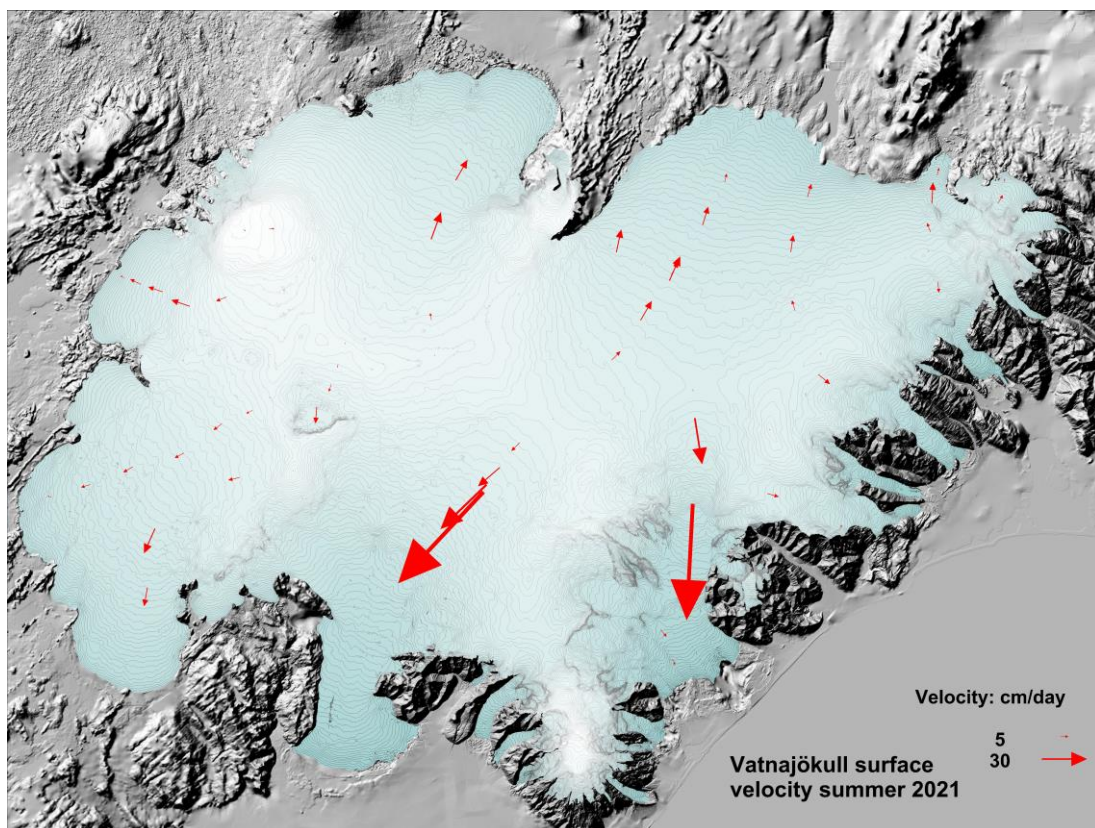


Figure 18. Average summer surface velocity at survey sites in 2019_21.

the centre areas of some of the outlets especially close to the equilibrium line, there is an increase in velocity during summer compared to winter. The summer velocity is typically in the order of two-fold the winter velocity. This suggests that basal sliding is increased in the melting season and is of the same magnitude as the deformation velocity.

To better understand the variable velocity continuous GPS has been run during summer at several sites.

From previous velocity measurements, surging of outlets has been predicted. Currently the increase in velocity at sites D05 and D07 (Fig. 20.) persists and suggests that Dyngjujökull may surge within a few years. The velocity at sites D07 and D05 is now similar that in 1997 prior to the surge in 1998-2000 and the accumulation zone has thickened. To monitor velocity changes leading up to a surge GPS instruments were set up in spring to continuously monitor movement at sites D05, D06 and D07.

The data collected allows for post-

processing to acquire more accuracy (~dm instead of ~m), but the processing has not been finished when this report is written.

A figure similar Fig 21. Showing the average summer velocity and elevation change record at the survey sites on Eyjabakkajökull. There is an increase in velocity at sites E01 (many-fold) and E02 (1.5-fold). This may be caused by the rapid recession of the glacier snout, and thus steeper surface slopes, but may also be signs of surge. Images of velocity and elevation records for other survey sites are displayed in Appendix F.

Most vehicles used in the survey are equipped with survey type GPS that collect data while driving. These are post-processed, to yield surface profiles with an accuracy of ~dm in horizontal and vertical. Location of all profiles surveyed in 2021 is shown in image 22. The profiles have proved of high importance to increase accuracy of remote sensing-based surface DEMs.

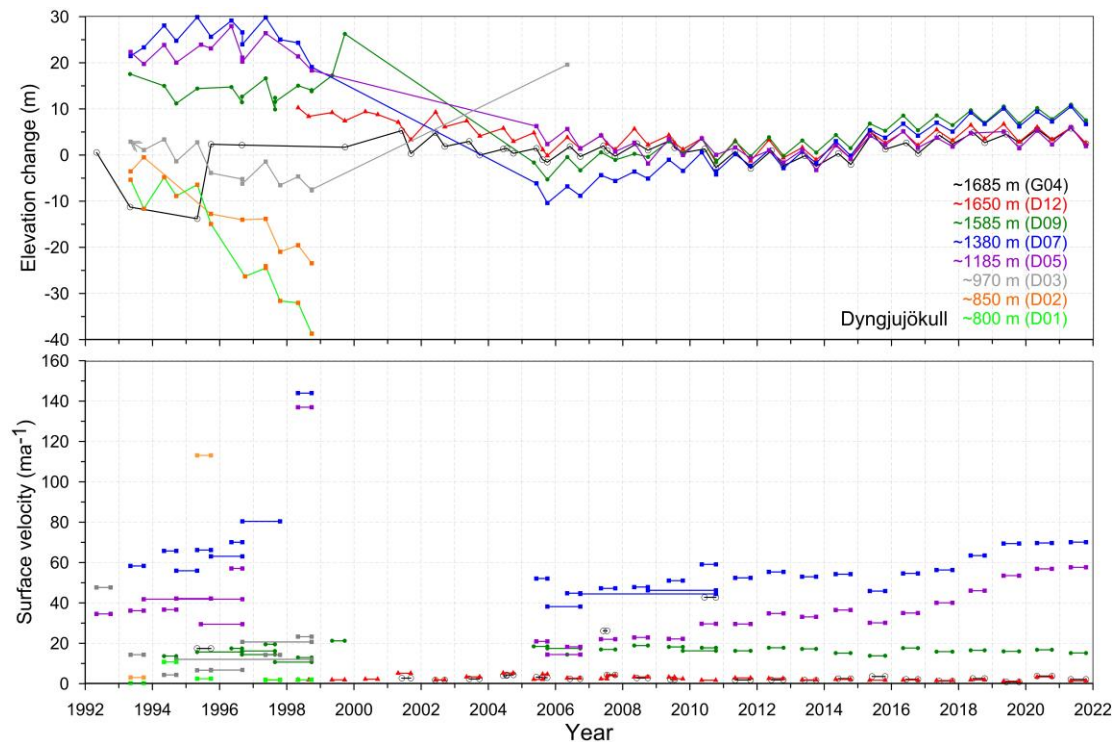


Figure 19. Surface elevation change relative to spring 2010 (upper panel) and average surface velocity (lower panel) at mb sites on Dyngjujökull in 1992 to 2021.

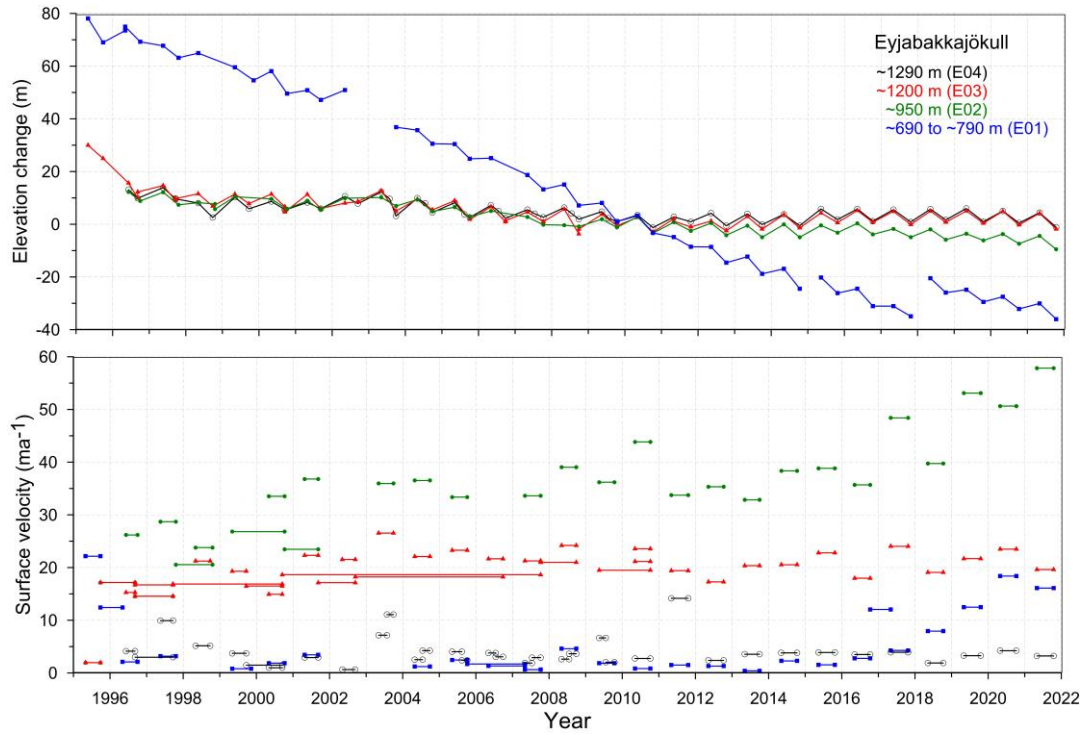


Figure 20. Surface elevation change relative to spring 2010 (upper panel) and average surface velocity (lower panel) at mb sites on Eyjabakkajökull in 1995 to 2021.

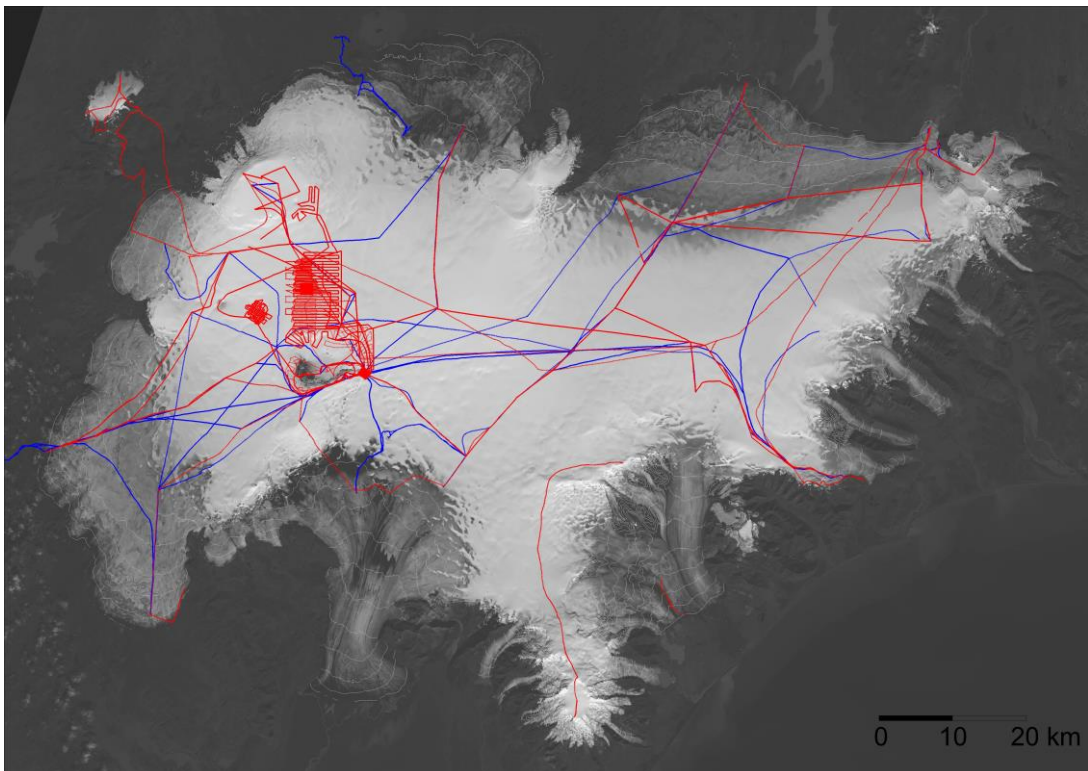


Figure 21. Location of surface elevation profiles surveyed in field trips on Vatnajökull in 2021. Survey in spring is shown with red and autumn survey in blue.

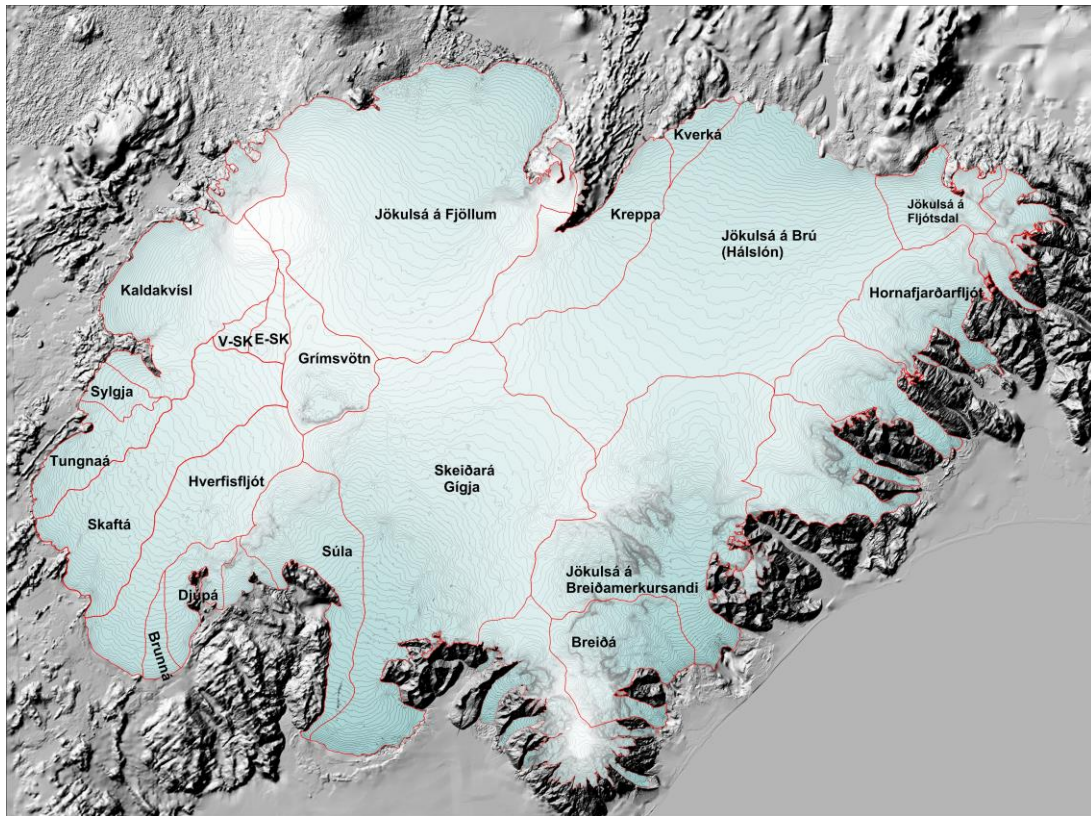


Figure 22. Water divides and drainage basins of selected rivers draining water from Vatnajökull, Súla is since summer 2016 diverted to Gígja.

5. Melt water runoff.

Water divides and drainage basins for rivers draining water from Vatnajökull have been defined from water pressure potential maps. The potential maps were produced from surface (year 2010) and bedrock DEMs.

Figure 22. shows the water divides and drainage areas for selected rivers draining melt water from Vatnajökull. The summer balance over the water basin is an estimate of meltwater contribution to rivers and groundwater storage. This estimate, however, does not include precipitation that falls as rain on the glacier, or snow that falls and melts during the summer. The meltwater contribution can be compared with river runoff at stream flow gauges closest to the glacier. For this comparison, we define the glaciological year from the start of October to the end of September and the period draining meltwater from the

glacier during the summer from June through September. It would be misleading to include May in the summer period because runoff from the glacier melt in May is delayed due

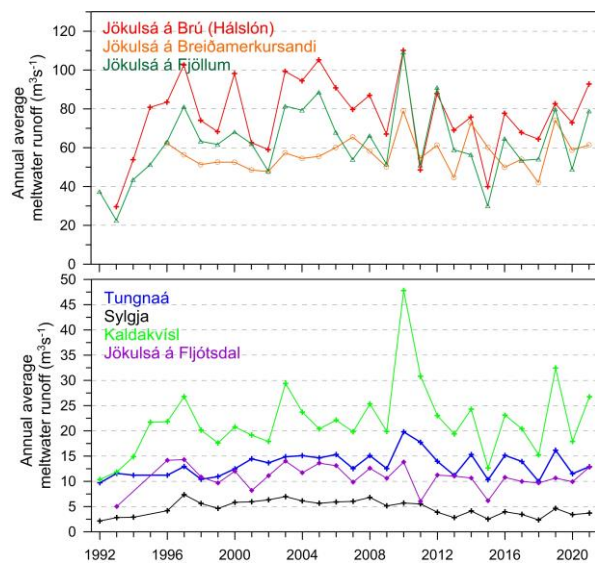


Figure 23. The temporal variation of average annual meltwater runoff to selected river catchments.

Table I. Melt water drainage to selected rivers in summer 2021.

Water Catchment:	Area (km ²)	ΣQ_s (10 ⁶ m ³)	Q_s (m ³ s ⁻¹)	Q_a (m ³ s ⁻¹)	q_s (ls ⁻¹ km ⁻²)
Vatnajökull	7771	20083	1905,3	636,8	82,0
Tungnaá	110	407	38,6	12,9	117,5
Sylgja	39	117	11,1	3,7	95,5
Kaldakvísl	344	844	80,1	26,8	77,8
Jökulsá á Fjöllum	1133	2488	236,0	78,9	69,6
Kreppa	289	578	54,8	18,3	63,5
Kverka	37	195	18,5	6,2	167,8
Háslón	1196	2926	277,6	92,8	77,6
Jökulsá á Fljótssdal	125	404	38,4	12,8	102,8
Jökulsá í Lóni	98	326	30,9	10,3	106,0
Hornafjarðarfjót	233	700	66,4	22,2	95,2
Jökulsá á Breiðamerkursandi	727	1936	183,6	61,4	84,4
Breiðá-Fjallsá	229	997	94,6	31,6	138,0
Skeiðará-Gígja	1394	3517	333,7	111,5	80,0
Brunná	32	160	15,2	5,1	159,6
Djúpá	74	270	25,6	8,6	115,6
Hverfisfjót	310	721	68,4	22,9	73,9
Skaftá	384	1023	97,1	32,4	84,4
Grímsvötn	173	106	10,0	3,4	19,4
Eystri Skaftárketill	39	35	3,3	1,1	28,1
Vestari Skaftárketill	25	22	2,0	0,7	27,3
Hólmsá	161	506	48,0	16,0	99,8
Heinabergsvötn	224	727	69,0	23,1	103,0
Skjálfafljót	107	186	17,6	5,9	54,9

ΣQ_s : total summer melt water; Q_s : average runoff (averaged over summer, 4 months, June – September)

Q_a : average runoff (averaged over a whole year); q_s : average runoff per km² (averaged over a whole year)

to refreezing during elimination of the cold wave and because of the contribution of the spring snow melt from the highlands to the runoff. Some melting also occurs during winter, especially in the terminus regions of the southern outlets.

Average melt water runoff to different rivers is given in Table I, and temporal variation of the average meltwater runoff in Fig. 24. The average specific runoff (q_s) differs from basin to basin from ~20 to ~170 ls⁻¹km⁻². This is mainly due to different elevation distributions, for example, the water drainage basins for Tungnaá and Kverká are within the ablation area, while that of Grímsvötn and Skaftárkatlar are high in the accumulation zone.

Runoff as function of elevation, estimated from summer balance, is tabulated for individual water catchments in Appendix E.

6. Conclusions

In the glaciological year 2020_21 the winter balance for Vatnajökull was 90% of the average, over the observation period from 1991_92.

The total summer mass loss was 17% more than average since 1995 (26% more than average since 1991_92).

The net balance was negative as it has been since 1994_95 (except 2014_15), and mass loss 2.6-fold the average since 1994_95 (1.9-fold the average since 1991_92).

Since 2010, after the 15-year period of high mass loss, the summer and net balance have been highly variable, even one year with positive mass balance in 2014_15 and close to zero in 2010_11, 2016_17 and 2017_18. In contrast 2018_19 and 2020_21 are both among years with highest surface mass loss of the survey period.

The total mass loss due to surface mass balance over the 30-year survey period is ice volume of $\sim 120 \text{ km}^3$, (average thinning of $\sim 15 \text{ m}$) since 1991_92. This volume loss since 1991_92 amounts to $\sim 4\%$ of total ice volume.

In addition to surface melt, mass is lost due to calving, geothermal melting at the glacier bed and melt from frictional energy due to ice deformation and sliding. This is estimated to be close to $0.2 \text{ m}_{\text{we}} \text{ a}^{-1}$ for Vatnajökull and amounts to $\sim 55 \text{ km}^3$ of ice in the survey period, leading to an estimation of the (Jóhannesson, T., Pálmason, B., Hjartarson,

Á., Jarosch, A., Magnússon, E., Belart, J., et al. (2020). Non-surface mass balance of glaciers in Iceland. *J. Glaciol.* 66, 685–697. doi:10.1017/jog.2020.37).

Glacier surface meltwater runoff in summer 2021 (estimated from summer surface balance only, summer rain and snow that falls and melts during summer, calving and geothermal and internal melting, is not included):

to Tungnaá 97% of the average, 123% of the average to Kaldakvísl, 127% of the average to Jökulsá á Fjöllum, 121% of the average to Háslón, 118% to Jökulsá í Fljótssdal and 108% to Jökulsá á Breiðamerkursandi.

(Averages refer to the survey period of each outlet.)

Surface velocity measurements suggest that Dyngjujökull is in the first phase of a surge and may complete a surge cycle within the next few years.

Surface mass balance summary 2020_21:

$$B_w = 11.34 \text{ km}^3_{\text{we}}$$

$$B_s = -20.08 \text{ km}^3_{\text{we}}$$

$$B_n = -8.74 \text{ km}^3_{\text{we}}$$

$$\text{AAR} = 49\%$$

Specific Values:

$$b_w = 1.46 \text{ m}_{\text{we}}$$

$$b_s = -2.59 \text{ m}_{\text{we}}$$

$$b_n = -1.13 \text{ m}_{\text{we}}$$

Appendix A: Surface mass balance at measurement sites 2020_21.

b_w: specific winter balance, **b_s**: specific summer balance, **b_n**: specific net balance, **l_a**: new snow in autumn (all in water equivalent).

Site	Position		Elevation (m a.s.l.)	Date in spring	Date in autumn	b_w (m)	b_s (m)	b_n (m)	l_a (m)
	Latitude	Longitude							
B09-21	64 44,6442	16 6,1145	727,4	20210502	2022016	0,06	-6,009	-5,949	0,05
B10-21	64 43,6833	16 6,7041	769,7	20210502	2022016	0,18	-6,026	-5,850	0,11
B11-21	64 40,9446	16 10,4751	948,9	20210502	2022016	1,13	-4,092	-2,961	0,19
B12-21	64 38,2660	16 14,1387	1078,8	20210502	2022016	1,29	-3,613	-2,322	0,21
B13-21	64 34,5751	16 19,6557	1222,2	20210502	2022015	1,61	-2,182	-0,572	0,22
B14-21	64 31,6465	16 24,7110	1322,8	20210501	2022015	1,66	-1,707	-0,052	0,18
B15-21	64 28,4936	16 30,0214	1405,3	20210501	2022015	1,87	-1,530	0,342	0,28
B16-21	64 24,1215	16 40,8974	1529,4	20210503	2022015	1,73	-1,034	0,699	0,25
B17-21	64 36,7339	16 28,7920	1218,2	20210501	2022016	1,35	-2,474	-1,125	0,25
Br1-21	64 5,9604	16 19,8222	101,9	20210507	2022015	-2,12	-9,440	-11,560	0
Br2-21	64 6,3585	16 22,5294	173,9	20210507	2021000	-1,23			
Br3-21	64 8,4339	16 24,0011	364,0	20210413	2021000	0,15			
Br5-21	64 13,5311	16 19,1855	671,4	20210501	2021000	0,50			
Br7-21	64 22,1325	16 16,9430	1246,4	20210501	2022015	2,00	-1,346	0,654	0,26
B07-21	64 25,7967	16 17,4775	1359,1	20210501	2022015	1,93	-1,311	0,618	0,21
BB0-21	64 22,7085	16 5,0539	1519,0	20210501	2022015	2,58	-0,332	2,244	0,21
Bru-21	64 39,7497	15 56,5444	894,7	20210501	2022015	0,92	-5,075	-4,158	0,12
Bud-21	64 35,9907	15 59,8802	1138,5	20210501	2022015	1,53	-2,861	-1,332	0,22
B18-21	64 31,5636	16 0,1214	1317,0	20210501	2022015	2,19	-1,753	0,440	0,2
B19-21	64 27,9908	15 55,9840	1439,7	20210501	2022015	2,51	-1,050	1,458	0,19
D05-21	64 42,2229	16 54,6816	1206,4	20210505	2022016	1,32	-3,265	-1,944	0,23
D07-21	64 38,2824	16 59,2486	1379,0	20210505	2022016	1,38	-1,867	-0,488	0,28
D09-21	64 31,7830	17 0,5908	1588,5	20210505	2022016	1,81	-1,104	0,702	0,33
D12-21	64 28,9716	17 0,1780	1650,6	20210505	2022016	2,11	-0,860	1,254	0,36
E01-21	64 40,6348	15 34,8580	760,2	20210502	2022015	0,65	-6,104	-5,454	0,01
E02-21	64 39,1241	15 35,9960	951,8	20210502	2022015	1,45	-4,667	-3,213	0,16
E03-21	64 36,6547	15 36,9094	1189,7	20210502	2022015	2,14	-2,382	-0,240	0,22
E04-21	64 34,9511	15 37,1435	1289,5	20210502	2022015	2,38	-1,630	0,750	0,16
K01-21	64 35,1745	17 51,8584	1042,8	20210505	2022017	0,58	-4,983	-4,401	0,05
K02-21	64 34,8090	17 49,6892	1170,1	20210505	2022017	0,73	-3,966	-3,240	0,11
K03-21	64 34,2376	17 46,4005	1293,5	20210505	2022017	1,00	-3,596	-2,601	0,14
K04-21	64 33,2090	17 42,2569	1487,3	20210504	2022017	1,30	-2,525	-1,222	0,2
K05-21	64 33,4360	17 35,4523	1679,8	20210505	2022017	1,84	-0,767	1,068	0,33
K06-21	64 38,3565	17 31,3201	1946,5	20210505	2022016	1,92			
K07-21	64 29,1058	17 42,0362	1532,4	20210504	2022017	1,32	-1,300	0,018	0,19
S01-21	64 7,0162	17 49,9749	709,7	20210504	2022127	0,43	-5,454	-5,022	0,05
S02-21	64 12,1590	17 48,9786	1002	20210504	2022127	0,91	-3,776	-2,871	0,18
S04-21	64 16,1767	17 48,1969	1158	20210504	2022020	1,48	-2,508	-1,026	0,06
S05-21	64 20,5113	17 33,9975	1451	20210504	2022017	1,73	-1,020	0,714	0,09
Haab-21	64 20,9565	17 24,1169	1731	20210503	2022016	1,95	-0,706	1,242	0,42

T01-21	64	19,0530	18	7,1750	730,4	20210504	2022127	0,18	-6,628	-6,453	5,25
T02-21	64	19,4790	18	4,5338	889,9	20210504	2022127	0,35	-4,693	-4,347	0,07
T03-21	64	20,2007	17	58,5813	1067,2	20210504	2022017	0,92	-3,302	-2,385	0,01
T04-21	64	21,3279	17	51,5139	1221,3	20210504	2022017	1,24	-2,328	-1,089	0,07
T05-21	64	22,2728	17	42,9967	1346,8	20210504	2022017	1,52	-1,524	-0,006	0,11
T06-21	64	24,2632	17	36,5068	1468,9	20210504	2022017	1,61	-1,226	0,384	0,21
T07-21	64	25,2904	17	31,2135	1564,2	20210504	2022017	1,72	-0,832	0,888	0,29
T08-21	64	26,2987	17	27,7525	1637,5	20210504	2022017	1,80	-1,047	0,756	0,4
Bor-21	64	24,9370	17	20,1469	1459,2	20210503	2022018	1,86	-1,669	0,186	0,27
Borth-21	64	25,0062	17	19,1939	1460,2	20210505	2022018	1,55	-1,257	0,294	0,27
G02-21	64	26,8571	17	17,7174	1568,1	20210505	2022016	1,81	-0,890	0,924	0,27
G03-21	64	28,4373	17	16,3313	1661,0	20210505	2022016	1,57	-0,929	0,642	0,28
G04-21	64	30,0201	17	15,0303	1690,1	20210505	2022016	1,73	-0,798	0,936	0,39
Go1-21	64	33,9686	17	24,9405	1761,3	20210505	2022016	1,76	-0,869	0,894	0,28
Barc-21	64	38,4148	17	26,7664	1900,2	20210608	2021000	2,36			
Skf00-21	64	15,4512	15	54,0652	951,8	20210501	2022015	2,11	-3,930	-1,818	0,05
Hof01-21	64	32,3386	15	35,8337	1142,7	20210502	2022015	2,00	-2,412	-0,416	0,08
Skf01-21	64	18,0179	16	5,0076	1284,6	20210501	2022015	2,44	-1,570	0,870	0,18
FI01-21	64	26,1537	15	55,6294	1347,5	20210501	2022015	2,27	-1,208	1,062	0,18
Ske02-21	64	15,9061	17	0,0660	1180,5	20210503	2022016	1,59	-1,89	-0,299	0,04
Ske03-21	64	18,0584	16	56,1545	1301,1	20210503	2022016	1,75	-1,248	0,498	0,14
Ske04-21	64	20,1345	16	51,8189	1400,4	20210503	2022016	1,56	-1,041	0,516	0,14
Ske05-21	64	22,2313	16	47,2341	1474,3	20210503	2022016	1,64	-0,992	0,648	0,16
oer01-21	63	59,8561	16	38,9983	1828,0	20210603	2021000	5,97			
E08-21	64	39,7173	15	23,8493	953	20210506	2022015	1,66	-4,837	-3,177	0,1
E07-21	64	38,4083	15	24,6746	1073	20210506	2022015	2,145	-4,359	-2,214	0,165
E07-20	64	38,4052	15	24,6752	1074	20200429	20201013	1,860	-2,724	-0,864	0,053

Appendix B: Surface mass balance distribution by elevation in 2020_21.

ΔS : area in elevation range, $\Sigma\Delta S$: cumulative area above given elevation, b_w : specific winter balance, b_s : specific summer balance. b_n : specific winter balance, ΔB_w : winter balance at a given elevation range, $\Sigma\Delta B_w$: cumulative winter balance above given elevation, ΔB_s summer balance at a given elevation range, $\Sigma\Delta B_s$: cumulative summer balance above given elevation, ΔB_n : net annual balance in a given elevation range, ΣB_n : cumulative net annual balance above given elevation.

Vatnajökull

Elevation			ΔS	$\Sigma\Delta S$	b_w	b_s	b_n	ΔB_w	$\Sigma\Delta B_w$	ΔB_s	$\Sigma\Delta B_s$	ΔB_n	ΣB_n
(m a.s.l.)			(km^2)	(km^2)	(mm)	(mm)	(mm)	(10^6m^3)	(10^6m^3)	(10^6m^3)	(10^6m^3)	(10^6m^3)	(10^6m^3)
2000	2050	2025	0,4	0,4	5537	-207	5329	2	2	0	0	1,9	2
1950	2000	1975	7,1	7,5	2750	-498	2251	19,4	21,4	-3,5	-3,6	15,9	17,8
1900	1950	1925	41,5	49,0	2232	-527	1705	92,6	114,1	-21,9	-25,5	70,8	88,6
1850	1900	1875	44	93,0	2577	-546	2031	113,4	227,4	-24	-49,5	89,3	177,9
1800	1850	1825	45,6	138,6	2825	-578	2246	128,9	356,3	-26,4	-75,9	102,5	280,4
1750	1800	1775	54,6	193,2	2349	-688	1660	128,3	484,6	-37,6	-113,5	90,7	371,1
1700	1750	1725	114	306,8	2016	-789	1226	229	713,6	-89,7	-203,2	139,3	510,4
1650	1700	1675	217	523,5	1949	-864	1085	422,4	1135,9	-187,2	-390,4	235,1	745,5
1600	1650	1625	372	895,2	1979	-911	1067	735,6	1871,5	-338,8	-729,2	396,8	1142,3
1550	1600	1575	358	1253,3	1891	-998	892	677,4	2549	-357,7	-1086,9	319,7	1462,1
1500	1550	1525	423	1676,1	1786	-1099	686	755,2	3304,2	-464,9	-1551,8	290,3	1752,4
1450	1500	1475	454	2130,2	1783	-1187	596	810,1	4114,3	-539,2	-2091	270,9	2023,3
1400	1450	1425	506	2636,2	1846	-1289	556	934,1	5048,5	-652,4	-2743,4	281,7	2305,1
1350	1400	1375	547	3183,0	1861	-1416	445	1018	6066,3	-774,5	-3517,9	243,4	2548,4
1300	1350	1325	539	3722,2	1815	-1580	235	979,1	7045,4	-852,3	-4370,2	126,8	2675,2
1250	1300	1275	506	4228,2	1774	-1854	-79	897,9	7943,3	-938,3	-5308,5	-40,4	2634,8
1200	1250	1225	447	4675,5	1643	-2206	-562	735,2	8678,5	-986,8	-6295,3	-251,6	2383,2
1150	1200	1175	397	5072,0	1517	-2604	-1087	601,9	9280,4	-1033	-7328,3	-431,1	1952,1
1100	1150	1125	353	5424,8	1391	-2966	-1575	490,8	9771,2	-1047	-8374,9	-555,9	1396,3
1050	1100	1075	311	5735,3	1257	-3310	-2052	390,6	10162	-1028	-9402,8	-637,3	759
1000	1050	1025	290	6025,2	1134	-3652	-2517	328,9	10491	-1059	-10462	-730	29,1
950	1000	975	259	6284,6	1047	-3992	-2945	271,7	10762	-1036	-11497	-764	-734,9
900	950	925	224	6509,0	937	-4305	-3367	210,5	10973	-966,3	-12464	-755,8	-1491
850	900	875	195	6704,3	812	-4663	-3850	158,7	11132	-910,8	-13375	-752,1	-2243
800	850	825	179	6883,4	690	-5018	-4327	123,8	11255	-899	-14273	-775,2	-3018
750	800	775	158	7041,6	579	-5325	-4746	91,7	11347	-842,5	-15116	-750,8	-3769
700	750	725	129	7170,4	483	-5542	-5059	62,2	11409	-713,8	-15830	-651,6	-4421
650	700	675	109	7278,9	427	-5661	-5233	46,4	11456	-614,3	-16444	-567,9	-4988
600	650	625	66,6	7345,5	420	-5782	-5361	28	11484	-385,3	-16829	-357,2	-5346
550	600	575	61,5	7407,0	401	-6066	-5664	24,7	11508	-373	-17202	-348,2	-5694
500	550	525	49,6	7456,6	351	-6344	-5993	17,5	11526	-314,8	-17517	-297,3	-5991
450	500	475	37,1	7493,7	261	-6710	-6448	9,7	11536	-249,2	-17766	-239,5	-6231
400	450	425	41,1	7534,8	159	-7092	-6932	6,6	11542	-291,4	-18058	-284,8	-6516
350	400	375	38,5	7573,3	24	-7461	-7437	0,9	11543	-287,5	-18345	-286,6	-6802
300	350	325	34,5	7607,8	-123	-7804	-7928	-4,3	11539	-269,5	-18615	-273,8	-7076
250	300	275	32,9	7640,7	-377	-8238	-8615	-12,4	11526	-270,8	-18885	-283,2	-7359
200	250	225	31,1	7671,8	-778	-8636	-9414	-24,2	11502	-268,8	-19154	-293	-7652
150	200	175	31	7702,8	-1205	-9021	-10226	-37,3	11465	-279,5	-19434	-316,8	-7969
100	150	125	27,3	7730,1	-1562	-9368	-10931	-42,7	11422	-256	-19690	-298,7	-8268
50	100	75	20,5	7750,6	-1813	-9612	-11425	-37,2	11385	-197,1	-19887	-234,3	-8502
0	50	25	19,9	7770,5	-1987	-9879	-11867	-39,5	11345	-196,2	-20083	-235,7	-8738

Tungnaárjökull

Elevation (m a.s.l.)			ΔS (km ²)	$\Sigma \Delta S$ (km ²)	b_w (mm)	b_s (mm)	b_n (mm)	ΔB_w (10 ⁶ m ³)	$\Sigma \Delta B_w$ (10 ⁶ m ³)	ΔB_s (10 ⁶ m ³)	$\Sigma \Delta B_s$ (10 ⁶ m ³)	ΔB_n (10 ⁶ m ³)	ΣB_n (10 ⁶ m ³)
1650	1700	1675	1,7	1,7	1776	-988	787	2,9	2,9	-1,6	-1,6	1,3	1,3
1600	1650	1625	12,2	13,9	1756	-939	816	21,4	24,3	-11,4	-13,1	9,9	11,2
1550	1600	1575	16,4	30,3	1688	-862	826	27,6	51,9	-14,1	-27,2	13,5	24,8
1500	1550	1525	15,9	46,2	1618	-916	702	25,7	77,7	-14,6	-41,7	11,2	35,9
1450	1500	1475	18,4	64,6	1557	-1130	427	28,6	106,3	-20,8	-62,5	7,9	43,8
1400	1450	1425	23,2	87,8	1537	-1319	218	35,6	141,9	-30,6	-93,1	5,1	48,9
1350	1400	1375	21,2	109,0	1489	-1438	50	31,6	173,5	-30,5	-123,6	1,1	49,9
1300	1350	1325	27,2	136,2	1404	-1656	-251	38,2	211,7	-45	-168,6	-6,8	43,1
1250	1300	1275	20,7	156,9	1338	-1945	-606	27,7	239,4	-40,2	-208,8	-12,5	30,5
1200	1250	1225	22,6	179,5	1250	-2319	-1068	28,2	267,6	-52,3	-261,1	-24,1	6,4
1150	1200	1175	20,8	200,3	1147	-2641	-1493	23,9	291,5	-55,1	-316,2	-31,1	-24,7
1100	1150	1125	18	218,3	1016	-2949	-1932	18,3	309,7	-53	-369,1	-34,7	-59,4
1050	1100	1075	17,3	235,6	893	-3327	-2433	15,4	325,2	-57,5	-426,6	-42,1	-101,5
1000	1050	1025	16,7	252,3	754	-3757	-3002	12,6	337,8	-62,8	-489,5	-50,2	-151,7
950	1000	975	16,1	268,4	592	-4147	-3555	9,5	347,3	-66,9	-556,3	-57,3	-209
900	950	925	16,3	284,7	456	-4574	-4118	7,5	354,8	-74,7	-631	-67,3	-276,2
850	900	875	12,5	297,2	358	-5109	-4751	4,5	359,3	-63,8	-694,8	-59,3	-335,5
800	850	825	12,9	310,1	295	-5635	-5340	3,8	363,1	-72,9	-767,7	-69,1	-404,6
750	800	775	10,5	320,6	233	-6301	-6067	2,4	365,5	-65,9	-833,6	-63,5	-468,1
700	750	725	7,2	327,8	194	-6797	-6603	1,4	366,9	-48,9	-882,5	-47,5	-515,6
650	700	675	2,4	330,2	185	-7036	-6851	0,4	367,4	-16,8	-899,3	-16,4	-532

Sylgjujökull

Elevation (m a.s.l.)			ΔS (km ²)	$\Sigma \Delta S$ (km ²)	b_w (mm)	b_s (mm)	b_n (mm)	ΔB_w (10 ⁶ m ³)	$\Sigma \Delta B_w$ (10 ⁶ m ³)	ΔB_s (10 ⁶ m ³)	$\Sigma \Delta B_s$ (10 ⁶ m ³)	ΔB_n (10 ⁶ m ³)	ΣB_n (10 ⁶ m ³)
1600	1650	1625	1,4	1,4	1688	-860	827	2,3	2,3	-1,2	-1,2	1,1	1,1
1550	1600	1575	5	6,4	1623	-892	730	8,1	10,4	-4,5	-5,7	3,7	4,8
1500	1550	1525	18,7	25,1	1413	-1065	348	26,4	36,9	-19,9	-25,6	6,5	11,3
1450	1500	1475	13,7	38,8	1320	-1206	114	18,1	54,9	-16,5	-42,1	1,6	12,9
1400	1450	1425	8,2	47,0	1316	-1290	25	10,8	65,8	-10,6	-52,7	0,2	13,1
1350	1400	1375	5,6	52,6	1303	-1373	-69	7,3	73,1	-7,7	-60,4	-0,4	12,7
1300	1350	1325	5,2	57,8	1253	-1645	-392	6,5	79,6	-8,5	-68,9	-2	10,7
1250	1300	1275	9,8	67,6	1184	-1967	-782	11,5	91,1	-19,2	-88,1	-7,6	3
1200	1250	1225	11,6	79,2	1104	-2352	-1247	12,9	104	-27,4	-115,5	-14,5	-11,5
1150	1200	1175	13,1	92,3	1012	-2648	-1635	13,3	117,3	-34,7	-150,2	-21,4	-32,9
1100	1150	1125	12,3	104,6	903	-2962	-2058	11,1	128,3	-36,3	-186,5	-25,3	-58,2
1050	1100	1075	11,4	116,0	802	-3423	-2620	9,1	137,5	-39	-225,5	-29,9	-88,1
1000	1050	1025	11,2	127,2	685	-4014	-3329	7,7	145,2	-45	-270,5	-37,3	-125,3
950	1000	975	3,6	130,8	614	-4217	-3602	2,2	147,4	-15,1	-285,6	-12,9	-138,2
900	950	925	1,5	132,3	563	-4372	-3809	0,9	148,2	-6,7	-292,3	-5,8	-144,1
850	900	875	0	132,3	527	-4500	-3973	0	148,3	-0,2	-292,5	-0,2	-144,2

Köldukvísarljökul

Elevation (m a.s.l.)			ΔS (km ²)	$\Sigma \Delta S$ (km ²)	b_w (mm)	b_s (mm)	b_n (mm)	ΔB_w (10 ⁶ m ³)	$\Sigma \Delta B_w$ (10 ⁶ m ³)	ΔB_s (10 ⁶ m ³)	$\Sigma \Delta B_s$ (10 ⁶ m ³)	ΔB_n (10 ⁶ m ³)	ΣB_n (10 ⁶ m ³)
1950	2000	1975	0,7	0,7	1895	-525	1369	1,3	1,3	-0,3	-0,3	0,9	0,9
1900	1950	1925	13,8	14,5	1908	-525	1383	26,4	27,7	-7,3	-7,6	19,1	20
1850	1900	1875	6,5	21,0	1828	-565	1262	11,9	39,6	-3,7	-11,3	8,2	28,3
1800	1850	1825	6,1	27,1	1789	-623	1166	10,9	50,5	-3,8	-15,1	7,1	35,4
1750	1800	1775	10,1	37,2	1752	-678	1074	17,6	68,1	-6,8	-21,9	10,8	46,2
1700	1750	1725	17,2	54,4	1751	-718	1032	30,1	98,2	-12,4	-34,3	17,8	63,9
1650	1700	1675	16	70,4	1767	-829	937	28,3	126,5	-13,3	-47,6	15	78,9
1600	1650	1625	14,2	84,6	1681	-1067	613	23,9	150,4	-15,2	-62,7	8,7	87,7
1550	1600	1575	18,6	103,2	1557	-1463	93	29	179,4	-27,2	-90	1,7	89,4
1500	1550	1525	20	123,2	1369	-1837	-468	27,3	206,7	-36,7	-126,6	-9,3	80
1450	1500	1475	19,3	142,5	1287	-2228	-940	24,8	231,5	-43	-169,6	-18,1	61,9
1400	1450	1425	15	157,5	1234	-2753	-1518	18,5	250	-41,2	-210,8	-22,7	39,2
1350	1400	1375	14,8	172,3	1158	-3154	-1996	17,2	267,1	-46,7	-257,5	-29,6	9,6
1300	1350	1325	17,1	189,4	1053	-3418	-2364	18,1	285,2	-58,6	-316,1	-40,5	-30,9
1250	1300	1275	17,9	207,3	938	-3631	-2692	16,8	302	-65	-381,1	-48,2	-79,1
1200	1250	1225	16,9	224,2	838	-3785	-2946	14,2	316,2	-63,9	-445	-49,7	-128,8
1150	1200	1175	16,2	240,4	750	-3990	-3239	12,1	328,3	-64,5	-509,5	-52,4	-181,2
1100	1150	1125	14,3	254,7	676	-4317	-3640	9,7	338	-61,7	-571,2	-52,1	-233,3
1050	1100	1075	12,9	267,6	620	-4636	-4015	8	346	-59,6	-630,9	-51,6	-284,9
1000	1050	1025	10,3	277,9	579	-4896	-4316	6	351,9	-50,5	-681,3	-44,5	-329,4
950	1000	975	8,8	286,7	553	-5140	-4587	4,9	356,8	-45,4	-726,7	-40,5	-369,9
900	950	925	2,6	289,3	543	-5324	-4781	1,4	358,2	-13,8	-740,6	-12,4	-382,4

Dyngjujökull

Elevation (m a.s.l.)			ΔS (km ²)	$\Sigma \Delta S$ (km ²)	b_w (mm)	b_s (mm)	b_n (mm)	ΔB_w (10 ⁶ m ³)	$\Sigma \Delta B_w$ (10 ⁶ m ³)	ΔB_s (10 ⁶ m ³)	$\Sigma \Delta B_s$ (10 ⁶ m ³)	ΔB_n (10 ⁶ m ³)	ΣB_n (10 ⁶ m ³)
1950	2000	1975	2,4	2,4	1916	-572	1343	4,5	4,5	-1,4	-1,4	3,2	3,2
1900	1950	1925	17,7	20,1	2099	-533	1565	37,2	41,8	-9,5	-10,8	27,8	31
1850	1900	1875	21,7	41,8	2253	-586	1667	48,8	90,6	-12,7	-23,5	36,1	67,1
1800	1850	1825	13,2	55,0	2219	-674	1544	29,2	119,9	-8,9	-32,4	20,3	87,4
1750	1800	1775	15,5	70,5	2115	-750	1365	32,7	152,6	-11,6	-44	21,1	108,5
1700	1750	1725	32,4	102,9	2050	-809	1240	66,5	219,1	-26,3	-70,3	40,2	148,8
1650	1700	1675	73,9	176,8	1987	-860	1126	146,9	366	-63,6	-133,9	83,3	232,1
1600	1650	1625	120	297,1	2025	-953	1072	243,7	609,7	-114,6	-248,6	129	361,1
1550	1600	1575	96,1	393,2	1946	-1108	838	187	796,6	-106,5	-355	80,5	441,6
1500	1550	1525	87,5	480,7	1828	-1289	538	160	956,7	-112,9	-467,9	47,2	488,7
1450	1500	1475	73	553,7	1672	-1486	185	122,1	1078,8	-108,6	-576,5	13,6	502,3
1400	1450	1425	60,5	614,2	1509	-1653	-143	91,3	1170,1	-100	-676,5	-8,7	493,6
1350	1400	1375	48,1	662,3	1415	-1874	-458	68	1238,1	-90,1	-766,6	-22,1	471,6
1300	1350	1325	36,5	698,8	1376	-2159	-783	50,3	1288,4	-78,9	-845,5	-28,6	443
1250	1300	1275	39,6	738,4	1360	-2496	-1135	53,9	1342,3	-98,9	-944,4	-45	398
1200	1250	1225	44	782,4	1352	-2951	-1599	59,5	1401,9	-130	-1074,3	-70,4	327,5
1150	1200	1175	44,4	826,8	1299	-3525	-2226	57,7	1459,6	-156,6	-1230,9	-98,9	228,7
1100	1150	1125	42,3	869,1	1134	-4073	-2939	47,9	1507,5	-172,2	-1403	-124,2	104,5
1050	1100	1075	30,6	899,7	874	-4469	-3594	26,8	1534,3	-136,8	-1539,8	-110	-5,5
1000	1050	1025	30,9	930,6	666	-4818	-4151	20,6	1554,9	-148,8	-1688,6	-128,2	-133,8
950	1000	975	28,8	959,4	505	-5255	-4749	14,6	1569,4	-151,3	-1839,9	-136,8	-270,5
900	950	925	24,2	983,6	383	-5666	-5282	9,3	1578,7	-137,2	-1977,1	-127,9	-398,4
850	900	875	21	1004,6	288	-6013	-5724	6,1	1584,8	-126,5	-2103,6	-120,4	-518,8
800	850	825	18,7	1023,3	231	-6338	-6106	4,3	1589,1	-118,5	-2222,1	-114,2	-633
750	800	775	12,3	1035,6	194	-6684	-6490	2,4	1591,5	-82,1	-2304,2	-79,7	-712,7
700	750	725	3,7	1039,3	171	-6999	-6828	0,6	1592,1	-25,7	-2329,9	-25,1	-737,8

Brúarjökull

Elevation (m a.s.l.)			ΔS (km ²)	$\Sigma \Delta S$ (km ²)	b_w (mm)	b_s (mm)	b_n (mm)	ΔB_w (10 ⁶ m ³)	$\Sigma \Delta B_w$ (10 ⁶ m ³)	ΔB_s (10 ⁶ m ³)	$\Sigma \Delta B_s$ (10 ⁶ m ³)	ΔB_n (10 ⁶ m ³)	ΣB_n (10 ⁶ m ³)
1900	1950	1925	0	0,0	1786	-581	1204	0	0	0	0	0	0
1850	1900	1875	1,2	1,2	1883	-531	1351	2,2	2,3	-0,6	-0,6	1,6	1,6
1800	1850	1825	4,4	5,6	1999	-558	1441	8,8	11,1	-2,5	-3,1	6,4	8
1750	1800	1775	2,8	8,4	2021	-656	1364	5,8	16,9	-1,9	-5	3,9	11,9
1700	1750	1725	3,9	12,3	2012	-730	1281	7,8	24,7	-2,8	-7,8	5	16,9
1650	1700	1675	5,5	17,8	2010	-797	1213	11	35,7	-4,4	-12,2	6,6	23,5
1600	1650	1625	51	68,8	2013	-885	1128	102,8	138,5	-45,2	-57,4	57,6	81,1
1550	1600	1575	47,4	116,2	1948	-967	980	92,3	230,8	-45,8	-103,2	46,4	127,5
1500	1550	1525	73,6	189,8	1852	-1068	783	136,4	367,2	-78,7	-182	57,7	185,2
1450	1500	1475	80,3	270,1	1907	-1229	677	153,1	520,2	-98,7	-280,6	54,4	239,6
1400	1450	1425	114	384,0	2067	-1317	750	235,5	755,7	-150	-430,6	85,5	325,1
1350	1400	1375	159	542,6	2029	-1477	551	321,8	1077,5	-234,4	-665	87,4	412,5
1300	1350	1325	148	691,0	1919	-1661	258	284,9	1362,4	-246,5	-911,5	38,3	450,8
1250	1300	1275	139	830,1	1856	-1892	-35	258,1	1620,5	-263,1	-1174,7	-5	445,8
1200	1250	1225	117	947,4	1713	-2258	-544	201	1821,5	-264,9	-1439,6	-63,9	381,9
1150	1200	1175	100	1047,4	1554	-2722	-1168	155,5	1977	-272,3	-1711,9	-116,8	265,1
1100	1150	1125	80,4	1127,8	1419	-3174	-1754	114,2	2091,2	-255,4	-1967,3	-141,2	123,9
1050	1100	1075	65,6	1193,4	1309	-3550	-2241	85,9	2177,1	-233	-2200,2	-147	-23,1
1000	1050	1025	57,9	1251,3	1214	-3833	-2618	70,4	2247,5	-222	-2422,2	-151,6	-174,7
950	1000	975	52,6	1303,9	1112	-4165	-3052	58,5	2306	-219	-2641,2	-160,5	-335,2
900	950	925	44,2	1348,1	951	-4581	-3629	42	2348	-202,3	-2843,5	-160,3	-495,5
850	900	875	39,3	1387,4	741	-5019	-4277	29,2	2377,2	-197,3	-3040,8	-168,1	-663,6
800	850	825	35,5	1422,9	534	-5419	-4885	18,9	2396,1	-192,1	-3233	-173,2	-836,8
750	800	775	32,5	1455,4	318	-5807	-5488	10,3	2406,5	-188,5	-3421,5	-178,2	-1015
700	750	725	26	1481,4	166	-6130	-5963	4,3	2410,8	-159,1	-3580,6	-154,8	-1170
650	700	675	12,5	1493,9	89	-6340	-6251	1,1	2411,9	-79,3	-3659,9	-78,2	-1248
600	650	625	1,1	1495,0	20	-6513	-6493	0	2411,9	-7,4	-3667,3	-7,3	-1255

Eyjabakkajökull

Elevation (m a.s.l.)			ΔS (km ²)	$\Sigma \Delta S$ (km ²)	b_w (mm)	b_s (mm)	b_n (mm)	ΔB_w (10 ⁶ m ³)	$\Sigma \Delta B_w$ (10 ⁶ m ³)	ΔB_s (10 ⁶ m ³)	$\Sigma \Delta B_s$ (10 ⁶ m ³)	ΔB_n (10 ⁶ m ³)	ΣB_n (10 ⁶ m ³)
1550	1600	1575	0	0,0	2890	-998	1891	0,1	0,1	0	0	0	0
1500	1550	1525	0	0,0	2876	-1019	1857	0,3	0,4	-0,1	-0,1	0,2	0,3
1450	1500	1475	1,1	1,1	2733	-1035	1698	3,1	3,5	-1,2	-1,3	2	2,2
1400	1450	1425	2,1	3,2	2695	-1094	1601	5,6	9,1	-2,3	-3,6	3,3	5,5
1350	1400	1375	2,7	5,9	2638	-1219	1419	7,1	16,2	-3,3	-6,9	3,8	9,3
1300	1350	1325	4,5	10,4	2575	-1413	1161	11,6	27,8	-6,4	-13,3	5,3	14,6
1250	1300	1275	13,8	24,2	2348	-1794	553	32,3	60,2	-24,7	-38	7,6	22,2
1200	1250	1225	13,3	37,5	2157	-2337	-180	28,6	88,7	-31	-68,9	-2,4	19,8
1150	1200	1175	14,2	51,7	1990	-3041	-1051	28,3	117	-43,2	-112,2	-14,9	4,9
1100	1150	1125	11,7	63,4	1806	-3514	-1708	21	138,1	-40,9	-153,1	-19,9	-15
1050	1100	1075	10	73,4	1633	-3777	-2144	16,3	154,4	-37,7	-190,8	-21,4	-36,4
1000	1050	1025	9,3	82,7	1501	-4093	-2592	14	168,3	-38,1	-228,9	-24,1	-60,6
950	1000	975	7,5	90,2	1353	-4451	-3098	10,1	178,5	-33,4	-262,3	-23,2	-83,8
900	950	925	5	95,2	1174	-4796	-3622	5,9	184,4	-23,9	-286,2	-18,1	-101,9
850	900	875	3,8	99,0	1026	-5071	-4044	3,9	188,3	-19,4	-305,6	-15,5	-117,4
800	850	825	2,9	101,9	902	-5388	-4486	2,7	190,9	-15,8	-321,5	-13,2	-130,5
750	800	775	1,9	103,8	717	-5880	-5162	1,4	192,3	-11,4	-332,9	-10	-140,6
700	750	725	1,7	105,5	555	-6402	-5846	1	193,3	-11,2	-344,1	-10,2	-150,8
650	700	675	1	106,5	434	-6816	-6381	0,4	193,8	-7	-351,1	-6,6	-157,4

Hoffellsjökull

Elevation (m a.s.l.)			ΔS (km ²)	$\Sigma \Delta S$ (km ²)	b_w (mm)	b_s (mm)	b_n (mm)	ΔB_w (10 ⁶ m ³)	$\Sigma \Delta B_w$ (10 ⁶ m ³)	ΔB_s (10 ⁶ m ³)	$\Sigma \Delta B_s$ (10 ⁶ m ³)	ΔB_n (10 ⁶ m ³)	ΣB_n (10 ⁶ m ³)
1450	1500	1475	1,2	1,2	2793	-1018	1775	3,3	3,3	-1,2	-1,2	2,1	2,1
1400	1450	1425	7,3	8,5	2598	-1201	1397	19	22,3	-8,8	-10	10,2	12,3
1350	1400	1375	10,2	18,7	2562	-1317	1244	26,1	48,4	-13,4	-23,4	12,7	25
1300	1350	1325	16,4	35,1	2459	-1501	958	40,4	88,8	-24,6	-48,1	15,7	40,7
1250	1300	1275	34,9	70,0	2300	-1748	552	80,4	169,1	-61,1	-109,1	19,3	60
1200	1250	1225	25,6	95,6	2131	-2009	121	54,5	223,6	-51,4	-160,5	3,1	63,1
1150	1200	1175	17,9	113,5	1961	-2269	-307	35,1	258,8	-40,6	-201,1	-5,5	57,6
1100	1150	1125	16,7	130,2	1729	-2525	-796	28,9	287,6	-42,2	-243,3	-13,3	44,3
1050	1100	1075	12,5	142,7	1499	-2922	-1423	18,8	306,4	-36,6	-279,9	-17,8	26,5
1000	1050	1025	9,7	152,4	1368	-3327	-1958	13,2	319,6	-32,1	-312	-18,9	7,6
950	1000	975	8,6	161,0	1261	-3744	-2482	10,8	330,4	-32,1	-344,1	-21,3	-13,7
900	950	925	6,4	167,4	1142	-4167	-3025	7,3	337,7	-26,5	-370,6	-19,2	-32,9
850	900	875	4,2	171,6	1023	-4504	-3480	4,3	342	-19	-389,6	-14,7	-47,6
800	850	825	3,6	175,2	936	-4732	-3795	3,4	345,4	-17,3	-406,9	-13,9	-61,5
750	800	775	3,8	179,0	856	-4915	-4059	3,3	348,7	-18,7	-425,6	-15,4	-76,9
700	750	725	3,3	182,3	692	-5277	-4584	2,3	351	-17,5	-443,1	-15,2	-92,1
650	700	675	3,5	185,8	533	-5634	-5100	1,9	352,8	-19,6	-462,7	-17,8	-109,8
600	650	625	2,5	188,3	446	-5885	-5439	1,1	353,9	-14,8	-477,4	-13,7	-123,5
550	600	575	1,7	190,0	395	-6104	-5709	0,7	354,6	-10,1	-487,6	-9,5	-133
500	550	525	1,5	191,5	338	-6367	-6029	0,5	355,1	-9,4	-497	-8,9	-141,9
450	500	475	0,9	192,4	228	-6750	-6521	0,2	355,3	-6,1	-503,1	-5,9	-147,8
400	450	425	0,7	193,1	71	-7182	-7110	0	355,4	-5,4	-508,5	-5,3	-153,2
350	400	375	0,7	193,8	-141	-7660	-7801	0	355,3	-5,1	-513,7	-5,2	-158,4
300	350	325	0,5	194,3	-327	-8047	-8375	-0,2	355,1	-4,2	-517,8	-4,4	-162,7
250	300	275	0,7	195,0	-472	-8396	-8868	-0,3	354,7	-6,2	-524,1	-6,6	-169,3
200	250	225	1,5	196,5	-673	-8733	-9407	-1	353,7	-13,3	-537,3	-14,3	-183,6
150	200	175	2,3	198,8	-901	-9057	-9959	-2,1	351,6	-21,3	-558,6	-23,4	-207
100	150	125	2,5	201,3	-1160	-9331	-10492	-2,9	348,7	-23,5	-582,1	-26,4	-233,5
50	100	75	1,9	203,2	-1393	-9623	-11017	-2,7	346	-18,4	-600,5	-21	-254,5
0	50	25	2,2	205,4	-1657	-9903	-11561	-3,6	342,4	-21,8	-622,3	-25,4	-279,9

Breiðamerkurjökull

Elevation (m a.s.l.)			ΔS (km ²)	$\Sigma \Delta S$ (km ²)	b_w (mm)	b_s (mm)	b_n (mm)	ΔB_w (10 ⁶ m ³)	$\Sigma \Delta B_w$ (10 ⁶ m ³)	ΔB_s (10 ⁶ m ³)	$\Sigma \Delta B_s$ (10 ⁶ m ³)	ΔB_n (10 ⁶ m ³)	ΣB_n (10 ⁶ m ³)
1900	1950	1925	0	0,0	4889	-261	4628	0,2	0,2	0	0	0,2	0,2
1850	1900	1875	0,4	0,4	4522	-355	4167	1,7	2	-0,1	-0,1	1,6	1,8
1800	1850	1825	0,5	0,9	4225	-456	3768	1,9	3,9	-0,2	-0,4	1,7	3,5
1750	1800	1775	0,9	1,8	3788	-490	3298	3,4	7,3	-0,4	-0,8	2,9	6,5
1700	1750	1725	2,6	4,4	3041	-568	2473	8,1	15,3	-1,5	-2,3	6,6	13
1650	1700	1675	6,2	10,6	2526	-668	1858	15,6	30,9	-4,1	-6,4	11,4	24,5
1600	1650	1625	17,7	28,3	2145	-749	1395	37,9	68,8	-13,2	-19,7	24,7	49,2
1550	1600	1575	26,2	54,5	2021	-873	1147	53	121,8	-22,9	-42,6	30,1	79,3
1500	1550	1525	32	86,5	1980	-967	1013	63,4	185,2	-31	-73,5	32,4	111,7
1450	1500	1475	46,4	132,9	2024	-985	1038	94	279,2	-45,8	-119,3	48,2	159,9
1400	1450	1425	58	190,9	1986	-1067	919	115,3	394,5	-62	-181,3	53,4	213,3
1350	1400	1375	88,8	279,7	1994	-1158	836	177,2	571,7	-102,9	-284,1	74,3	287,5
1300	1350	1325	95,3	375,0	1951	-1232	719	186	757,7	-117,4	-401,6	68,6	356,1
1250	1300	1275	57,4	432,4	1900	-1368	531	109	866,7	-78,5	-480,1	30,5	386,6
1200	1250	1225	39,4	471,8	1841	-1575	266	72,7	939,4	-62,1	-542,3	10,5	397,1
1150	1200	1175	31,8	503,6	1752	-1853	-101	55,8	995,2	-59	-601,3	-3,2	393,9
1100	1150	1125	27	530,6	1650	-2183	-533	44,6	1039,8	-59	-660,3	-14,4	379,5
1050	1100	1075	23,8	554,4	1563	-2486	-922	37,2	1077	-59,1	-719,4	-21,9	357,6
1000	1050	1025	22,1	576,5	1495	-2738	-1242	33,1	1110,1	-60,6	-780	-27,5	330
950	1000	975	24,4	600,9	1429	-2972	-1543	34,8	1144,9	-72,5	-852,5	-37,6	292,4
900	950	925	26,6	627,5	1315	-3335	-2020	34,9	1179,9	-88,6	-941,1	-53,7	238,7
850	900	875	23,7	651,2	1165	-3865	-2699	27,6	1207,4	-91,4	-1032,6	-63,8	174,9
800	850	825	24,3	675,5	1056	-4246	-3190	25,6	1233,1	-103,1	-1135,7	-77,5	97,4
750	800	775	25,4	700,9	883	-4645	-3762	22,4	1255,5	-118	-1253,6	-95,5	1,9
700	750	725	20,3	721,2	673	-5004	-4331	13,7	1269,2	-101,4	-1355,1	-87,8	-85,9
650	700	675	30	751,2	502	-5403	-4900	15,1	1284,2	-162	-1517,1	-146,9	-232,8
600	650	625	25,9	777,1	440	-5689	-5249	11,4	1295,6	-147,4	-1664,5	-136	-368,8
550	600	575	26,8	803,9	429	-6048	-5619	11,5	1307,2	-162,2	-1826,7	-150,7	-519,6
500	550	525	18	821,9	378	-6342	-5963	6,8	1314	-113,8	-1940,6	-107	-626,6
450	500	475	13,1	835,0	291	-6782	-6491	3,8	1317,8	-88,8	-2029,4	-85	-711,6
400	450	425	16,6	851,6	212	-7160	-6947	3,5	1321,3	-118,7	-2148,1	-115,2	-826,8
350	400	375	12,8	864,4	115	-7539	-7423	1,5	1322,8	-96,4	-2244,4	-94,9	-921,7
300	350	325	10,6	875,0	0	-7859	-7860	0	1322,8	-83,6	-2328,1	-83,6	-1005
250	300	275	10,8	885,8	-274	-8199	-8474	-3	1319,8	-88,1	-2416,2	-91,1	-1096
200	250	225	9,4	895,2	-789	-8548	-9337	-7,4	1312,4	-80,1	-2496,3	-87,5	-1184
150	200	175	9,8	905,0	-1340	-8944	-10284	-13,1	1299,3	-87,5	-2583,8	-100,6	-1285
100	150	125	8,1	913,1	-1772	-9352	-11125	-14,3	1285	-75,4	-2659,2	-89,7	-1374
50	100	75	6,5	919,6	-2015	-9635	-11651	-13	1272	-62,2	-2721,3	-75,2	-1449
0	50	25	3	922,6	-2147	-9795	-11943	-6,5	1265,5	-29,8	-2751,1	-36,3	-1486

Síðujökull

Elevation (m a.s.l.)			ΔS (km ²)	$\Sigma \Delta S$ (km ²)	b_w (mm)	b_s (mm)	b_n (mm)	ΔB_w (10 ⁶ m ³)	$\Sigma \Delta B_w$ (10 ⁶ m ³)	ΔB_s (10 ⁶ m ³)	$\Sigma \Delta B_s$ (10 ⁶ m ³)	ΔB_n (10 ⁶ m ³)	ΣB_n (10 ⁶ m ³)
1700	1750	1725	0,9	0,9	1906	-746	1160	1,7	1,7	-0,7	-0,7	1	1
1650	1700	1675	5,9	6,8	1858	-886	972	11	12,7	-5,2	-5,9	5,7	6,8
1600	1650	1625	11,2	18,0	1828	-932	896	20,4	33,1	-10,4	-16,3	10	16,8
1550	1600	1575	11,5	29,5	1804	-873	931	20,7	53,9	-10	-26,4	10,7	27,5
1500	1550	1525	21,3	50,8	1785	-879	906	38,1	92	-18,8	-45,1	19,3	46,8
1450	1500	1475	38,2	89,0	1749	-963	785	66,8	158,8	-36,8	-81,9	30	76,9
1400	1450	1425	24,9	113,9	1715	-1156	559	42,7	201,5	-28,8	-110,7	13,9	90,8
1350	1400	1375	21,1	135,0	1683	-1370	313	35,6	237,1	-29	-139,7	6,6	97,4
1300	1350	1325	17,2	152,2	1621	-1588	33	28	265	-27,4	-167	0,6	98
1250	1300	1275	15,6	167,8	1571	-1850	-279	24,4	289,5	-28,8	-195,8	-4,3	93,6
1200	1250	1225	21,2	189,0	1520	-2074	-554	32,2	321,6	-43,9	-239,7	-11,7	81,9
1150	1200	1175	17,9	206,9	1436	-2396	-960	25,7	347,3	-42,9	-282,6	-17,2	64,7
1100	1150	1125	17	223,9	1284	-2782	-1497	21,8	369,1	-47,2	-329,7	-25,4	39,3
1050	1100	1075	15,4	239,3	1110	-3241	-2130	17,1	386,2	-50	-379,8	-32,9	6,4
1000	1050	1025	19,3	258,6	952	-3623	-2670	18,4	404,6	-70	-449,8	-51,6	-45,2
950	1000	975	19,8	278,4	818	-4020	-3202	16,2	420,8	-79,6	-529,4	-63,4	-108,6
900	950	925	20,3	298,7	713	-4357	-3644	14,5	435,3	-88,5	-617,9	-74	-182,6
850	900	875	19	317,7	637	-4652	-4014	12,1	447,4	-88,3	-706,2	-76,2	-258,7
800	850	825	18,8	336,5	580	-4921	-4341	10,9	458,4	-92,6	-798,8	-81,7	-340,4
750	800	775	21,4	357,9	526	-5171	-4645	11,3	469,6	-110,7	-909,5	-99,4	-439,8
700	750	725	21,5	379,4	457	-5397	-4939	9,8	479,5	-115,9	-1025,4	-106,1	-545,9
650	700	675	20,6	400,0	373	-5666	-5293	7,7	487,2	-117	-1142,4	-109,3	-655,2
600	650	625	9,7	409,7	309	-5870	-5561	3	490,2	-57,2	-1199,5	-54,2	-709,4
550	600	575	0,2	409,9	281	-5934	-5653	0	490,2	-1,1	-1200,6	-1	-710,4

Skaftárjökull

Elevation (m a.s.l.)			ΔS (km ²)	$\Sigma \Delta S$ (km ²)	b_w (mm)	b_s (mm)	b_n (mm)	ΔB_w (10 ⁶ m ³)	$\Sigma \Delta B_w$ (10 ⁶ m ³)	ΔB_s (10 ⁶ m ³)	$\Sigma \Delta B_s$ (10 ⁶ m ³)	ΔB_n (10 ⁶ m ³)	ΣB_n (10 ⁶ m ³)
1400	1450	1425	0	0,0	1643	-1354	289	0	0	0	0	0	0
1350	1400	1375	2,5	2,5	1611	-1446	164	4	4	-3,6	-3,6	0,4	0,4
1300	1350	1325	5,3	7,8	1561	-1640	-78	8,3	12,3	-8,7	-12,3	-0,4	0
1250	1300	1275	4	11,8	1499	-1915	-415	6	18,3	-7,7	-20	-1,7	-1,7
1200	1250	1225	6,4	18,2	1427	-2218	-791	9,1	27,4	-14,1	-34,1	-5	-6,7
1150	1200	1175	7,6	25,8	1335	-2526	-1190	10,1	37,5	-19,2	-53,3	-9	-15,8
1100	1150	1125	10,9	36,7	1198	-2849	-1650	13	50,6	-30,9	-84,2	-17,9	-33,7
1050	1100	1075	12,1	48,8	1042	-3230	-2187	12,6	63,2	-39,2	-123,4	-26,5	-60,2
1000	1050	1025	12,8	61,6	883	-3628	-2745	11,3	74,5	-46,4	-169,8	-35,1	-95,3
950	1000	975	8,7	70,3	722	-4051	-3329	6,3	80,8	-35,3	-205,1	-29	-124,3
900	950	925	5,6	75,9	602	-4398	-3796	3,4	84,2	-24,7	-229,8	-21,3	-145,6
850	900	875	4,9	80,8	508	-4714	-4206	2,5	86,7	-23	-252,8	-20,5	-166,1
800	850	825	4,9	85,7	443	-5038	-4594	2,2	88,8	-24,7	-277,5	-22,6	-188,7
750	800	775	4,5	90,2	400	-5290	-4890	1,8	90,6	-24	-301,5	-22,2	-210,9
700	750	725	4,1	94,3	357	-5559	-5202	1,5	92,1	-23	-324,5	-21,5	-232,4
650	700	675	2,9	97,2	324	-5826	-5502	0,9	93,1	-17	-341,4	-16	-248,4
600	650	625	0,5	97,7	305	-6017	-5711	0,1	93,2	-2,8	-344,2	-2,6	-251

Vestari Skaftárketill

Elevation (m a.s.l.)			ΔS (km ²)	$\Sigma \Delta S$ (km ²)	b_w (mm)	b_s (mm)	b_n (mm)	ΔB_w (10 ⁶ m ³)	$\Sigma \Delta B_w$ (10 ⁶ m ³)	ΔB_s (10 ⁶ m ³)	$\Sigma \Delta B_s$ (10 ⁶ m ³)	ΔB_n (10 ⁶ m ³)	ΣB_n (10 ⁶ m ³)
1900	1950	1925	0,6	0,6	1985	-528	1457	1,1	1,1	-0,3	-0,3	0,8	0,8
1850	1900	1875	0,6	1,2	1964	-554	1410	1,2	2,3	-0,3	-0,6	0,9	1,7
1800	1850	1825	0,8	2,0	1889	-623	1266	1,5	3,8	-0,5	-1,1	1	2,7
1750	1800	1775	2,6	4,6	1757	-748	1008	4,4	8,2	-1,9	-3	2,5	5,2
1700	1750	1725	5,5	10,1	1737	-771	966	9,4	17,6	-4,2	-7,2	5,2	10,4
1650	1700	1675	6,6	16,7	1761	-799	961	11,4	29	-5,2	-12,4	6,2	16,7
1600	1650	1625	7,6	24,3	1714	-857	857	12,3	41,3	-6,2	-18,5	6,2	22,8
1550	1600	1575	5,5	29,8	1633	-923	709	8,2	49,5	-4,6	-23,1	3,6	26,4
1500	1550	1525	1,5	31,3	1573	-961	611	4,2	53,7	-2,6	-25,7	1,6	28

Eystri Skaftárketill

Elevation (m a.s.l.)			ΔS (km ²)	$\Sigma \Delta S$ (km ²)	b_w (mm)	b_s (mm)	b_n (mm)	ΔB_w (10 ⁶ m ³)	$\Sigma \Delta B_w$ (10 ⁶ m ³)	ΔB_s (10 ⁶ m ³)	$\Sigma \Delta B_s$ (10 ⁶ m ³)	ΔB_n (10 ⁶ m ³)	ΣB_n (10 ⁶ m ³)
1750	1800	1775	1,1	1,1	1740	-807	933	1,9	1,9	-0,9	-0,9	1	1
1700	1750	1725	10,2	11,3	1734	-872	862	17	18,9	-8,6	-9,5	8,5	9,5
1650	1700	1675	16,5	27,8	1759	-911	847	27,2	46,1	-14,1	-23,5	13,1	22,6
1600	1650	1625	9,7	37,5	1749	-885	864	16,2	62,3	-8,2	-31,7	8	30,6
1550	1600	1575	2,4	39,9	1736	-869	866	7,4	69,7	-3,7	-35,4	3,7	34,3

Gjálp

Elevation (m a.s.l.)			ΔS (km ²)	$\Sigma \Delta S$ (km ²)	b_w (mm)	b_s (mm)	b_n (mm)	ΔB_w (10 ⁶ m ³)	$\Sigma \Delta B_w$ (10 ⁶ m ³)	ΔB_s (10 ⁶ m ³)	$\Sigma \Delta B_s$ (10 ⁶ m ³)	ΔB_n (10 ⁶ m ³)	ΣB_n (10 ⁶ m ³)
1900	1950	1925	0,4	0,4	2034	-521	1512	0,7	0,7	-0,2	-0,2	0,5	0,5
1850	1900	1875	0,7	1,1	2007	-571	1435	1,5	2,2	-0,4	-0,6	1,1	1,6
1800	1850	1825	1,1	2,2	1908	-687	1221	2,2	4,4	-0,8	-1,4	1,4	3
1750	1800	1775	4,9	7,1	1776	-829	946	9,8	14,2	-4,6	-6	5,2	8,2
1700	1750	1725	18,8	25,9	1722	-903	818	40,5	54,7	-21,2	-27,2	19,3	27,5
1650	1700	1675	13,5	39,4	1718	-934	784	13,9	68,6	-7,6	-34,8	6,4	33,8

Grímsvötn

Elevation (m a.s.l.)			ΔS (km ²)	$\Sigma \Delta S$ (km ²)	b_w (mm)	b_s (mm)	b_n (mm)	ΔB_w (10 ⁶ m ³)	$\Sigma \Delta B_w$ (10 ⁶ m ³)	ΔB_s (10 ⁶ m ³)	$\Sigma \Delta B_s$ (10 ⁶ m ³)	ΔB_n (10 ⁶ m ³)	ΣB_n (10 ⁶ m ³)
1700	1750	1725	1,4	1,4	1712	-910	801	2,3	2,3	-1,2	-1,2	1,1	1,1
1650	1700	1675	41	42,4	1746	-944	801	71,6	74	-38,7	-40	32,9	34
1600	1650	1625	30,9	73,3	1800	-1026	773	55,6	129,5	-31,7	-71,7	23,9	57,9
1550	1600	1575	20	93,3	1821	-1054	766	36,4	166	-21,1	-92,8	15,3	73,2
1500	1550	1525	16,8	110,1	1840	-1128	711	30,8	196,8	-18,9	-111,7	11,9	85,1
1450	1500	1475	9,7	119,8	1848	-1281	567	18	214,8	-12,5	-124,1	5,5	90,7
1400	1450	1425	13,8	133,6	1805	-1441	364	24,9	239,7	-19,9	-144,1	5	95,7
1350	1400	1375	1,5	135,1	1838	-1310	527	2,8	242,5	-2	-146	0,8	96,5

Appendix C: Coordinates of the velocity measurement stakes in 2021.

Position of the velocity measurement stakes determined by GPS sub-metre differential (I), fast static (FS) and kinematic (K). (Accuracy of horizontal position 0.5 – 1.0 m, and vertical accuracy 1-2 m for DGPS, about 1cm for fast static, and 3 cm for kinematic).

The station Hofn in Höfn í Hornafirði is used as a stationary reference for all measurements, ÍSN93 datum, h_1 is elevation above ellipsoid, dL antenna height, N estimated difference between ellipsoid and sea-level, H elevation in metres above sea level ($H = h_1 + N + dL$). X and Y are ÍSN93 Lambert conformal conic projected coordinates. M is a quality marker.

Site	Calender					Latitude	Longitude	h_1 (m a. e.)	dL (m)	N (m)	H (m a. s. l.)	X	Y	M		
	time	Date	#	Year	Day											
B07-21	16,216	1	5	121	2021	64	25,7967	16	17,4775	1426,1	0	-67,1	1359,1	630456,9	439245,3	K
B07-21	13,869	15	10	288	2021	64	25,7955	16	17,4765	1422	0	-67,1	1355	630457,8	439243,1	K
B09-21	16,675	2	5	122	2021	64	44,6442	16	6,11445	794,11	0	-66,7	727,43	637967	474631,6	K
B09-21	12,908	16	10	289	2021	64	44,6444	16	6,11565	787,37	0	-66,7	720,69	637966	474631,8	K
B10-20	16,055	2	5	122	2021	64	43,6837	16	6,6948	836,26	0	-66,7	769,55	637588,4	472827,7	K
B10-21	16,173	2	5	122	2021	64	43,6833	16	6,70414	836,39	0	-66,7	769,68	637581	472826,7	K
B10-21	12,453	16	10	289	2021	64	43,6828	16	6,70414	829,73	0	-66,7	763,02	637581	472825,8	K
B11-21	13,015	2	5	122	2021	64	40,9446	16	10,4751	1015,7	0	-66,8	948,86	634816,6	467607,9	K
B11-21	11,832	16	10	289	2021	64	40,9495	16	10,4708	1010,3	0	-66,8	943,52	634819,6	467617,2	K
B12-21	12,716	2	5	122	2021	64	38,266	16	14,1387	1145,7	0	-66,9	1078,8	632122,5	462507	K
B12-21	11,455	16	10	289	2021	64	38,2766	16	14,1289	1141,4	0	-66,9	1074,5	632129,4	462526,9	K
B13-21	11,451	2	5	122	2021	64	34,5751	16	19,6557	1289,2	0	-67	1222,2	628020,2	455466,5	K
B13-21	14,5	15	10	288	2021	64	34,5872	16	19,6412	1285,6	-0,91	-67	1217,7	628030,8	455489,4	K
B13ror15	17,99	1	5	121	2021	64	34,6264	16	19,6081	1287	0	-67	1220	628054,1	455563,3	K
B13ror15	13,893	16	10	289	2021	64	34,6382	16	19,5928	1282,4	3,85	-67	1219,3	628065,5	455585,7	K
B14-21	18,348	1	5	121	2021	64	31,6465	16	24,711	1389,9	0	-67,1	1322,8	624209	449861,8	K
B14-21	19,13	15	10	288	2021	64	31,6558	16	24,6948	1385,8	0	-67,1	1318,7	624221,3	449879,6	K
B15-21	17,204	1	5	121	2021	64	28,4936	16	30,0214	1472,5	0	-67,2	1405,3	620195,2	443837,4	K
B15-21	19,691	15	10	288	2021	64	28,4992	16	30,0085	1467,7	0	-67,2	1400,5	620205,2	443848,2	K
B16-21	12,421	3	5	123	2021	64	24,1215	16	40,8974	1596,7	0	-67,3	1529,4	611781	435387,3	K
B16-21	16,026	15	10	288	2021	64	24,1216	16	40,8966	1592,8	0	-67,3	1525,4	611781,6	435387,6	K
B17-21	19,775	1	5	121	2021	64	36,7339	16	28,792	1285,4	0	-67,1	1218,2	620569,9	459174,7	K
B17-21	10,894	16	10	289	2021	64	36,7443	16	28,7856	1281,3	0	-67,1	1214,1	620574,2	459194,3	K
B18-21	15,43	1	5	121	2021	64	31,5636	16	0,12141	1383,9	0	-66,9	1317	643870,7	450576,8	K
B18-21	11,994	15	10	288	2021	64	31,5694	16	0,12456	1379,4	0	-66,9	1312,5	643867,7	450587,6	K
B19-21	14,734	1	5	121	2021	64	27,9908	15	55,984	1506,6	0	-66,9	1439,7	647499,3	444105,2	K
B19-21	11,509	15	10	288	2021	64	27,9912	15	55,9843	1502,1	0	-66,9	1435,2	647499	444105,9	K
BB0-21	12,911	1	5	121	2021	64	22,7085	16	5,05385	1585,9	0	-66,9	1519	640687,1	433957	K
BB0-21	10,968	15	10	288	2021	64	22,7083	16	5,05447	1581,1	0	-66,9	1514,3	640686,6	433956,7	K
Bor-21	16,905	3	5	123	2021	64	24,937	17	20,1469	1526,9	0	-67,7	1459,2	580209,5	435908,4	K
Bor-21	17,927	18	10	291	2021	64	24,9277	17	20,1492	1536,1	0	-67,7	1468,4	580208	435891,1	K
Br1-21	13	13	4	103	2021	64	5,96039	16	19,8222	169,44	-1,6	-65,9	101,94	630131,9	402341,8	K
Br2-21	14,333	13	4	103	2021	64	6,35847	16	22,5294	241,49	-1,6	-66	173,85	627903,1	402988,7	K
Br3-21	15,167	13	4	103	2021	64	8,43391	16	24,0011	431,9	-1,6	-66,3	364,04	626549,8	406792,3	K
Br5-21	10,996	1	5	121	2021	64	13,5311	16	19,1855	737,94	0	-66,6	671,38	630052,6	416417,8	K
Br7-21	15,033	1	5	121	2021	64	22,1325	16	16,943	1313,4	0	-67	1246,4	631178,2	432461,8	K
Br7-21	13,449	15	10	288	2021	64	22,1046	16	16,9357	1307,5	0	-67	1240,5	631186,3	432410,2	K
Bru-21	16,559	1	5	121	2021	64	39,7497	15	56,5444	961,5	0	-66,8	894,71	645994,1	465905,9	K
Bru-21	17,3	15	10	288	2021	64	39,7577	15	56,5415	955,9	0	-66,8	889,11	645995,7	465920,7	K
Bud-21	16,126	1	5	121	2021	64	35,9907	15	59,8802	1205,4	0	-66,9	1138,5	643673	458802,2	K
Bud-21	17,747	15	10	288	2021	64	36,0016	15	59,8778	1200,6	0	-66,9	1133,8	643674	458822,5	K

D05-21	19,991	5	5	125	2021	64	42,2229	16	54,6816	1273,7	0	-67,4	1206,4	599597,4	468615,3	K
D05-21	14,423	16	10	289	2021	64	42,2346	16	54,6639	1268,9	0	-67,4	1201,5	599610,8	468637,4	K
D07-21	18,29	5	5	125	2021	64	38,2824	16	59,2486	1446,5	0	-67,5	1379	596202,1	461179,8	K
D07-21	12,547	16	10	289	2021	64	38,298	16	59,2331	1441,6	0	-67,5	1374,1	596213,5	461209,2	K
D09-21	17,167	5	5	125	2021	64	31,783	17	0,59083	1656,1	0	-67,6	1588,5	595513,2	449075,9	K
D09-21	11,594	16	10	289	2021	64	31,7866	17	0,59212	1652,6	0	-67,6	1585	595512	449082,7	K
D12-21	19,316	5	5	125	2021	64	28,9716	17	0,17804	1718,1	0	-67,6	1650,6	596008,3	443865,4	K
D12-21	10,968	16	10	289	2021	64	28,9719	17	0,17769	1714,6	0	-67,6	1647,1	596008,5	443866	K
E01-21	17,442	2	5	122	2021	64	40,6348	15	34,858	826,96	0	-66,7	760,24	663147,4	468432	K
E01-21	16,437	15	10	288	2021	64	40,6383	15	34,8537	820,56	0	-66,7	753,84	663150,4	468438,6	K
E02-21	16,549	2	5	122	2021	64	39,1241	15	35,996	1018,6	0	-66,8	951,77	662394,1	465580,3	K
E02-21	13,961	15	10	288	2021	64	39,1381	15	35,9916	1012,1	0	-66,8	945,27	662396,2	465606,5	K
E03-21	15,472	2	5	122	2021	64	36,6547	15	36,9094	1256,5	0	-66,9	1189,7	661913,2	460959,8	K
E03-21	13,405	15	10	288	2021	64	36,6593	15	36,9124	1250,3	0	-66,9	1183,4	661910,4	460968,2	K
E04-21	14,722	2	5	122	2021	64	34,9511	15	37,1435	1356,3	0	-66,8	1289,5	661895,9	457789	K
E04-21	12,876	15	10	288	2021	64	34,9519	15	37,143	1350,8	0	-66,8	1283,9	661896,3	457790,5	K
E07e-21	13,98	6	5	126	2021	64	38,4083	15	24,6746	1139,6	0	-66,6	1073	671472,3	464750,7	K
E07e-21	15,544	15	10	288	2021	64	38,4121	15	24,6652	1133	0	-66,6	1066,4	671479,4	464758,1	K
E08-21	14,419	6	5	126	2021	64	39,7173	15	23,8493	1019,8	0	-66,6	953,27	671990,3	467216,2	K
E08-21	15,75	15	10	288	2021	64	39,7184	15	23,8471	1013,8	0	-66,6	947,23	671991,9	467218,4	K
FI01-21	13,95	1	5	121	2021	64	26,1537	15	55,6294	1414,3	0	-66,8	1347,5	647949,1	440709,7	K
FI01-21	11,314	15	10	288	2021	64	26,1472	15	55,6136	1408,7	0	-66,8	1341,9	647962,4	440698,2	K
G02-21	16,025	5	5	125	2021	64	26,8571	17	17,7174	1635,8	0	-67,7	1568,1	582064,3	439526,6	K
G02-21	20,641	16	10	289	2021	64	26,8525	17	17,7215	1632,2	0	-67,7	1564,4	582061,3	439518,1	K
G03-21	15,369	5	5	125	2021	64	28,4373	17	16,3313	1728,7	0	-67,7	1661	583095,9	442491,8	K
G03-21	20,241	16	10	289	2021	64	28,4354	17	16,3325	1725,3	0	-67,7	1657,6	583095,1	442488,3	K
G04-21	14,736	5	5	125	2021	64	30,0201	17	15,0303	1757,8	0	-67,7	1690,1	584057,1	445460,3	K
G04-21	19,639	16	10	289	2021	64	30,0206	17	15,0297	1754,5	0	-67,7	1686,8	584057,6	445461,1	K
Go1-21	11,217	5	5	125	2021	64	33,9686	17	24,9405	1829,2	0	-67,8	1761,3	575939,2	452584,9	K
Go1-21	16,626	16	10	289	2021	64	33,9671	17	24,9393	1825,7	0	-67,8	1757,9	575940,2	452582,2	K
Haab-21	15,791	3	5	123	2021	64	20,9565	17	24,1169	1798,7	0	-67,5	1731,2	577208,1	428432,8	K
Haab-21	20,822	16	10	289	2021	64	20,957	17	24,1168	1794,8	0	-67,5	1727,2	577208,1	428433,7	K
Hof01-21	13,859	2	5	122	2021	64	32,3386	15	35,8337	1209,3	0	-66,7	1142,7	663201,5	452998,2	K
Hof01-21	12,528	15	10	288	2021	64	32,3323	15	35,833	1204,4	0	-66,7	1137,7	663202,6	452986,5	K
Imau-Bre	11,375	1	5	121	2021	64	13,1582	16	18,31	708,32	0	-66,5	641,8	630789,8	415755,5	K
K01-21	16,257	5	5	125	2021	64	35,1745	17	51,8584	1110,4	0	-67,6	1042,8	554398,1	454362,4	K
K02-21	16,633	5	5	125	2021	64	34,809	17	49,6892	1237,8	0	-67,6	1170,1	556142,1	453715	K
K03-21	17,212	5	5	125	2021	64	34,2376	17	46,4005	1361,1	0	-67,7	1293,5	558788,4	452703,5	K
K03-21	12,161	17	10	290	2021	64	34,2403	17	46,4187	1356,3	0	-67,7	1288,6	558773,8	452708,1	K
K04-21	20,411	4	5	124	2021	64	33,209	17	42,2569	1555	0	-67,7	1487,3	562136,9	450858,7	K
K05-21	10,459	5	5	125	2021	64	33,436	17	35,4523	1747,6	0	-67,8	1679,8	567565,3	451396,7	K
K05-21	11,091	17	10	290	2021	64	33,4331	17	35,4672	1743,3	0	-67,8	1675,5	567553,5	451391,1	K
K06-21	12,842	5	5	125	2021	64	38,3565	17	31,3201	2014,4	0	-67,9	1946,5	570653,2	460612	K
K06-21	17,99	16	10	289	2021	64	38,3559	17	31,3187	2011,4	0	-67,9	1943,5	570654,3	460610,8	K
K07-21	19,472	4	5	124	2021	64	29,1058	17	42,0362	1600,1	0	-67,7	1532,4	562470	443240,2	K
K07-21	16,798	20	10	293	2021	64	29,106	17	42,0377	1596,6	0	-67,7	1528,9	562468,7	443240,5	K
Oer01-21	15,9	3	6	154	2021	63	59,8561	16	38,9983	1894,4	0	-66,3	1828	614982	390388,9	K
S01-21	13,379	4	5	124	2021	64	7,01622	17	49,9749	776,53	0	-66,8	709,69	556867,3	402080,4	K
S01-21	12,1	27	11	331	2021	64	7,01927	17	49,9773	772,41	-1,65	-66,8	703,92	556865,3	402086	K
S02-21	12,709	4	5	124	2021	64	12,159	17	48,9786	1069,1	0	-67,1	1002	557497,4	411649,2	K
S02-21	11,5	27	11	331	2021	64	12,1466	17	48,9847	1066,2	-2,05	-67	997,12	557492,9	411626,1	K
S04-21	12,082	4	5	124	2021	64	16,1767	17	48,1969	1225,1	0	-67,2	1157,9	557989	419124,7	K
S04-21	16,022	20	10	293	2021	64	16,1634	17	48,211	1220,8	0	-67,2	1153,6	557978	419099,8	K
S05-21	11,321	4	5	124	2021	64	20,5113	17	33,9975	1518,9	0	-67,5	1451,4	569272,1	427415	K
S05-21	16,865	17	10	290	2021	64	20,5097	17	34,013	1515,5	0	-67,5	1448	569259,7	427411,7	K
SkGPS-21	17,35	26	11	330	2021	64	15,5866	17	14,8005	1037,7	-2	-67	968,66	584984,8	418658,1	K
Ske02-21	12,984	3	5	123	2021	64	15,9061	17	0,06596	1247,6	0	-67,1	1180,5	596865,5	419604,6	K
Ske02-21	15,422	16	10	289	2021	64	15,8512	17	0,19293	1239,2	0	-67,1	1172,1	596766,2	419499,4	K
Ske03-21	11,903	3	5	123	2021	64	18,0584	16	56,1545	1368,3	0	-67,2	1301,1	599893	423703	K
Ske03-21	17,896	16	10	289	2021	64	18,0319	16	56,222	1362,1	-0,4	-67,2	1294,5	599840,1	423652,2	K
Ske04-21	10,921	3	5	123	2021	64	20,1345	16	51,8189	1467,7	0	-67,3	1400,4	603258,4	427674,5	K
Ske04-21	15	16	10	289	2021	64	20,123	16	51,85	1464,1	0	-67,3	1396,8	603234	427652,2	K
Ske05-21	10,371	3	5	123	2021	64	22,2313	16	47,2341	1541,7	0	-67,4	1474,3	606814	431695,1	K
Ske05-21	14,733	16	10	289	2021	64	22,2262	16	47,2461	1537,7	0	-67,4	1470,4	606804,6	431685,1	K

Skf00-21	10,196	1	5	121	2021	64	15,4512	15	54,0652	1017,8	0	-66	951,8	650177,7	420909,6	K
Skf00-21	10,475	15	10	288	2021	64	15,4525	15	54,0641	1011,4	0	-66	945,37	650178,5	420911,9	K
Skf01-21	11,928	1	5	121	2021	64	18,0179	16	5,00759	1351,2	0	-66,6	1284,6	641126,2	425252,9	K
Skf01-21	11,07	15	10	288	2021	64	18,0153	16	4,99139	1345,3	0	-66,6	1278,7	641139,5	425248,6	K
T01-21	18,028	4	5	124	2021	64	19,053	18	7,17503	797,62	0	-67,3	730,37	542588,7	424216,7	K
T01-21	14,433	27	11	331	2021	64	19,0526	18	7,17422	791,72	-1,61	-67,3	722,86	542589,4	424215,9	K
T02-21	19,274	4	5	124	2021	64	19,479	18	4,53382	957,2	0	-67,3	889,94	544706,4	425038,5	K
T02-21	13,933	27	11	331	2021	64	19,4789	18	4,54009	953,74	-1,68	-67,3	884,79	544701,4	425038,2	K
T03-21	17,806	4	5	124	2021	64	20,2007	17	58,5813	1134,5	0	-67,3	1067,2	549482,1	426453,1	K
T03-21	14,347	17	10	290	2021	64	20,199	17	58,5926	1130,4	0	-67,3	1063,1	549473	426449,9	K
T04-21	15,962	4	5	124	2021	64	21,3279	17	51,5139	1288,6	0	-67,4	1221,3	555137,6	428644,7	K
T04-21	13,377	17	10	290	2021	64	21,3239	17	51,5285	1284,6	0	-67,4	1217,3	555125,9	428637,1	K
T05-21	15,403	4	5	124	2021	64	22,2728	17	42,9967	1414,2	0	-67,5	1346,8	561958,2	430531,5	K
T05-21	12,533	17	10	290	2021	64	22,2692	17	43,0105	1410,4	0	-67,5	1342,9	561947,2	430524,5	K
T06-21	14,548	4	5	124	2021	64	24,2632	17	36,5068	1536,6	0	-67,6	1468,9	567097,9	434339,2	K
T06-21	11,45	17	10	290	2021	64	24,2592	17	36,5189	1532,7	0	-67,6	1465,1	567088,3	434331,5	K
T07-21	12,844	4	5	124	2021	64	25,2904	17	31,2135	1631,9	0	-67,7	1564,2	571306,3	436343,8	K
T07-21	10,723	17	10	290	2021	64	25,2883	17	31,2223	1628,4	0	-67,7	1560,7	571299,3	436339,7	K
T08-21	12,057	4	5	124	2021	64	26,2987	17	27,7525	1705,2	0	-67,8	1637,5	574039,8	438283	K
T08-21	10,164	17	10	290	2021	64	26,2984	17	27,7542	1701,1	0	-67,8	1633,4	574038,5	438282,4	K

Appendix D: Measured surface velocity at marked sites on Vatnajökull in 2021.

Site	Calendar		Calendar		# of days	translation		velocity	
	day date	#	day date	#		(m)	(°)	(cm/day)	(m/annum)
B07-21	210501	121	211015	288	167	2,40	160	1,44	5,25
B09-21	210502	122	211016	289	167	0,99	285	0,59	2,16
B10-20	201009	283	210502	122	204	7,07	160	3,47	12,66
B10-21	210502	122	211016	289	167	0,91	180	0,54	1,98
B11-21	210502	122	211016	289	167	9,78	21	5,85	21,37
B12-21	210502	122	211016	289	167	21,05	22	12,61	46,02
B13-21	210502	122	211015	288	166	25,22	27	15,20	55,46
B13ror15	201009	283	210501	121	203	7,41	28	3,65	13,32
B13ror15	210501	121	211016	289	168	25,06	29	14,92	54,45
B14-21	210501	121	211015	288	167	21,54	37	12,90	47,07
B15-21	210501	121	211015	288	167	14,65	45	8,77	32,02
B16-21	210503	123	211015	288	165	0,69	70	0,42	1,53
B17-21	210501	121	211016	289	168	19,92	15	11,86	43,28
B18-21	210501	121	211015	288	167	11,18	347	6,69	24,43
B19-21	210501	121	211015	288	167	0,65	340	0,39	1,42
BB0-21	210501	121	211015	288	167	0,56	243	0,34	1,23
Bor-21	210503	123	211018	291	168	17,24	186	10,26	37,45
Br7-21	210501	121	211015	288	167	52,00	174	31,14	113,66
Bru-21	210501	121	211015	288	167	14,85	9	8,89	32,46
Bud-21	210501	121	211015	288	167	20,28	5	12,14	44,32
D05-21	210505	125	211016	289	164	25,82	33	15,74	57,46
D07-21	210505	125	211016	289	164	31,41	23	19,15	69,90
D09-21	210505	125	211016	289	164	6,82	351	4,16	15,18
D12-21	210505	125	211016	289	164	0,66	25	0,40	1,46
E01-21	210502	122	211015	288	166	7,31	28	4,41	16,08
E02-21	210502	122	211015	288	166	26,22	8	15,79	57,65
E03-21	210502	122	211015	288	166	8,90	344	5,36	19,57
E04-21	210502	122	211015	288	166	1,46	18	0,88	3,21
E07e-21	210506	126	211015	288	162	10,17	47	6,28	22,92
E08-21	210506	126	211015	288	162	2,70	40	1,67	6,09
FI01-21	210501	121	211015	288	167	17,55	134	10,51	38,37
G02-21	210505	125	211016	289	164	9,00	201	5,49	20,04
G03-21	210505	125	211016	289	164	3,60	196	2,19	8,00
G04-21	210505	125	211016	289	164	0,96	32	0,59	2,14
Go1-21	210505	125	211016	289	164	2,89	160	1,76	6,44
Haab-21	210503	123	211016	289	166	0,87	2	0,52	1,91
Hof01-21	210502	122	211015	288	166	11,70	178	7,05	25,72
K03-21	210505	125	211017	290	165	15,36	289	9,31	33,98
K05-21	210505	125	211017	290	165	13,07	246	7,92	28,92
K06-21	210505	125	211016	289	164	1,63	137	0,99	3,62
K07-21	210504	124	211020	293	169	1,30	287	0,77	2,81
S01-21	210504	124	211127	331	207	5,98	341	2,89	10,55
S02-21	210504	124	211127	331	207	23,51	192	11,36	41,45
S04-21	210504	124	211020	293	169	27,18	205	16,08	58,69
S05-21	210504	124	211017	290	166	12,76	257	7,69	28,06

Ske02-21	210503	123	211016	289	166	144,38	225	86,97	317,46
Ske03-21	210503	123	211016	289	166	73,25	228	44,12	161,05
Ske04-21	210503	123	211016	289	166	33,02	230	19,89	72,61
Ske05-21	210503	123	211016	289	166	13,62	225	8,21	29,95
Skf00-21	210501	121	211015	288	167	2,47	21	1,48	5,39
Skf01-21	210501	121	211015	288	167	13,95	111	8,35	30,49
T01-21	210504	124	211127	331	207	0,99	139	0,48	1,74
T02-21	210504	124	211127	331	207	5,06	266	2,45	8,93
T03-21	210504	124	211017	290	166	9,59	252	5,78	21,10
T04-21	210504	124	211017	290	166	13,92	238	8,38	30,60
T05-21	210504	124	211017	290	166	12,96	239	7,81	28,49
T06-21	210504	124	211017	290	166	12,33	232	7,43	27,11
T07-21	210504	124	211017	290	166	8,15	241	4,91	17,91
T08-21	210504	124	211017	290	166	1,48	247	0,89	3,25

Appendix E: Melt water runoff to selected rivers in summer 2021, derived from summer surface balance.

ΔS : area in a given elevation range where summer balance is negative, $\Sigma\Delta S$: cumulative area above a given elevation, ΔQ_s : melt water runoff from a given elevation range, $\Sigma\Delta Q_s$: cumulative melt water runoff from an area above given elevation.

Tungnaá water drainage basin

Elevation (m a. s. l.)		ΔS km ²	$\Sigma\Delta S$ km ²	ΔQ_s (10 ⁶ m ³)	$\Sigma\Delta Q_s$ (10 ⁶ m ³)
1350	1400	0,3	0,3	0,5	0,5
1300	1350	6,0	6,4	10,1	10,6
1250	1300	10,0	16,3	20,0	30,6
1200	1250	10,9	27,2	26,3	56,8
1150	1200	9,5	36,7	25,9	82,7
1100	1150	11,4	48,1	34,2	116,9
1050	1100	10,8	58,9	36,6	153,5
1000	1050	9,5	68,4	35,7	189,1
950	1000	9,1	77,5	37,2	226,3
900	950	8,8	86,2	39,5	265,8
850	900	6,6	92,9	34,2	300,0
800	850	6,8	99,6	39,4	339,4
750	800	5,7	105,4	36,6	376,1
700	750	3,7	109,1	25,6	401,6
650	700	0,8	109,9	5,6	407,2

Sylgja water drainage basin

Elevation (m a. s. l.)		ΔS km ²	$\Sigma\Delta S$ km ²	ΔQ_s (10 ⁶ m ³)	$\Sigma\Delta Q_s$ (10 ⁶ m ³)
1300	1350	1,1	1,1	2,0	2,0
1250	1300	3,4	4,5	6,9	8,8
1200	1250	5,5	10,0	12,9	21,8
1150	1200	8,2	18,2	21,4	43,2
1100	1150	5,8	24,0	17,0	60,2
1050	1100	6,2	30,2	21,2	81,4
1000	1050	5,8	36,0	23,5	104,9
950	1000	1,9	37,9	8,0	113,0
900	950	0,8	38,7	3,4	116,4
850	900	0,0	38,7	0,2	116,6

Western Skaftá cauldron water drainage basin

Elevation (m a. s. l.)		ΔS km ²	$\Sigma\Delta S$ km ²	ΔQ_s (10 ⁶ m ³)	$\Sigma\Delta Q_s$ (10 ⁶ m ³)
1700	1750	2,2	2,2	1,7	1,7
1650	1700	7,2	9,4	5,8	7,5
1600	1650	7,9	17,3	6,8	14,3
1550	1600	5,1	22,4	4,7	19,0
1500	1550	2,6	25,1	2,5	21,6
1450	1500	0,0	25,1	0,0	21,6

Eastern Skaftár cauldron water drainage basin

Elevation (m a. s. l.)		ΔS km ²	$\Sigma \Delta S$ km ²	ΔQ_s (10 ⁶ m ³)	$\Sigma \Delta Q_s$ (10 ⁶ m ³)
1750	1800	2,4	2,4	1,9	1,9
1700	1750	9,7	12,1	8,4	10,3
1650	1700	13,7	25,8	12,6	22,9
1600	1650	9,4	35,2	8,3	31,2
1550	1600	4,1	39,3	3,6	34,8

Grímsvötn water drainage basin

Elevation (m a. s. l.)		ΔS km ²	$\Sigma \Delta S$ km ²	ΔQ_s (10 ⁶ m ³)	$\Sigma \Delta Q_s$ (10 ⁶ m ³)
1900	1950	0,4	0,4	0,2	0,2
1850	1900	1,3	1,8	0,8	1,0
1800	1850	1,7	3,5	1,1	2,1
1750	1800	4,8	8,3	4,0	6,1
1700	1750	23,8	32,1	21,6	27,6
1650	1700	48,6	80,7	45,8	73,4
1600	1650	30,9	111,5	31,7	105,1
1550	1600	20,0	131,6	21,1	126,2
1500	1550	16,6	148,2	18,8	145,0
1450	1500	9,7	157,9	12,5	157,5
1400	1450	13,8	171,7	19,9	177,4
1350	1400	1,5	173,2	2,0	179,4

Kaldakvísl water drainage basin

Elevation (m a. s. l.)		ΔS km ²	$\Sigma \Delta S$ km ²	ΔQ_s (10 ⁶ m ³)	$\Sigma \Delta Q_s$ (10 ⁶ m ³)
1950	2000	1,2	1,2	0,7	0,7
1900	1950	14,1	15,3	7,4	8,1
1850	1900	6,4	21,7	3,6	11,7
1800	1850	6,2	27,9	3,8	15,6
1750	1800	10,8	38,7	7,4	23,0
1700	1750	20,2	58,9	14,6	37,6
1650	1700	16,8	75,7	13,9	51,5
1600	1650	14,4	90,1	15,3	66,8
1550	1600	18,5	108,6	27,2	94,0
1500	1550	24,0	132,6	42,2	136,2
1450	1500	28,0	160,6	54,0	190,2
1400	1450	22,4	183,0	50,9	241,1
1350	1400	20,8	203,8	55,1	296,2
1300	1350	20,2	224,0	63,7	359,9
1250	1300	21,1	245,1	71,1	431,0
1200	1250	20,4	265,5	71,9	502,8
1150	1200	19,3	284,8	73,0	575,8
1100	1150	17,3	302,1	70,5	646,3
1050	1100	16,1	318,1	70,5	716,8
1000	1050	14,1	332,3	66,1	782,9
950	1000	9,2	341,5	47,1	830,0
900	950	2,6	344,1	13,8	843,9

Jökulsá á Fjöllum water drainage basin

Elevation (m a. s. l.)		ΔS km ²	$\Sigma\Delta S$ km ²	ΔQ_s (10 ⁶ m ³)	$\Sigma\Delta Q_s$ (10 ⁶ m ³)
1950	2000	2,8	2,8	1,6	1,6
1900	1950	20,3	23,1	11,0	12,6
1850	1900	24,9	48,0	14,5	27,1
1800	1850	18,4	66,4	12,0	39,1
1750	1800	21,8	88,2	15,9	55,0
1700	1750	39,1	127,4	31,3	86,3
1650	1700	80,5	207,8	69,1	155,4
1600	1650	122,3	330,1	116,4	271,8
1550	1600	100,7	430,8	111,5	383,3
1500	1550	93,3	524,1	120,3	503,6
1450	1500	80,0	604,1	118,7	622,3
1400	1450	69,0	673,1	114,1	736,4
1350	1400	54,7	727,7	102,6	839,0
1300	1350	43,2	770,9	93,7	932,7
1250	1300	46,8	817,7	117,7	1050,5
1200	1250	49,8	867,5	147,5	1198,0
1150	1200	49,6	917,1	174,9	1372,8
1100	1150	43,8	961,0	178,9	1551,8
1050	1100	31,3	992,3	140,2	1692,0
1000	1050	31,4	1023,7	151,4	1843,4
950	1000	29,1	1052,8	153,1	1996,5
900	950	24,4	1077,2	138,5	2135,0
850	900	21,1	1098,3	126,8	2261,8
800	850	18,7	1117,0	118,6	2380,3
750	800	12,3	1129,3	82,1	2462,4
700	750	3,7	1133,0	25,7	2488,1

Kreppa and Kverká water drainage basin

Elevation (m a. s. l.)		ΔS km ²	$\Sigma \Delta S$ km ²	ΔQ_s (10 ⁶ m ³)	$\Sigma \Delta Q_s$ (10 ⁶ m ³)
1900	1950	0,0	0,0	0,0	0,0
1850	1900	1,3	1,4	0,7	0,8
1800	1850	4,4	5,9	2,5	3,3
1750	1800	2,7	8,5	1,7	5,0
1700	1750	3,8	12,3	2,8	7,8
1650	1700	5,2	17,5	4,1	11,9
1600	1650	41,4	58,9	36,7	48,6
1550	1600	20,5	79,4	20,0	68,6
1500	1550	13,4	92,8	14,9	83,5
1450	1500	16,4	109,2	20,5	104,0
1400	1450	20,0	129,2	28,7	132,8
1350	1400	26,2	155,4	42,0	174,8
1300	1350	20,4	175,7	35,6	210,3
1250	1300	15,5	191,2	30,1	240,4
1200	1250	18,1	209,3	42,2	282,7
1150	1200	17,4	226,7	49,6	332,2
1100	1150	16,0	242,7	52,0	384,2
1050	1100	10,5	253,2	37,5	421,7
1000	1050	12,1	265,3	45,8	467,5
950	1000	13,3	278,6	55,6	523,1
900	950	12,6	291,2	58,9	582,0
850	900	12,6	303,8	64,5	646,5
800	850	10,4	314,2	57,3	703,8
750	800	7,3	321,5	43,7	747,5
700	750	3,5	325,0	22,3	769,8
650	700	0,4	325,4	2,9	772,7

Hálslón water drainage basin

Elevation (m a. s. l.)		ΔS km ²	$\Sigma \Delta S$ km ²	ΔQ_s (10 ⁶ m ³)	$\Sigma \Delta Q_s$ (10 ⁶ m ³)
1600	1650	11,4	11,4	10,2	10,2
1550	1600	33,1	44,5	31,7	42,0
1500	1550	65,3	109,8	69,3	111,3
1450	1500	70,0	179,9	86,2	197,5
1400	1450	99,0	278,8	127,7	325,2
1350	1400	133,7	412,6	194,2	519,3
1300	1350	130,3	542,9	214,4	733,7
1250	1300	123,4	666,3	232,6	966,3
1200	1250	98,2	764,5	220,5	1186,8
1150	1200	82,2	846,7	221,7	1408,5
1100	1150	64,5	911,2	203,3	1611,8
1050	1100	55,1	966,3	195,7	1807,5
1000	1050	46,1	1012,4	177,0	1984,6
950	1000	39,4	1051,8	164,0	2148,6
900	950	31,6	1083,4	143,8	2292,4
850	900	26,8	1110,1	133,3	2425,7
800	850	25,1	1135,3	134,9	2560,5
750	800	25,2	1160,5	144,7	2705,3
700	750	22,4	1182,9	136,7	2842,0
650	700	12,1	1194,9	76,4	2918,4
600	650	1,1	1196,1	7,4	2925,8

Jökulsá á Fljótsdal water drainage basin

Elevation (m a. s. l.)		ΔS km ²	$\Sigma \Delta S$ km ²	ΔQ_s (10 ⁶ m ³)	$\Sigma \Delta Q_s$ (10 ⁶ m ³)
1550	1600	0,0	0,0	0,0	0,0
1500	1550	0,1	0,1	0,1	0,1
1450	1500	1,1	1,2	1,2	1,3
1400	1450	2,1	3,4	2,3	3,6
1350	1400	3,1	6,5	3,9	7,5
1300	1350	5,9	12,4	8,5	16,0
1250	1300	16,1	28,5	29,0	45,0
1200	1250	15,8	44,3	36,5	81,5
1150	1200	17,0	61,3	50,2	131,7
1100	1150	14,3	75,6	49,3	181,0
1050	1100	11,9	87,6	45,2	226,1
1000	1050	11,1	98,6	45,7	271,9
950	1000	8,7	107,3	38,9	310,7
900	950	5,5	112,8	26,6	337,3
850	900	4,2	117,0	21,0	358,3
800	850	3,1	120,1	16,5	374,8
750	800	1,9	122,0	11,4	386,2
700	750	1,7	123,8	11,2	397,4
650	700	1,0	124,8	7,0	404,4

Hornafjarðarfljót water drainage basin

Elevation (m a. s. l.)		ΔS km ²	$\Sigma \Delta S$ km ²	ΔQ_s (10 ⁶ m ³)	$\Sigma \Delta Q_s$ (10 ⁶ m ³)
1450	1500	1,2	1,2	1,2	1,2
1400	1450	8,2	9,4	10,0	11,2
1350	1400	12,7	22,2	17,0	28,2
1300	1350	19,2	41,4	29,3	57,5
1250	1300	37,9	79,3	66,7	124,2
1200	1250	28,8	108,1	58,0	182,1
1150	1200	20,3	128,4	46,4	228,5
1100	1150	18,9	147,3	47,9	276,5
1050	1100	14,2	161,5	41,3	317,8
1000	1050	11,1	172,5	36,6	354,4
950	1000	10,4	182,9	38,4	392,9
900	950	8,1	191,0	33,3	426,1
850	900	5,4	196,3	24,2	450,3
800	850	4,5	200,8	21,2	471,5
750	800	4,1	204,9	20,2	491,7
700	750	3,4	208,4	18,2	509,9
650	700	3,6	212,0	20,2	530,1
600	650	2,6	214,5	15,2	545,3
550	600	1,8	216,4	11,1	556,4
500	550	1,7	218,1	11,1	567,5
450	500	1,2	219,3	8,0	575,5
400	450	1,1	220,4	7,9	583,4
350	400	0,8	221,3	6,4	589,8
300	350	0,6	221,9	4,9	594,6
250	300	0,8	222,7	6,9	601,5
200	250	1,6	224,3	13,7	615,2
150	200	2,3	226,6	21,3	636,5
100	150	2,5	229,1	23,5	660,0
50	100	1,9	231,0	18,4	678,4
0	50	2,2	233,2	21,8	700,2

Jökulsá á Breiðamerkursandi water drainage basin

Elevation (m a. s. l.)		ΔS km ²	$\Sigma \Delta S$ km ²	ΔQ_s (10 ⁶ m ³)	$\Sigma \Delta Q_s$ (10 ⁶ m ³)
1700	1750	1,0	1,0	0,7	0,7
1650	1700	4,2	5,2	3,1	3,8
1600	1650	14,2	19,5	11,2	15,1
1550	1600	19,0	38,5	16,8	31,8
1500	1550	22,9	61,4	22,4	54,2
1450	1500	36,1	97,5	34,4	88,6
1400	1450	51,2	148,7	54,2	142,8
1350	1400	83,5	232,2	96,7	239,5
1300	1350	83,4	315,6	102,4	341,9
1250	1300	51,7	367,3	70,3	412,2
1200	1250	34,7	401,9	54,4	466,6
1150	1200	28,3	430,3	52,6	519,3
1100	1150	23,8	454,0	51,9	571,2
1050	1100	20,4	474,4	50,9	622,1
1000	1050	17,5	492,0	48,5	670,6
950	1000	19,2	511,2	57,3	727,9
900	950	19,8	531,0	66,1	793,9
850	900	18,5	549,5	71,3	865,2
800	850	18,7	568,1	78,4	943,6
750	800	19,9	588,1	91,1	1034,6
700	750	16,7	604,8	82,8	1117,4
650	700	27,3	632,0	147,8	1265,1
600	650	19,3	651,3	109,6	1374,7
550	600	19,0	670,3	114,8	1489,5
500	550	10,3	680,6	64,4	1553,9
450	500	5,1	685,7	34,1	1588,0
400	450	7,1	692,8	51,0	1639,0
350	400	5,0	697,8	37,6	1676,6
300	350	4,5	702,2	35,3	1711,9
250	300	5,3	707,6	43,8	1755,6
200	250	4,4	712,0	38,0	1793,6
150	200	5,0	717,0	44,8	1838,3
100	150	4,6	721,6	43,2	1881,6
50	100	3,8	725,5	37,2	1918,8
0	50	1,7	727,2	16,7	1935,5

Breiðárlón/Fjallsárlón water drainage basin

Elevation (m a. s. l.)		ΔS km ²	$\Sigma \Delta S$ km ²	ΔQ_s (10 ⁶ m ³)	$\Sigma \Delta Q_s$ (10 ⁶ m ³)
2000	2050	0,0	0,0	0,0	0,0
1950	2000	0,6	0,7	0,1	0,2
1900	1950	0,9	1,6	0,2	0,4
1850	1900	1,6	3,3	0,5	0,9
1800	1850	2,1	5,4	0,9	1,8
1750	1800	2,6	8,0	1,3	3,1
1700	1750	2,9	10,9	1,5	4,6
1650	1700	3,1	14,0	1,6	6,2
1600	1650	4,2	18,2	2,2	8,5
1550	1600	4,4	22,6	2,5	11,0
1500	1550	5,8	28,3	3,8	14,8
1450	1500	5,0	33,3	3,8	18,6
1400	1450	5,3	38,6	4,8	23,4
1350	1400	6,4	45,0	7,0	30,4
1300	1350	12,9	57,9	16,2	46,7
1250	1300	6,2	64,0	9,1	55,7
1200	1250	5,8	69,8	9,6	65,4
1150	1200	4,8	74,6	9,0	74,4
1100	1150	4,5	79,1	10,0	84,5
1050	1100	5,0	84,1	12,3	96,8
1000	1050	6,1	90,2	16,5	113,3
950	1000	6,7	96,9	20,1	133,4
900	950	7,9	104,7	26,4	159,9
850	900	6,2	110,9	23,9	183,8
800	850	7,6	118,5	32,3	216,1
750	800	8,6	127,1	39,9	256,0
700	750	6,6	133,6	33,0	289,0
650	700	6,2	139,9	33,7	322,7
600	650	7,3	147,2	41,9	364,6
550	600	8,2	155,4	49,8	414,4
500	550	8,3	163,6	53,2	467,6
450	500	8,8	172,4	59,8	527,3
400	450	10,4	182,8	74,2	601,5
350	400	8,7	191,5	65,8	667,4
300	350	7,0	198,5	54,8	722,2
250	300	6,4	204,9	52,4	774,6
200	250	6,0	210,9	51,4	826,0
150	200	6,0	216,9	53,5	879,6
100	150	4,5	221,4	42,1	921,6
50	100	3,7	225,1	35,6	957,2
0	50	4,1	229,2	40,2	997,4

Skeiðarársandur (Gígja) water drainage basin

Elevation ΔS $\Sigma \Delta S$ ΔQ_s $\Sigma \Delta Q_s$
(m a. s. l.) km^2 km^2 (10^6m^3) (10^6m^3)

1700	1750	1,9	1,9	1,4	1,4
1650	1700	21,5	23,5	18,6	20,0
1600	1650	82,0	105,5	70,4	90,4
1550	1600	86,0	191,5	77,4	167,8
1500	1550	110,8	302,3	106,6	274,4
1450	1500	106,5	408,8	106,6	381,0
1400	1450	104,2	513,0	110,2	491,3
1350	1400	91,4	604,4	102,4	593,6
1300	1350	77,9	682,4	94,2	687,9
1250	1300	69,6	751,9	96,8	784,6
1200	1250	60,5	812,4	100,1	884,7
1150	1200	54,6	867,0	105,9	990,6
1100	1150	51,4	918,4	112,8	1103,4
1050	1100	46,3	964,8	117,6	1221,0
1000	1050	41,5	1006,3	121,3	1342,3
950	1000	40,3	1046,6	134,3	1476,6
900	950	37,2	1083,8	138,2	1614,7
850	900	38,6	1122,5	156,7	1771,5
800	850	32,6	1155,1	146,3	1917,8
750	800	27,3	1182,4	132,6	2050,4
700	750	25,2	1207,6	129,5	2179,9
650	700	20,2	1227,8	110,4	2290,3
600	650	15,5	1243,4	89,4	2379,7
550	600	23,3	1266,6	141,8	2521,5
500	550	20,5	1287,2	131,4	2652,9
450	500	13,5	1300,7	91,3	2744,2
400	450	12,0	1312,7	86,5	2830,7
350	400	13,0	1325,7	97,9	2928,6
300	350	14,1	1339,8	110,0	3038,6
250	300	12,2	1352,0	100,5	3139,1
200	250	12,1	1364,1	104,3	3243,4
150	200	11,2	1375,3	101,7	3345,1
100	150	9,8	1385,1	91,7	3436,8
50	100	6,0	1391,1	57,4	3494,2
0	50	2,4	1393,5	23,2	3517,3

Djúpá water drainage basin

Elevation (m a. s. l.)		ΔS km ²	$\Sigma \Delta S$ km ²	ΔQ_s (10 ⁶ m ³)	$\Sigma \Delta Q_s$ (10 ⁶ m ³)
1450	1500	0,1	0,1	0,1	0,1
1400	1450	0,3	0,4	0,3	0,4
1350	1400	0,7	1,1	0,7	1,2
1300	1350	3,5	4,6	4,3	5,5
1250	1300	3,3	7,9	4,0	9,5
1200	1250	2,9	10,8	4,4	13,9
1150	1200	3,3	14,2	6,7	20,6
1100	1150	5,3	19,5	13,1	33,7
1050	1100	5,5	24,9	16,9	50,5
1000	1050	8,8	33,7	29,8	80,4
950	1000	7,4	41,1	29,1	109,5
900	950	7,4	48,5	31,7	141,2
850	900	6,3	54,8	28,7	169,9
800	850	6,6	61,4	32,0	201,9
750	800	6,0	67,4	31,0	232,9
700	750	3,5	70,9	19,3	252,2
650	700	2,5	73,4	14,1	266,3
600	650	0,6	74,0	3,6	269,8

Brunná water drainage basin

Elevation (m a. s. l.)		ΔS km ²	$\Sigma \Delta S$ km ²	ΔQ_s (10 ⁶ m ³)	$\Sigma \Delta Q_s$ (10 ⁶ m ³)
1000	1050	0,8	0,8	3,0	3,0
950	1000	2,1	3,0	8,7	11,7
900	950	4,0	7,0	17,4	29,1
850	900	4,0	10,9	18,4	47,5
800	850	3,7	14,7	18,4	65,9
750	800	4,1	18,8	21,2	87,2
700	750	5,0	23,8	26,7	113,9
650	700	5,2	29,0	29,7	143,6
600	650	2,8	31,8	16,5	160,1

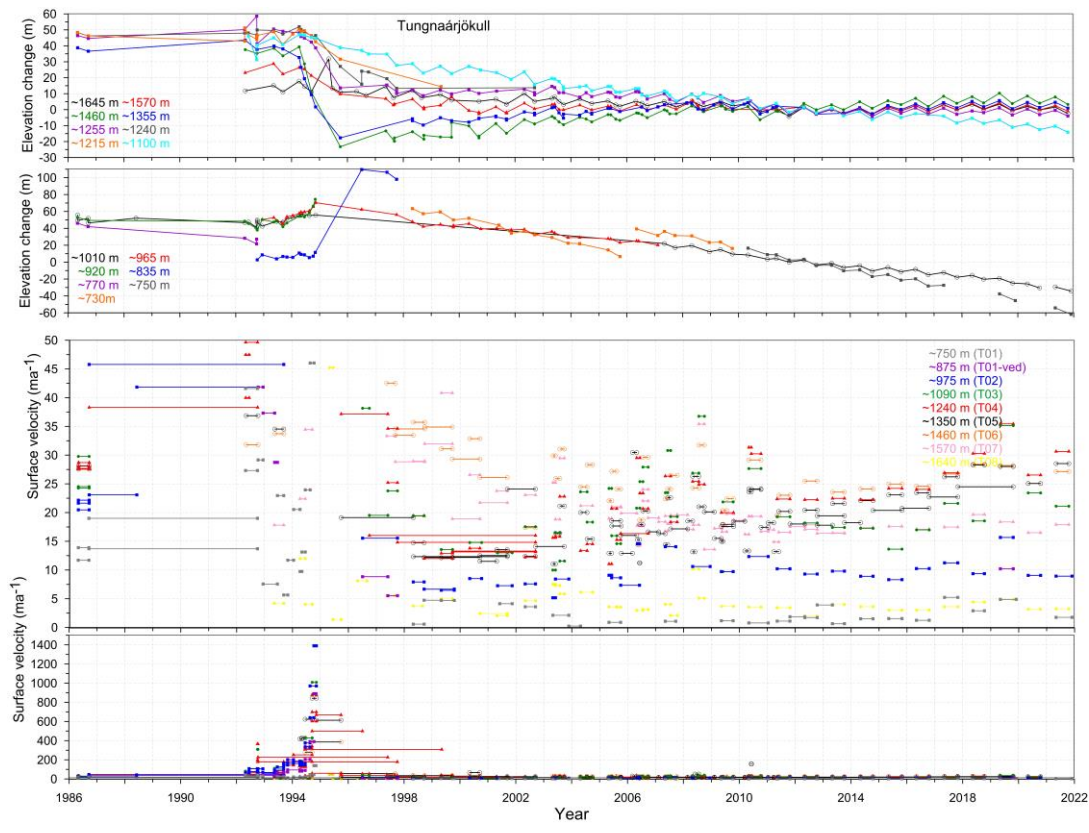
Hverfisfljót water drainage basin

Elevation (m a. s. l.)		ΔS km ²	$\Sigma \Delta S$ km ²	ΔQ_s (10 ⁶ m ³)	$\Sigma \Delta Q_s$ (10 ⁶ m ³)
1700	1750	0,9	0,9	0,7	0,7
1650	1700	5,9	6,8	5,2	5,9
1600	1650	9,1	15,9	8,4	14,3
1550	1600	10,4	26,3	9,1	23,3
1500	1550	20,8	47,1	18,3	41,6
1450	1500	40,3	87,4	38,7	80,3
1400	1450	26,6	114,0	31,0	111,3
1350	1400	24,2	138,2	33,2	144,5
1300	1350	22,7	160,9	36,2	180,8
1250	1300	17,6	178,5	32,7	213,5
1200	1250	20,3	198,8	42,2	255,7
1150	1200	14,4	213,2	34,4	290,1
1100	1150	10,9	224,1	30,5	320,6
1050	1100	9,3	233,4	30,3	351,0
1000	1050	8,7	242,0	31,5	382,4
950	1000	8,6	250,6	34,4	416,8
900	950	7,9	258,5	34,3	451,2
850	900	7,8	266,3	36,3	487,5
800	850	6,8	273,1	33,5	520,9
750	800	8,5	281,6	43,6	564,6
700	750	10,7	292,2	57,5	622,1
650	700	11,2	303,4	63,3	685,3
600	650	6,0	309,4	35,0	720,3
550	600	0,2	309,6	1,1	721,4

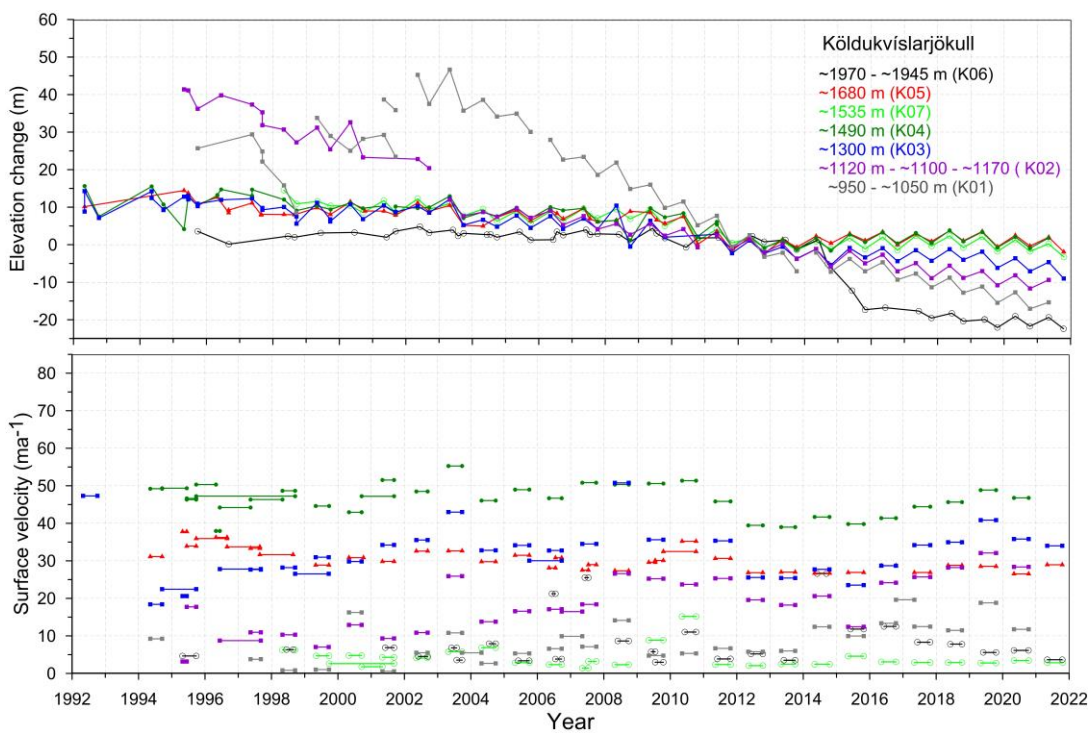
Skaftá water drainage basin

Elevation (m a. s. l.)		ΔS km ²	$\Sigma \Delta S$ km ²	ΔQ_s (10 ⁶ m ³)	$\Sigma \Delta Q_s$ (10 ⁶ m ³)
1650	1700	1,9	1,9	1,9	1,9
1600	1650	14,8	16,7	14,0	15,9
1550	1600	22,8	39,5	19,9	35,8
1500	1550	31,7	71,1	30,0	65,8
1450	1500	24,9	96,0	28,0	93,8
1400	1450	22,5	118,4	29,7	123,5
1350	1400	20,5	138,9	29,5	153,0
1300	1350	22,2	161,1	36,6	189,6
1250	1300	15,1	176,2	29,1	218,8
1200	1250	20,5	196,7	46,0	264,8
1150	1200	22,3	219,0	57,3	322,1
1100	1150	23,3	242,3	67,1	389,2
1050	1100	22,7	264,9	73,5	462,8
1000	1050	25,2	290,1	92,1	554,9
950	1000	20,2	310,3	82,6	637,5
900	950	16,8	327,1	75,5	713,0
850	900	13,5	340,6	65,2	778,3
800	850	14,2	354,8	73,5	851,8
750	800	12,4	367,2	69,5	921,3
700	750	9,9	377,1	58,7	980,0
650	700	6,3	383,4	38,1	1018,1
600	650	0,8	384,2	4,9	1023,0

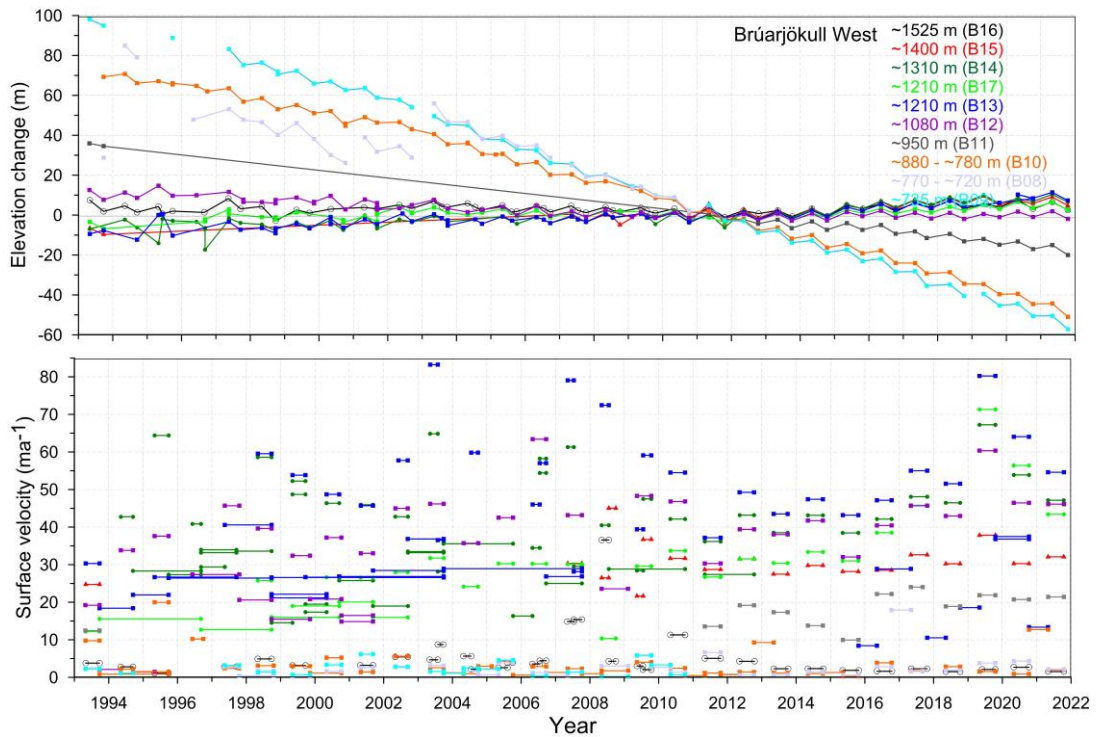
Appendix F: Records of surface elevation change and surface velocity at mass balance survey sites on Vatnajökull.



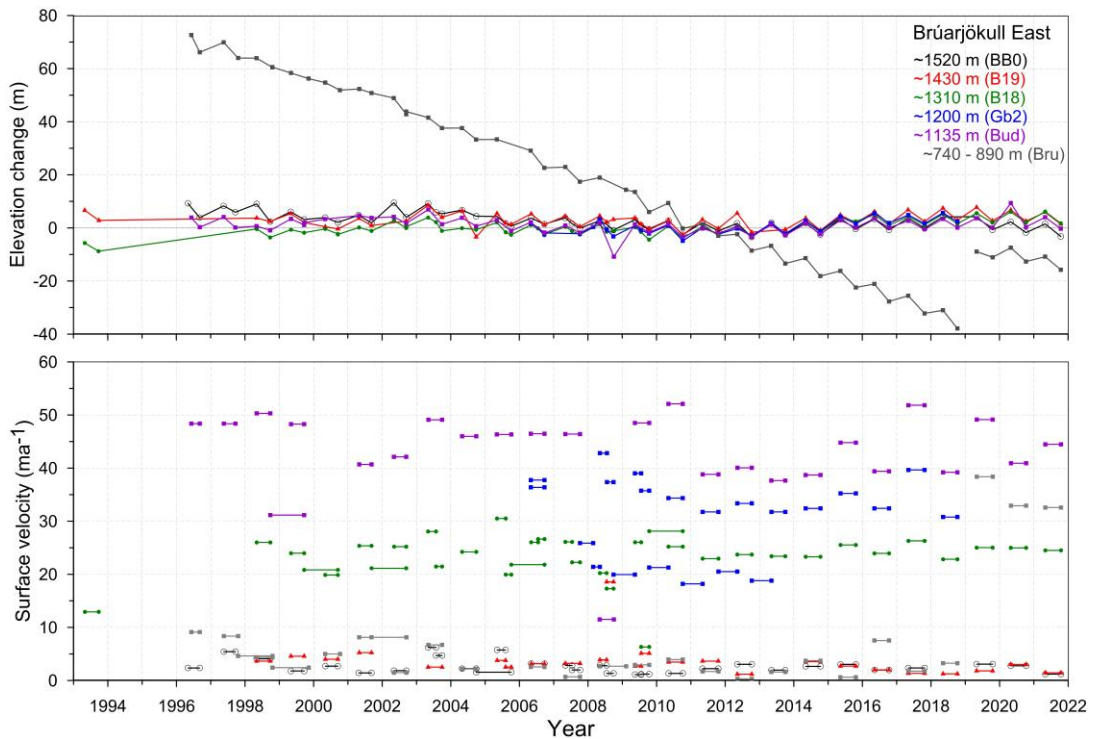
Surface elevation change relative to spring 2010 (upper panel) and average surface velocity (lower panel) at mb sites on Tungnaárjökull in 1986 to 2021.



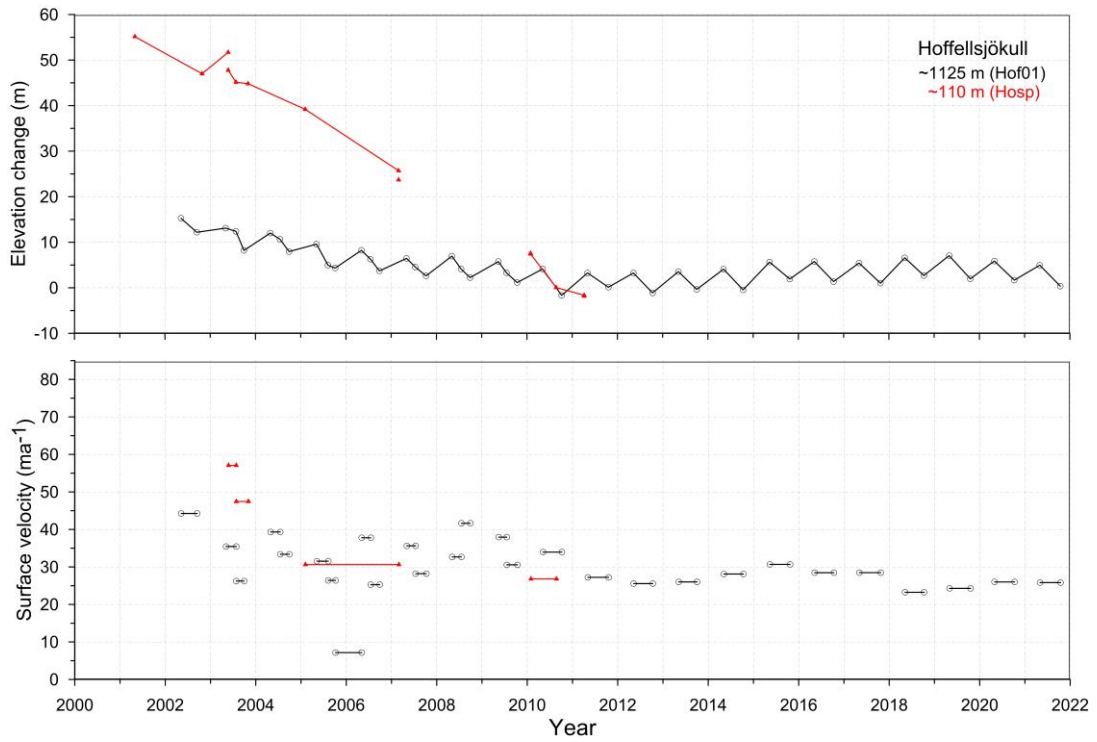
Surface elevation change relative to spring 2010 (upper panel) and average surface velocity (lower panel) at mb sites on Köldukvíslarjökull in 1992 to 2021.



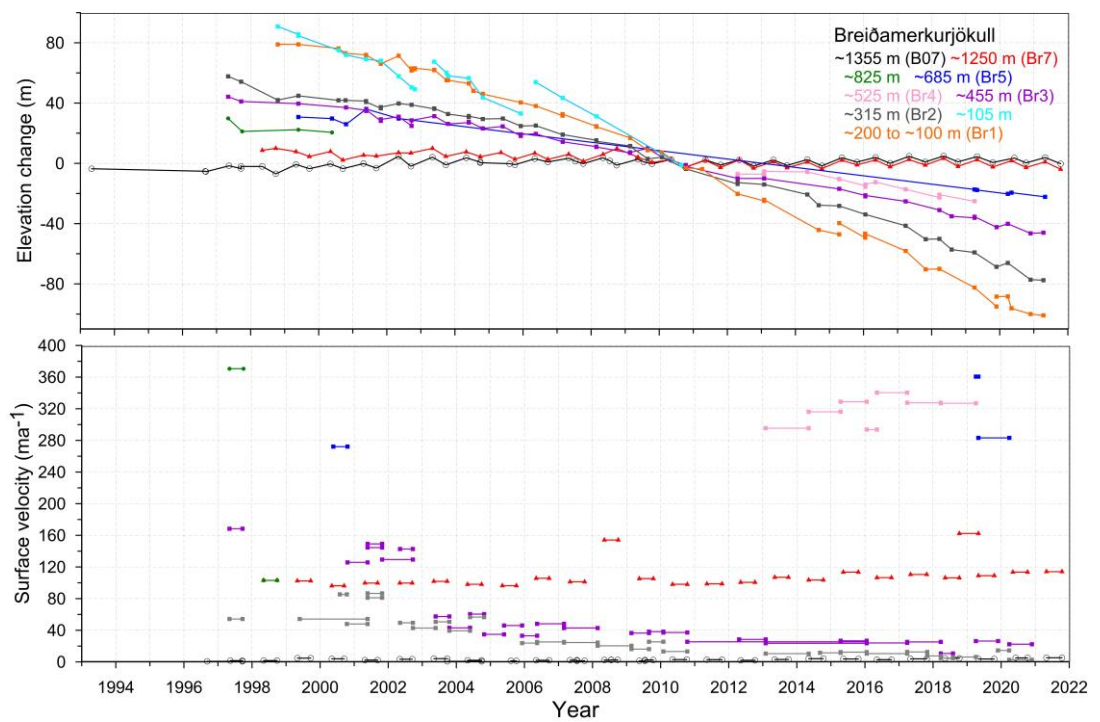
Surface elevation change relative to spring 2010 (upper panel) and average surface velocity at mb sites (lower panel) on W-Brúarjökull in 1993 to 2021.



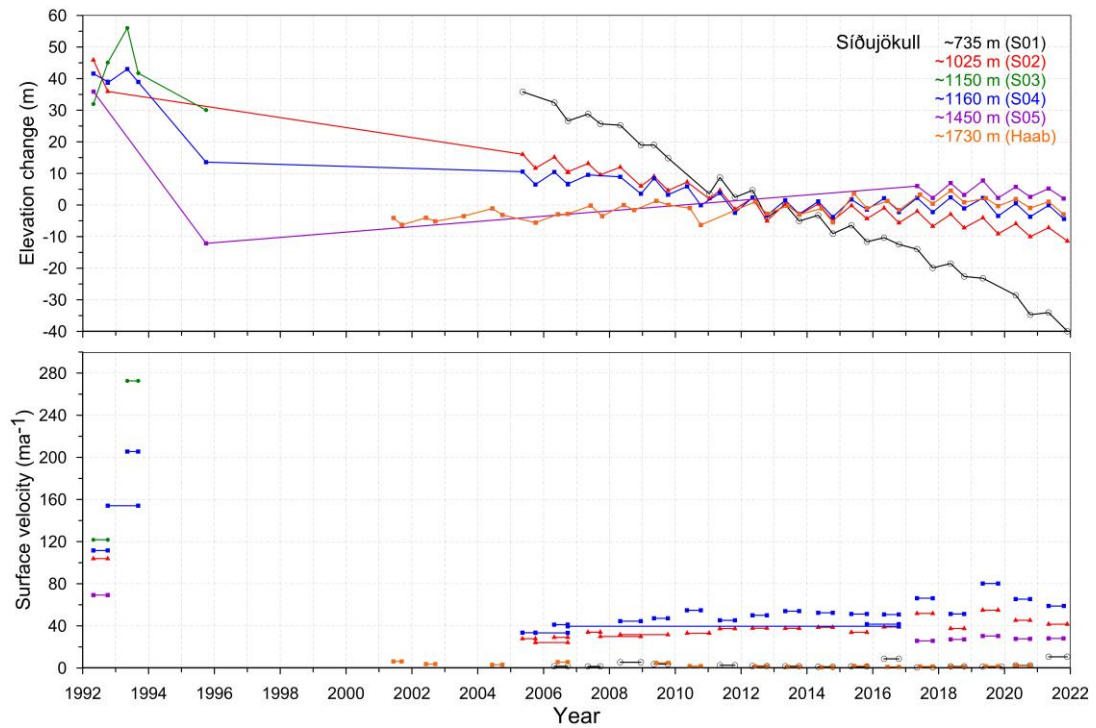
Surface elevation change relative to spring 2010 (upper panel) and average surface velocity at mb sites (lower panel) on E-Brúarjökull in 1993 to 2021.



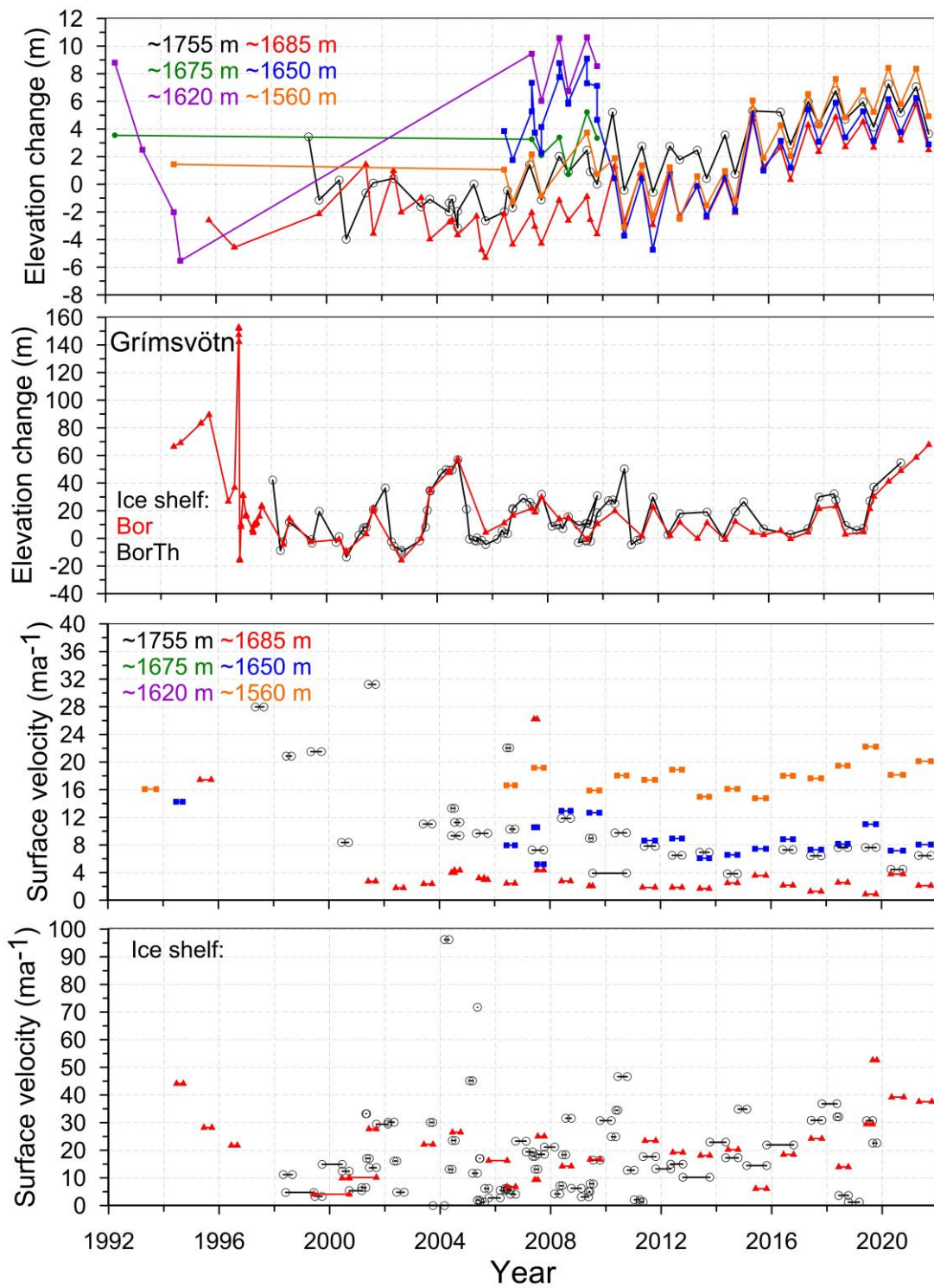
Surface elevation change relative to spring 2010 (upper panel) and average surface velocity) at mb sites (lower panel) on Hoffellsjökull in 2000 to 2021.



Surface elevation change relative to spring 2010 (upper panel) and average surface velocity at mb sites (lower panel) on Breiðamerkurjökull in 1993 to 2021.



Surface elevation change relative to spring 2010 (upper panel) and average surface velocity at mb sites (lower panel) on Síðujökull in 1992 to 2021.



Surface elevation change relative to spring 2010 (upper panel) and average surface velocity at mb sites (lower panel) in Grímsvötn ice catchment in 1993 to 2021.

